Glycan polymeric prodrugs against pulmonary intracellular alveolar infections

Jasmin Chen

A dissertation

submitted in partial fulfillment of the

requirements for the degree of

Doctor of Philosophy

University of Washington

2017

Reading Committee:

Daniel Ratner, Chair

David Danley

Patrick Stayton

Program Authorized to Offer Degree:

Bioengineering

University of Washington

Abstract

Glycan polymeric prodrugs against pulmonary intracellular alveolar infections

Jasmin Chen

Chair of the Supervisory Committee:
Professor Daniel Ratner
Bioengineering

Intracellular pathogens are a major cause of global morbidity and mortality due to their complex and intricate ability to replicate within host cells while evading the innate immune defense system. Many intracellular pathogens, such as *F. tularensis* and *B. pseudomallei*, are highly infectious and can cause severe and fatal diseases. They are designated as Tier 1 select agents by the Centers for Disease Control and Prevention due to their high infectivity and mortality, transmission by pulmonary route of infection, and potential development as a bioweapon. Current antibiotics are limited by poor pharmacokinetic properties, and consequently require high frequency dosing at high concentrations to show promising clinical success. The physicochemical properties may also limit the route of administration of drugs – a critical factor to consider when select target tissues are of importance. To date, intravenous administration followed by oral tablets are the common routes of administration to deliver drugs; however, in a mass casualty setting, intravenous injections may not be practical. Therefore, new strategies are needed to improve the effectiveness of antibiotics in treating intracellular pulmonary infections.

This work utilizes RAFT polymerization techniques to explore synthetic multivalent glycopolymer prodrug systems. Prodrugs are inactive forms of the drug, but when administered undergo hydrolysis to release the pharmacologically active drug. We hypothesized that

engineering mannose glycopolymer prodrugs to target the macrophage mannose receptor on alveolar macrophage cells would eradicate or minimize bacterial replication and allow for better protection against intracellular infections.

We have demonstrated that our mannose polymeric prodrug systems provided significantly improved protection against intracellular *F. novicida* infection in mice challenge models compared to free antibiotic. When intratracheally administered to the lungs of mice in a prophylactic setting, poly(Man-co-CTM) improved survival in 50% of the mice and in a post-infection treatment setting, the survival of mice increased to 87.5%. In both studies, mice treated with free antibiotics remained ineffective. We also show that these results are due to the improved pharmacokinetic and pharmacodynamic properties of ciprofloxacin, in which targeted mannose polymer prodrugs had more than double elimination half-life time in the lungs compared to non-specific polymer prodrugs. We are excited about the promising results of the work presented here, but even more so at the modularity of the prodrug system such that it can be expanded and fine-tuned to be utilized for other diseases and applications.

Table of Contents

List of Figures

List of Tables

Preface: Motivation and specific aims

P.1. Research motivation

Infectious diseases continue to be a major threat to public health and are now spreading geographically much faster than at any time in history[1]. Focus on infectious diseases remains necessary to prevent global spread, enhance economic development, and increase health equity[2].

Burkholderia psuedomallei and *Francisella Tularensis* are intracellular bacteria which are the causative agents of melioidosis and tularemia, respectively. Both pathogens lead to severe systemic disease and sepsis, and have mortality rates ranging from 20-40% and rise to 80-95% for patients with septic shock despite appropriate antimicrobial therapy [3]. *B. pseudomallei* is a soil saprophyte endemic in northern Australia and northeast Thailand, while *F. tularensis* is found predominantly in the Northern Hemisphere[3,4]. Both pathogens infect the host by three potential routes: percutaneously, by ingestion, and by inhalation. However, the lung is involved in about 50% of clinical melioidosis cases[5]. Owing to the high mortality rates, low infectious doses, and severity of disease, both *B. pseudomallei* and *F. tularensis* are categorized by the Centers for Disease Control and Prevention (CDC) as potential Tier 1 select agents. Therefore, there is significant interest in the development of improved antimicrobial and prophylactic strategies to combat these pathogens.

Current clinical standards of care for melioidosis and tularemia involve treatment with antibiotics, including intravenous antibiotic therapy for 10-14 days, followed by 3-6 months of oral antibiotic therapy[6,7]. However, even with prolonged therapy, relapse and failure rates can range from 0-33%[8]. The challenges with current antibiotic therapy are largely due to the pathogenesis of these intracellular bacteria, in which they hide, reside, and proliferate for prolonged periods within phagocytic host immune cells[9]. Intravenous and oral administration lead to systemic dissemination of the antibiotics and limitations posed by the chemical properties of the antibiotics,

such as lack of specificity and the inability to cross cellular membranes and penetrate tissue, ultimately lead to laborious and exhaustive dosing regimens that may cause unwanted side effects. **To this end, there is a clinical unmet need for new drug delivery systems that address these current limitations.**

This research dissertation focuses on a modular approach towards the development of a targeted polymeric antibiotic prodrug system to combat intracellular pathogens. Carbohydrate-receptor mediated targeting on macrophage cells is investigated, and ultimately leveraged to evaluate the *in vivo* efficacy of this engineered prodrug system for treatment and prophylaxis.

P.2. Scientific Rationale

Utilizing the macrophage mannose receptor on alveolar macrophages as a route for targeted and intracellular delivery of ciprofloxacin prodrug polymers may enable prophylaxis and treatment of *F. tularensis* and *B. pseudomallei* infections. The goals of this research proposal are motivated by the following key observations:

First, alveolar macrophages (AMs) resident to the lung are the predominant effector cells of the pulmonary innate immune response. AMs express high levels of the mannose receptor CD206, a C-type lectin pattern-recognition receptor, that enables them to recognize pathogen-associated glycans, localize and isolate infectious events, and trigger adaptive immunity [10–12]. The calcium-dependent carbohydrate recognition domain (CRD) of the C-type lectins allows for high affinity carbohydrate binding[12,13].

Second, ciprofloxacin is a potent and broad-spectrum antibiotic used to treat most gram-negative and gram-positive bacteria. Ciprofloxacin has shown to penetrate most tissues compared to other antibiotics and accumulates in cells such as macrophages and neutrophils.

Ciprofloxacin disseminates to other organs such as liver, lungs, spleen, and lymph nodes which make it a good candidate to reach infections sites during intracellular bacterial infections[14,15]. However, ciprofloxacin does not preferentially accumulate at these tissues and cells of interest, has a terminal half-life of approximately 4 hours, and has extremely limited solubility in aqueous conditions[16].

Third, polymeric carriers and, more specifically, polymerizable drug monomers provide an attractive route for controlled-release drug delivery[17,18]. Sophisticated linkage chemistries and architectures allow for the development of disease-specific release strategies[19–20]. Recently, various drug linker designs were incorporated onto ciprofloxacin monomers and polymerized via reverse addition-fragmentation chain-transfer (RAFT) polymerization[21]. Drug release kinetics were studied and compared, in which phenolic ester linkages were shown to provide faster hydrolysis rates than aliphatic ester linkages.

Based on these observations, this research is motivated by the ultimate goal of designing and engineering a functional ciprofloxacin prodrug system capable of probing and targeting endogenous receptors on alveolar macrophages to promote intracellular delivery and ultimately combat intracellular pathogens either prophylactically or after the onset of infection.

P.3. Specific Aims

P.3.A Investigate carbohydrate receptor-mediated targeting via nano-structured glycopolymer functional liposomes

Hypothesis: Stealth liposomes augmented with synthetic multi-valent mannosylated glycopolymers will enhance intracellular uptake in macrophage cells via the macrophage mannose receptor, CD206, thereby presenting a promising strategy for targeted drug delivery.

Mannose receptors highly expressed on alveolar macrophages (AMs) are favorable targets for receptor-mediated delivery strategies. However, in-depth *in vitro* carbohydrate receptor-mediated studies in alveolar macrophages are complicated by limited access to primary alveolar macrophages. As a result, most studies are conducted using alternative primary cells or cell lines, even though cells obtained from disparate anatomical sites or cell lines differ phenotypically from one another[22,23]. The implications of cell phenotype on carbohydrate receptor expression and subsequent targeting are poorly understood and require further elaboration. To this end, we have synthesized and formulated multivalent mannose and galactose glycopolymer augmented liposomes to investigate and compare receptor-mediated uptake in various macrophage cell lines. The objective of this study is to explore and elucidate the carbohydrate receptor-targeting paradigm for molecular and nanomaterial delivery systems in *in vitro* alveolar macrophage models.

P.3.B Evaluate glycopolymer ciprofloxacin prodrugs towards targeting host alveolar macrophages

Hypothesis: Mannosylated ciprofloxacin prodrug polymers will improve the chemical property limitations of free ciprofloxacin. The CD206 receptor-mediated targeting, intracellular delivery, and sustained antibiotic release will also improve the efficacy of killing intracellular bacteria

compared to non-specific prodrug polymers. Polymeric carriers and, more specifically, polymerizable drug monomers provide an attractive route for controlled-release drug delivery[17,18]. Sophisticated linkage chemistries and architectures allow for the development of disease-specific release strategies[19–21]. To study the potential role of carbohydrate-receptors as an efficacious route for targeted drug delivery, ciprofloxacin-(phenol) methacrylates have been copolymerized with methacrylate mannose monomers to produce antibiotic prodrug polymers. The mannosylated ciprofloxacin prodrug polymers, along with non-specific analogs such as galactose and zwitterionic ciprofloxacin prodrug polymers will be investigated for their ability to kill intracellular bacteria.

P.3.C Demonstrate *in vivo* efficacy of glycopolymer ciprofloxacin prodrugs to combat intracellular pathogens in murine challenge models

Hypothesis: The receptor-mediated targeting and subsequent uptake of mannosylated ciprofloxacin prodrug polymers in alveolar macrophage cells will allow for better protection in murine challenge models nebulized with F.novicida. To study whether CD206 mediated targeting improves efficacy towards combating intracellular bacteria, the viability of infected mice administered with mannosylated ciprofloxacin prodrug polymers were compared with those administered with non-specific galactose prodrug polymers as well as free ciprofloxacin. We then evaluated the potential for the mannosylated ciprofloxacin prodrugs to act as prophylactic or post-exposure treatment via lethal *F. novicida* infected mice. Viability and bacterial counts in organs were evaluated and analyzed. Furthermore, biodistribution and pharmacokinetic studies were conducted to investigate whether the mannosylated prodrug polymers improve ciprofloxacin retention in mice compared to free ciprofloxacin administration.

Summary

My dissertation research combines synthetic carbohydrate chemistry and RAFT polymerization techniques with applied molecular and cellular biology to engineer and design functional multivalent neoglycopolymer prodrugs and drug delivery systems to investigate carbohydrate-receptor mediated targeting and uptake in macrophage cells. The ultimate goal is to leverage this knowledge and improve current limitations associated with free antibiotic treatment in order to efficiently combat intracellular pathogens. Current progress has shown that multivalent mannosylated glycopolymers increase intracellular uptake in macrophage cells significantly via CD206 interaction. We have also shown *in vitro* and *in vivo* that the macrophage mannose receptor is a promising route for targeting and uptake of antibiotics for efficient killing of intracellular pathogens. More importantly, when mice were lethally challenged with *F. novicida*, protection against infection was observed for mice treated with targeted mannose ciprofloxacin prodrug polymers whereas mice treated with free ciprofloxacin did not survive. This was ultimately due to the significantly improved pharmacokinetic and pharmacodynamic properties of ciprofloxacin in our polymer prodrug system. Retention of ciprofloxacin above the MIC for *F. tularensis* lasted 72 hours after a single dose administration, while peak serum concentrations were observed to be low to prevent systemic side effects. Overall, we present an inhalable targeted ciprofloxacin polymeric prodrug system that efficiently combats alveolar intracellular respiratory infections.

P.4. Preface References

1. World Health Organization. *World Health Report*. (2007). at <http://www.who.int/whr/2007/overview/en/index1.html>
2. De Cock, K. M., Simone, P. M., Davison, V. & Slutsker, L. The New Global Health. *Emerg. Infect. Dis.* **19,** (2013).
3. Cheng, A. C. & Currie, B. J. Melioidosis: epidemiology, pathophysiology, and

management. *Clin. Microbiol. Rev.* **18,** 383–416 (2005).
4. Tärnvik, A. & Berglund, L. Tularaemia. *Eur. Respir. J.* **21,** 361–373 (2003).
5. West, T. E., Myers, N. D., Liggitt, H. D. & Skerrett, S. J. Murine pulmonary infection and inflammation induced by inhalation of Burkholderia pseudomallei. *Int. J. Exp. Pathol.* **93,** 421–428 (2012).
6. Centers for Disease Control and Prevention. Melioidosis: Treatment. at <https://www.cdc.gov/melioidosis/treatment.html>
7. Prevention, C. for D. C. and. Tularemia: Diagnosis & Treatment. at <http://www.cdc.gov/tularemia/diagnosistreatment/>
8. Enderlin, G., Morales, L., Jacobs, R. F. & Cross, L. T. Streptomycin and alternative agents for the treatment of tularaemia; review of literature. *Clin. Infect. Dis.* **19,** 42–47 (1994).
9. Wiersinga, W. J., van der Poll, T., White, N. J., Day, N. P. & Peacock, S. J. Melioidosis: insights into the pathogenicity of Burkholderia pseudomallei. *Nat. Rev. Microbiol.* **4,** 272–82 (2006).
10. Zhang, J. *et al.* Negative regulatory role of mannose receptors on human alveolar macrophage proinflammatory cytokine release in vitro. *J. Leukoc. Biol.* **78,** 665–74 (2005).
11. Gordon, S. Alternative activation of macrophages. *Nat. Rev. Immunol.* **3,** 23–35 (2003).
12. Fraser, I. P., Koziel, H. & Ezekowitz, R. A. B. The serum mannose-binding protein and the macrophage mannose receptor are pattern recognition molecules that link innate and adaptive immunity. *Semin. Immunol.* **10,** 363–372 (1998).
13. Stahl, P. D. The mannose receptor and other macrophage lectins. *Curr. Opin. Immunol.* **4,** 49–52 (1992).
14. Nix, D. E., Goodwin, D., Peloquin, C. A., Rotella, D. L. & Schentag, J. J. Antibiotic tissue penetration and its relevance: models of tissue penetration and their meaning. *Antimicrob. Agents Chemother.* **35,** 1947–1950 (1991).
15. Bergan, T., Dalhoff, A. & Rohwedder, R. Pharmacokinetics of ciprofloxacin. *Infection* **16,** 3–13 (1988).
16. Hoffken, G., Lode, H., Prinzing, C., Borner, K. & Koeppe, P. Pharmacokinetics of ciprofloxacin after oral and parenteral administration. *Antimicrob. Agents Chemother.* **27,** 375–379 (1985).
17. Duncan, R. & Kopeček, J. Soluble synthetic polymers as potential drug carriers. *Adv. Polym. Sci.* **57,** 51–101 (2005).
18. Zhang, Y., Ma, L., Deng, X. & Cheng, J. Trigger-responsive chain-shattering polymers. *Polym. Chem.* **4,** 224–228 (2013).
19. Dizman, B., Elasri, M. O. & Mathias, L. J. Synthesis, characterization, and antibacterial activities of novel methacrylate polymers containing norfloxacin. *Biomacromolecules* **6,** 514–520 (2005).
20. Conejos-Sánchez, I. *et al.* Polymer-doxycycline conjugates as fibril disrupters: An approach towards the treatment of a rare amyloidotic disease. *J. Control. Release* **198,** 80–90 (2015).
21. Das, D. *et al.* RAFT polymerization of ciprofloxacin prodrug monomers for the controlled intracellular delivery of antibiotics. *Polym. Chem.* **7,** 826–837 (2015).
22. Murray, P. J. & Wynn, T. a. Protective and pathogenic functions of macrophage subsets. *Nat. Rev. Immunol.* **11,** 723–737 (2011).
23. Gordon, S. & Taylor, P. R. Monocyte and macrophage heterogeneity. *Nat. Rev. Immunol.* **5,** 953–964 (2005).

Acknowledgements

The thesis is the culmination of my research work over the past 4 years I have been in graduate school; however, the work presented was by no means done all by myself. Throughout the years, I have been fortunate and extremely thankful to have family, friends, mentors, coworkers, colleagues, and collaborators help me along this arduous journey – and I could not have gotten this far without them.

I would like to thank my adviser, Prof. Daniel Ratner, for the past 4 years since I have joined his lab. I came to Dan's lab fortuitously as I grew an immense passion for drug delivery. I had intended to conduct research in point-of-care diagnostics, but had a change of interest early in my graduate path. Dan trusted the naïve and inexperienced first-year me, and gave me the opportunity to work on drug delivery despite having minimal research experience in this field. I quickly came to acknowledge and respect Dan's sharp intelligence (especially in chemistry), and his ability to absorb new knowledge, but more importantly I appreciate his genuine curiosity and open optimism for research. I am extremely thankful for Dan's unique mentoring style – rather than having the conventional reserved boss-to-employee relationship, I felt as if we were partners or colleagues working to bud his drug delivery research group together. Because of his unique mentoring style, I have grown to become the independent and proactive researcher I am now. Altogether, I feel grateful for getting to know Dan and thankful for him advising me through the PhD.

This work would not have been possible if not for the support of our collaborators whose expertise was integral towards the success of the project. I would like to thank Prof. Patrick Stayton, who has given me the opportunity to work on such an interesting and exciting project. To learn from one of the most experienced investigators in drug delivery has been a unique and telling experience. I would also like to thank Dr. Anthony Convertine – the mastermind behind our intricate drug delivery systems. I have learned so much about RAFT polymerization, and that is all due to Dr. Convertine's patience in teaching the students. I would like to give special thanks to Dr. Hye-nam Son, who taught me a lot about cell and tissue culture experimental design. Her constant optimism and efficient time-management have inspired me to be a hard-working, yet positive researcher regardless of the countless failed experiments I have encountered. I am thankful to have had such an intelligent, patient, and supportive research mentor and partner. I would also like to thank Dr. Selvi Srinivasan, the person I can always go to for chemistry advice and guidance. Last, but certainly not least, I would like to thank our clinical collaborators, Dr. Shawn Skerrett and Dr. Eoin West, for their insightful and significant clinical input and

spearheading our many animal challenge studies. Without them, our *in vivo* challenge studies would not have been possible.

I also thank my Supervisory Committee for their advice and valuable feedback on my research direction: Prof. Dan Ratner, Prof. Patrick Stayton, Dr. David Danley, Dr. Eoin West, Prof. Kim Woodrow, and Prof. Cole DeForest. I appreciate all the time they have put to attending my committee meetings and for providing constructive feedback as well as providing challenging questions.

The work presented in this thesis reflects just one aspect of a much larger effort. Without the hard work of all the students and research technicians, we would not have the promising and exciting results we have today. I would like to thank colleagues Jojo Das and Ida Su for working together with me on this challenging project. Abby Kelly and previous postdoc Dr. David Chiu helped establish many of the *in vivo* toxicity studies as well as *in vitro* MIC bacterial studies that we all use for our current project. Research technicians from Dr. Shawn Skerrett's lab, Brian Lee and Frank Radella, have played an integral role in helping us complete our *in vivo* challenge studies. Many thanks to Dale Whittington and Scott Edgar from UW Department of Medicinal Chemistry's Mass Spec center for having the patience and expertise in teaching me all I know about LC-MS/MS. I would also like to thank my current and former undergraduate students, Taylor Monroe-Jones and Julia Swanson, for their hard-work and opportunity to practice mentorship.

Each and every encounter I have made with my previous mentors, small or large, has played a significant role at where I am today. I would like to thank my first research mentor, Dr. Kelly Trego for taking me in as her undergraduate research mentee, despite being a young sophomore with zero benchwork experience. Thank you for seeing potential in me and introducing the world of research to me. I would also like to thank my other undergraduate mentors, Dr. Leo Wan and Dr. John Waldeisen from Prof. Gordana Vunjak-Novakovic and Prof. Luke Lee's labs, respectively. Meeting them further instilled my passion for research and cemented my decision to pursue a PhD in bioengineering (but in the field of POC-diagnostics). I thank Prof. Paul Yager's wisdom and bountiful years of research experience. Despite a short rotation stay, he taught me the fundamentals of proper experimental design and motivated me to continually challenge myself. I would also like to thank Prof.. Suzie Pun for her amazing and awe-inspiring mentoring style and sharp intelligence. The short, yet impactful 10-week rotation in her lab opened doors to the drug delivery realm and inspired me to pursue my PhD thesis in drug delivery.

Finally, thanks to my support system for keeping me positive throughout this difficult yet fruitful journey. I would like to first thank my parents, Keyno and Cindy Chen, for their endless support and love. They have always emphasized the importance of a good education and the

opportunities that arise from hard work. The love and support I have received from them cannot be described in words, but I believe my thesis reflects the hard work and ambition they have instilled in me. A special thank you to my partner in crime (and climbing partner), Dr. Shin Inoue, for being there almost every step of the way. His unwavering love and encouragement has pulled me through the tough days. I am amazed at his unfazed optimism and cheerfulness, and this has made me become a better person and scientist. I would like to thank my best college friend, Winnie Wong, for being such a great friend and support despite being on the opposite end of the country from me. It has been with immense pleasure being able to pursue our PhD journeys together and to share the joys and struggles of graduate school. I would also like to thank my first and best friend in Seattle, Jia Jun Chia – I could not have asked for a better roommate to go bargain shopping with. Thanks to Jerry and Marsa Lee for the numerous delicious dinners and for introducing strategy boardgames to me. I would also like to acknowledge other friends who have been a part of this great support team: Dr. Kevin Tan, Dr. Susan Liu, Gary Liu (for long lunch and boba breaks), Dr. Ted Chen (thanks for all the 85˚C bread and drinks), Lige Tonggu (for learning top-rope with me), Karen Fong, Henry Cheung, Ritu Garg, the 2012 UW BioE grad cohort, and many others.

1. Chapter 1: Introduction

1. A. The threat of intracellular pathogens and select agents

The ability of many pathogenic bacteria to survive intracellularly after the invasion of host eukaryotic cells is crucial as the intracellular niche provides protection from several aspects of host immunity, such as antibodies and the complement. After entry into the target cells, bacteria are internalized within membrane-bound vesicles[1]. Under static conditions, the vacuole progressively acidifies and develops into degradative phagolysosomes; however, many intracellular pathogens are capable of surviving such conditions by initiating mechanisms that prevent vacuole-lysosome fusion, by modifying the environment within the phagosome, or by escaping the vacuole as a whole[2–4]. After escaping from the vacuole, the remaining stages of intracellular pathogens involve replication within the cytosol and manipulation of the innate immune response triggered in the cytosol[3]. Provided that the primary function of innate immune cells is to destroy pathogens, the survival of intracellular pathogens in the cytosol remains a paradox. Their complexity is why intracellular pathogens are a major cause of global morbidity and mortality, and as a result, they establish immediate medical precedence.

The severity of public threat posed by certain pathogens requires the Department of Health and Human Services to establish and regulate a list of biological agents and toxins that have potential to harm public health and safety (www.selectagents.gov). Certain select agents and toxins are further subcategorized as Tier 1 agents, in which they present the greatest risk of deliberate misuse with significant potential for mass casualties or may present devastating effects to the economy[5]. Two facultative intracellular bacteria, *Burkholderia pseudomallei* and *Francisella tularensis*, are classified as Tier 1 select agents and are the focus of infection models for this research dissertation.

1.A.1. Burkholderia Thailandensis and its pathogenicity

Soil saprophyte *B. thailandensis* is the causative agent of the tropical disease melioidosis and is endemic to regions of Southeast Asia, northern Australia, and northeast Thailand[6,7]. Melioidosis accounts for 20% of all community-acquired pneumonia and 40% of sepsis-related mortality in northeast Thailand[8]. The most severe clinical manifestation of melioidosis is septic shock which is associated with pneumonia, system-wide bacterial dissemination, and organ failure. Current treatment involves intravenous antibiotic therapy for 10-14 days, followed by 3-6 months of oral antibiotic therapy[9]. The overall mortality rate is 50%

in northeast Thailand of which 35% constitute children and 20% in the developed country of northern Australia[10].

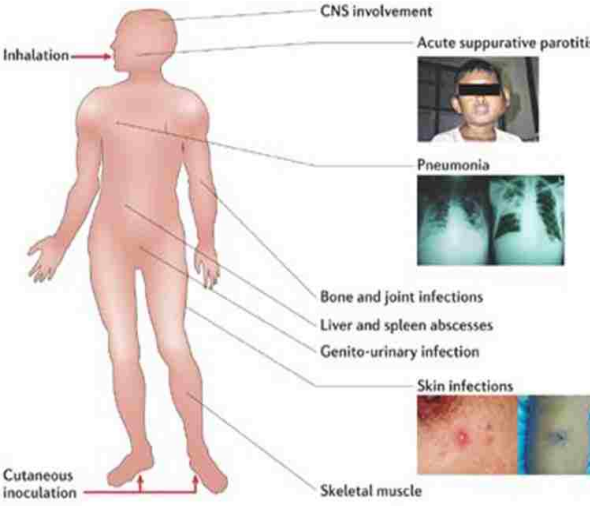

Figure 1-1 Clinical signs and symptoms of melioidosis. Melioidosis affects the entire host system. The most severe clinical manifestation is septic shock in which *B. pseodomallei* disseminates to distant sites such as the lungs, liver, and spleen. The lung, however, is the primary site of inhabitation in which pulmonary infection, chronic lung disease, abscess formation, empyema are some of the notable clinical signs and symptoms observed. Figure from [Wiersinga][10].

Individuals exposed to environments containing *B. pseudomallei* can be infected via percutaneous, ingestion, or inhalation routes. The lungs are the most commonly affected organ in adults. Bacterial localization and dissemination in the lungs lead to pulmonary infection, chronic lung disease, abscess formation, and empyema[6,8,10].

Cells of the innate immune system are the first to encounter and recognize foreign pathogens via pathogen-associated molecular patterns and pattern recognition receptors. *B. pseudomallei* survives and replicates within neutrophils and monocytes and utilizes multiple mechanisms to escape macrophage phagocytosis and evade host immunity[11]. Although there is no confirmed single mechanism for

intracellular survival of *B. pseudomallei*, multiple hypotheses have been observed and demonstrated. Some of the mechanisms of host evasion include resistance to human defensis and inhibition of DNA and protein synthesis within the host cell[11,12]. *B. pseudomallei* have also shown to have the ability to survive and grow in the acidic environments of phagolysosomes[13]. These bacteria can also lyse the endosome membranes within 15 minutes of internalization thereby escaping from endocytic vesicles into the cytoplasm[14]. Lastly, *B. pseudomallei* induce actin polymerization which results in membrane protrusions in host cells. The protrusions are then used to project into adjacent cells, ultimately leading to bacterial dissemination and infection[15]. The ability of *B. pseudomallei* to utilize the cytosol as a niche for replication and to evade the host innate immune response further highlights the importance for efficacious antimicrobial treatments.

1.A.2. *Francisella tularensis* and its pathogenicity

Francisella tularensis is a highly infectious intracellular pathogen and the causative agent of tularemia. As low as 25 colony-forming units can cause illness in 50% of individuals contacted, and half of these cases would result in a 25% case-fatality rate[16]. Tularemia is a zoonosis and spreads infection via rodents, hares, and rabbits[17]. The global incidence of tularemia resides in the northern hemisphere. After 3-5 days of bacterial incubation in a host, the onset of disease is rapid which includes clinical symptoms of fever, chills, malaise, sore throat, and headache[18].

Similar to *B. thailandensis* infection, individuals exposed to mammals infected with *F. tularensis* can acquire pathogens via percutaneous, ingestion, and inhalation routes. Those acquired through the skin or mucous membranes develop ulcerglandular tularemia in which primary ulcers develop at the site of infection. If ulcergladular tularemia is not treated with antibiotics within 7-10 days, lymph nodes enlarge and 30-40% of cases suppuration, or pus, develops. Infection by inhalation leads to respiratory tularemia in which *F. tularensis* subspecies

tularensis is the most dangerous form of tularemia, leading up to a case-fatality ratio of 30% if left untreated[18,19].

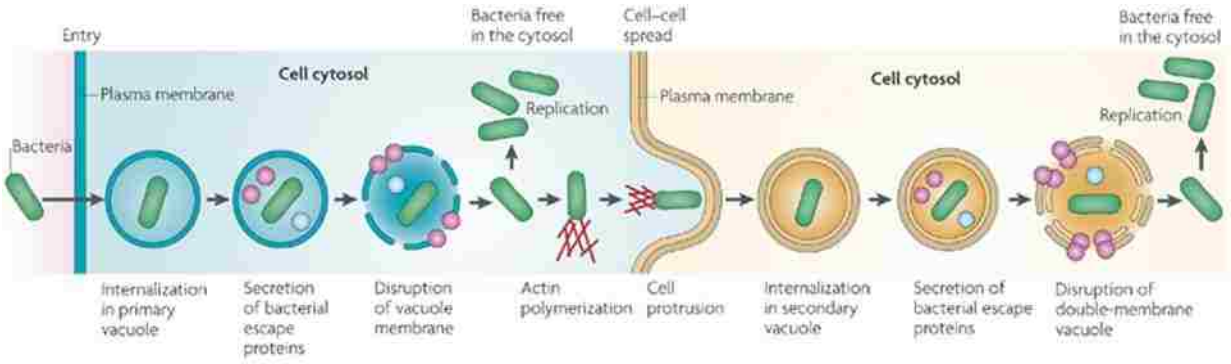

Figure 1-2 Intracellular bacteria encounter target host cells and are subsequently engulfed via primary vacuoles. The bacteria are able to escape the vacuoles and consequently, mature phago-lysosomes, by secreting facilitating proteins capable of disrupting vacuole membranes. Within the cytosol, bacteria replicate. Most intracellular bacteria, except *F. tularensis*, polymerize actin at the bacterial pole which enables intracellular as well as intercellular motility. The bacteria are then capable of disseminating the infection. Figure from [Ray][3].

F. tularensis primarily infect macrophage cells[20]. Upon entry into macrophages, bacteria are contained in the phagosomes in which they replicate; however, mechanisms by which *F. tularensis* are able to survive in these conditions remain unclear. Subsequent interactions between *F. tularensis* and macrophage cells depend on the activation state as well as the population-type of the macrophage. The phagosomal membrane degrades by acquiring fibrillary coatings on the cytoplasmic face which disintegrates the membrane, allowing the bacteria to escape the phagosomes and into the cytosol[21,22]. *F. tularensis* are notable for their fast replication rates in which the numbers of bacteria per cell can increase by 1.5-2.5 log within 24 hours of infection[22].

1.A.3. Current treatment regimens and limitations

With the introduction to antibiotics and antimicrobial treatment, mortality from tularemia has decreased from about 60% in severely ill patients with pneumonia or typhoidal disease to less than 5%[23,24]. Morbidity rates may also be minimized if effectively treated at early stages.

Therefore, antimicrobial therapy is the current standard method administered to patients suspected with tularemia; however, there are currently no specific antibiotic approaches or set regimens. Conventional approaches to treatment involve observational data trends of frequency of cure and relapse associated with different antimicrobial agents[25]. No controlled clinical trials have been conducted comparing different drug regimens or optimizing duration of therapy.

Historically, aminoglycosides, specifically streptomycin have generally been the drug of choice due to their high cure rate and minimal relapses[25]. However, streptomycin is now rarely used and is no longer readily available in many western European countries due to toxic side effects to the cochlea or auditory nerve and the vestibular system[25,26]. Streptomycin is still occasionally used in combination with drugs that penetrate the cerebrospinal fluid. Gentamicin, however, has become the alternative aminoglycoside[27]. Due to the exhaustive dosing regimen (7 to 14 days) of antimicrobial therapy, and the need for continuous monitoring of serum levels, aminoglycosides are now generally used only for severe cases of tularemia in which no alternative treatments are available.

Fluoroquinolones, particularly ciprofloxacin, have shown excellent microbiological and clinical success in treating *F. tularensis* infections in both children and adults[28–32]. Although tetracyclines such as doxycycline have excellent pharmacokinetic properties, some clinicians prefer fluoroquinolones given their lower likelihood of relapse[28,33,34]. Treatment failures of ciprofloxacin have been reported only when treatment was delayed for several weeks. Oral administration of ciprofloxacin has been noted as the preferred therapeutic strategy in a mass casualty setting[35,36].

Ciprofloxacin, however, presents several limitations. Due to poor aqueous solubility properties, ciprofloxacin is currently administered only via intravenous (I.V.) injections or oral tablets. Maximum serum concentrations for oral tablets are attained 1 to 2 hours after oral dosing and the serum elimination half-life in human patients with normal renal function is approximately 4 hours. Approximately 40 to 50% of orally administered ciprofloxacin is excreted in the urine as

unchanged drug, and complete urinary excretion occurs within 24 hours[37]. Although, both I.V. and oral administration of ciprofloxacin result in systemic distribution of the drug, no preferential accumulation at target tissues occurs therefore proper therapeutic levels at target tissue sites, such as the lungs, may not be reached.

1. B. The lung and the lower respiratory tract

The lungs are the largest organs in the lower respiratory tract and have a surface area of 90 m^2, which is greater than that of the gut and the skin[38]. The lower airway of the respiratory tract has a branched organization analogous to trees. The trachea is the largest tube in the respiratory tract and branches off into two bronchial tubes, which then branch into smaller secondary and tertiary bronchi. The bronchi further branch into smaller tubes known as the bronchioles. The bronchioles terminate into millions of highly vascularized and thin-walled alveoli, where gas exchange between oxygen and carbon dioxide occur. The distal airways filter approximately 8,000-9,000 liters of air every day and are consequently exposed to inhaled solid and liquid particles, allergens, and airborne microbes. Lung resident macrophages and dendritic cells (DCs) are the first-line of defense cells in charge of removing debris and pathogens. Crosstalk between anti-inflammatory macrophages, lung DCs, and airway epithelial cells are responsible for proper balance between clearance of the pathogen, repair of tissue, and restraint of inflammation[39].

1.B.1. The respiratory tract as a route of infection

The respiratory epithelium has mucosal surfaces that filter chronically exposed non-pathogenic and pathogenic antigens. The mucosa contains dense networks of DCs and macrophages which are strategically localized for antigen uptake within and beneath the surface epithelium[40]. T cells are also found in the mucosa in which they provide local “default” immune responses as non-imflammatory, T helper 2 cells. The columnar epithelium also has mucus and

ciliated cells, which constitute the mucociliary escalator. The secreted mucus containing trapped foreign particles are brought up from within the lungs into the oesophagus where material is coughed up or swallowed to the acidic environment of the stomach[41].

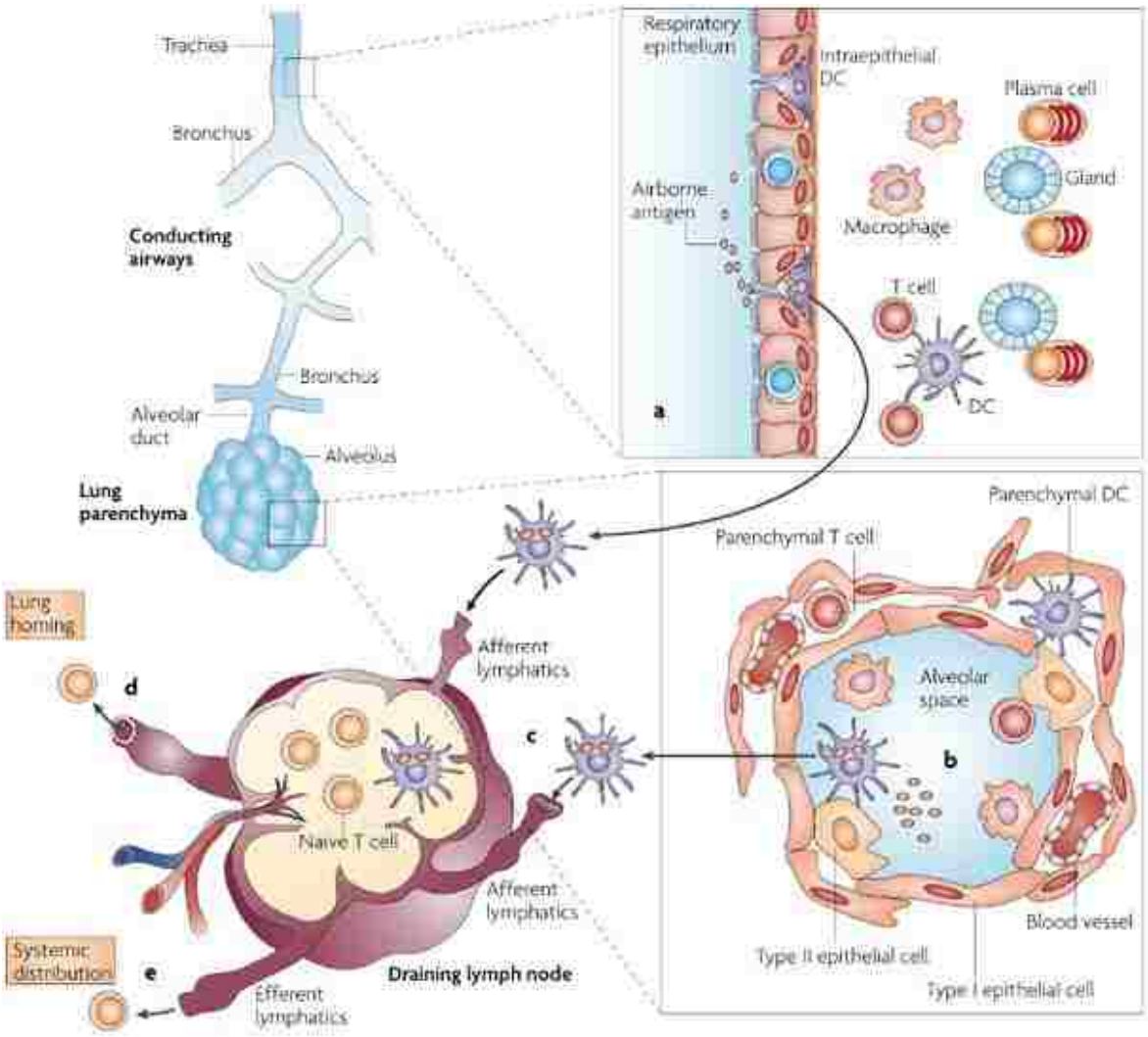

Figure 1-3 The lower respiratory tract comprises of a trachea which branches into the left and right bronchus, bronchioles, and alveoli. Lung resident immune cells, which include lung-resident macrophages and dendritic cells, capture airborne pathogens in which they present to naïve antigen-specific T cells. Activated T cells proliferate and migrate through the lymphatics and lymph nodes into the bloodstream. Figure from [Holt][40].

1.B.2. Function of alveolar macrophages in defense

The three predominant types of macrophages that reside in the lungs are bronchial macrophages, interstitial macrophages (IMs), and alveolar macrophages (AMs). Interstitial macrophages are located in the interstitium between adjacent alveoli, in which they interact with DCs and interstitial lymphocytes. IMs play a role in the immune response via antigen presentation to interstitial T cells and have also been shown to inhibit DC activation via IL-10[42]. Alveolar macrophages are found in the alveoli and constitute 90% of the cellular content in steady state[39]. The ontogeny and function of IMs, bronchial macrophages, and other lung resident macrophages are not well known and deem further studies.

In steady state mode, AMs balance the responses of alveolar epithelial cells, DCs, and lung T cells via phagocytosis, filtration of antigens, and production of IL-10 and transforming growth factor-β[43]. AMs also protect the host from inflammatory acute lung injury via intercommunication of sessile AMs located in different alveoli. Gap junctions are formed with alveolar epithelial cells (AECs) and AMs subsequently synchronize calcium release to balance the recruitment of neutrophils to the alveoli thereby inhibiting inflammation[44]. Another mechanism by which AMs prevent inflammatory responses is through receptor and ligand interaction between AMs and AECs respectively[45,46].

In the presence of pathogens, AMs are the first line of innate cellular defense in the lower airways. They are attached to AECs and encounter microbes that are transported to the alveoli via alveolar liquid flow[44]. The key roles that AMs play in immunity are defending against pathogens and immunological homeostasis after infection-mediated damage[40]. AMs are essential for the clearance of fungal and bacterial lung infections due to their phagocytic ability[47]. Despite the quiescent state of AMs during steady state, they are capable of producing low amount of pro-inflammatory cytokines, but more importantly, can be activated in response to extrinsic and intrinsic stimuli such as cytokines, microorganisms, and particulates. This activation shifts the role

of AMs into effector cells which increases their functionality in phagocytosis, killing, and coordination of innate immune responses[48].

The polar extremes of macrophage activation are classified into two groups: M1 and M2. M1 and M2 macrophages differ in receptor expression, cytokine and chemokine expression, and effector functions. M1 macrophages are microbicidal and pro-inflammatory whereas M2 macrophages are immunomodulators and anti-inflammatory[49]. In actuality, macrophage polarization or activation involve a highly complex gradient of functional states. The plasticity of macrophages enables them to constantly and rapidly play roles in both inflammation and immunosuppression. In the context of infectious diseases and bacterial infections, the M1 activation state is usually associated with acute infectious diseases[50]. However, prolonged M1 states may be dangerous for the host as M1 programs have been shown to relate to the onset of sepsis as production of type I cytokines and chemokines activate the endothelium and contribute to cardiac failure, loss of organ perfusion, and death[51,52]. The M2 activation state is usually associated with chronic infectious diseases in which interleukin (IL)-10 and IL-4 are involved[50].

1.B.3. Pulmonary drug delivery

Pulmonary inhalation of medications dates back to before the Common Era. However, utilizing this method as a route of administration for drug delivery has been sparse. Prior to the approval of the first inhaled insulin, pulmonary delivery was doubtful as it seemed impractical, complex, inefficient and unreliable, and its safety was unknown. Recent developments have emerged since, including Pfizer's recombinant DNA human insulin powder to treat both type I and type II diabetes[53].

The large surface area of the lung, good epithelial permeability, and vast dispersion of aerosols allow for rapid systemic absorption and delivery of small molecules via pulmonary administration and inhalation[54]. This leads to high bioavailabilities of small molecules[55,56]. In contrast to oral delivery, inhaled drugs are less likely to be degraded because the lungs have

lower drug-metabolizing enzymes than the gastrointestinal tract and the liver[57]. The rapid absorption and systemic dissemination, however, result in rapid clearance, thereby limiting inhalation as a route of small molecule drug delivery. Current strategies in pulmonary drug delivery design need to be modified to allow for slower adsorption, and ultimately, increased systemic circulation.

Year	Formulation/device	Molecule(s)	Disease
1500 BC	Egyptians used 'vapors'	?	?
1662 AD	Bennet's inhalation treatment	?	Tuberculosis
1802	Potter's cigarettes	?	Asthma
1860	Sales-Giron's portable nebulizer	?	?
1925	Aqueous/nebulizer	Insulin	Diabetes
1945	Aqueous/nebulizer	Penicillin	Lung infections
1951	Aqueous/nebulizer	Isoprenaline	Asthma
1955	Aqueous/nebulizer	Hydrocortisone	Asthma
1956	First metered-dose inhaler (MDI) (freon)	Albuterol	Asthma
1960	First dry powder inhaler (DPI)	Norsadrenaline	Asthma
1988	First multidose DPI	Terbutaline	Asthma
1996	First protein aqueous/nebulizer	DNAse	Cystic fibrosis
1998	First antibiotic aqueous/nebulizer	Tobramycin	Cystic fibrosis
1997	First hydrofluoralkane MDI	Albuterol	Asthma
2006	First protein DPI	Insulin	Diabetes

Figure 1-4 Inhaled medicines. Figure from [Patton][53].

A variety of mechanisms may be altered to increase the lung retention time. Increasing hydrophobicity can improve lung retention for hours, days, and possibly weeks due to tissue binding[58]. Drug molecules with log octanol-water partition coefficients greater than 1 are absorbed rapidly; however decreasing the log octanol-water partition coefficient to -1 or lower can increase the half-life[59]. Lipophilic compounds with positive charge under physiological conditions have also

shown to bind to lung tissue[60]. Another way to increase lung retention in aerosol delivery is increasing the molecular mass of the drug via conjugation or polymerization to water-soluble molecules or ligands, such as polyethylene glycol or carbohydrate structures. The lung epithelium has transport mechanisms for molecules as large as 160 kDa. Although small molecules can be absorbed in seconds, soluble higher-molecular weight systems may be absorbed in hours, days, and possibly weeks.

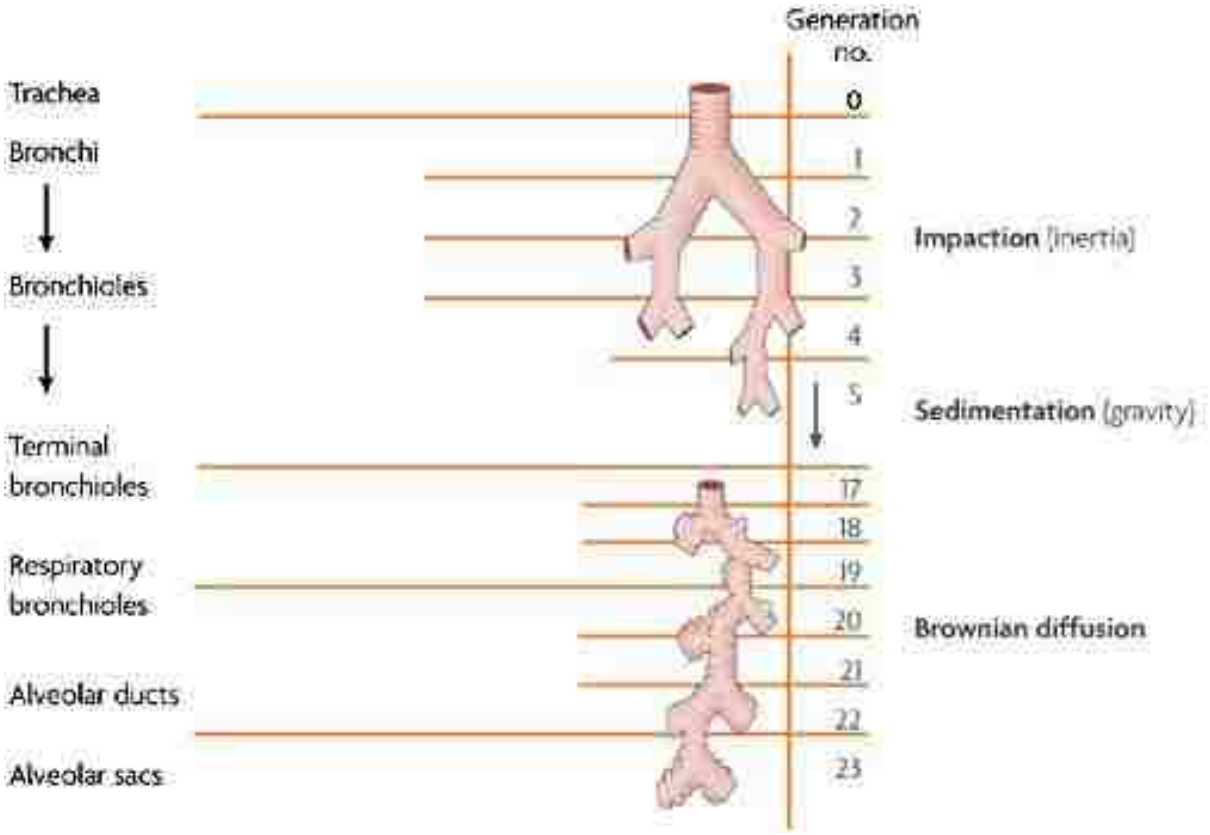

Figure 1-5 The force that dominates the motion of particles is the key factor that determines the deposition of inhaled particles. Larger particles deposit in the upper airways as their inertial force allows them to overcome the streamlines of lung flow. Impaction clears these larger particles. Smaller particles sediment to the middle airways via gravitational sedimentation. Small particles are governed by Brownian diffusion and deposit in the alveolar region. Figure from [Patton][53].

1C. Exploitation of the macrophage mannose receptor in infectious disease therapeutics

Macrophage cells express surface receptors that regulate a myriad of functions including differentiation, growth and survival, adhesion, migration, phagocytosis, activation, and cytotoxicity. Their ability to recognize endogenous and exogenous ligands are key roles to homeostasis and host defense in innate and adaptive immunity[61]. Opsonins such as Toll-like receptors and Nod-like receptors have been extensively studied[62,63]; however, macrophages also express non-opsonic receptors which mediate phagocytosis, such as the mannose receptor.

The macrophage mannose receptor (CD206) is a transmembrane glycoprotein known for its selective binding to mannose structures, although it has been shown to also bind fucose and N-acetylglucosamine. CD206 contains eight C-type lectin-like domains (CTLDs or CRDs) which have protein conformations containing two α-helices and two antiparallel β-sheets and are Ca^{2+} dependent to enable carbohydrate recognition. CRDs 4-8 have been shown to be the CRDs responsible for high-affinity binding[64,65]. It is a recycling receptor present in the endocytic compartment, and its cytoplasmic tail contains two internalization motifs. The main role of CD206 seems to be phagocytosis and physiological clearance. Aside from clearing endogenous high mannose *N*-linked glycoproteins, CD206 plays key roles in pathogen recognition and antigen presentation[66,67]. The macrophage mannose receptor is upregulated by IL-4 and IL-10 and is downregulated by IFN-γ[68].

1.C.1 CD206 and pathogen recognition

The macrophage mannose receptor recognizes a variety of Gram-negative and Gram-positive bacteria, yeasts, parasites, and mycobacteria. The expression of CD206 correlates with the activation state of macrophage cells[50]. One of the best characterized CD206 expression modulators during innate immunity is IFN-γ, in which receptor expression is downregulated. It was

shown that IFN-γ induced human monocyte-derived macrophages increased their capacity to phagocytose and kill *Candida albicans* despite the downregulation of CD206. It is hypothesized that with the induction of IFN-γ, enhanced coupling between CD206 and the microbes occurs[69]. Surprisingly, Th2 cytokine IL-4, which usually antagonizes the responses of IFN-γ, counteracts with IFN-γ to increase CD206 expression. This may indicate that during inflammation, the two cytokines signal for both clearance of bacteria and tissue remodeling[67]. The mannose receptor also plays a role in adaptive immunity via antigen recognition and presentation. It has been shown that once antigens are bound to the CRDs they are directed to appropriate effector cells via the cysteine-rich domain. It is hypothesized that a cleaved soluble form of the receptor with antigen bound go to lymphoid organs and interact with ligands which recognize the cysteine-rich region[70].

Phagocytosis is an extremely complex process in which no single model can fully explain the structures, mechanisms, and signal of events associated with particle internalization. Despite the complexity of phagocytosis, several fundamental events occur. First, in order for internalization to occur, specific cell-surface receptors need to interact with ligands on the surface of the particles. Second, actin polymerization at the site of internalization occurs via an actin-based mechanism. Then, actin sheds from the phagosome as it matures by a series of fusion and fission events with components of the endocytic pathway, ultimately forming mature phagolysosomes[47]. The macrophage mannose receptor is a pattern recognition receptor that has high affinity for multivalent mannosylated oligosaccharides, or pathogen-associated molecular patterns, which make it a phagocytic receptor with broad pathogen specificity.

1.C.2 Rationale for CD206 targeting

The mannose receptor presents a promising route for targeted drug delivery. Aside from its non-opsonic phagocytic properties and the fact that CD206 is expressed at high levels on macrophages, several other functions and abilities of CD206 allow for an encouraging and relatively new route of targeted drug delivery.

The multiple CRDs in the extracellular domain of macrophage cells cooperate to achieve high affinity binding to complex ligands. Individual CRDs have demonstrated weak affinity for single sugars, while clustering of CRDs achieves high affinity binding to oligosaccharides. Rather than oligomerization of multiple polypeptides each with a single CRD, the mannose receptor has multiple interactions that are achieved through having multiple active CRDs in a single polypeptide[65]. The affinity for oligosaccharides is in the micromolar range as a result of the binding of multiple sugar units to extended binding sites on the receptors. Binding at the secondary binding subsites is driven by favorable enthalpy, while entropy costs are also decreased due to a decrease in the overall motion and conformational freedom from the oligosaccharide that has already been bound at the primary binding site[71]. Multivalency has shown to lead to significantly higher binding affinities[72], thereby allowing synthetic strategies such as glycopolymers to be utilized for targeted drug delivery.

The mannose receptor is a rapid recycling receptor, thereby allowing significantly greater amounts of particles internalized. Research has shown that following internalization, receptors are continually recycled back to the cell surface, or that a group of CD206 stays present within cells and is rapidly and continually replacing those which have been internalized. Internalization of prebound ligand occurs very rapidly at 37ºC ($t_{1/2}$ < 5 min) and following internalization, binding activity is rapidly recovered ($t_{1/2}$ < 5 min)[73]. Enhanced uptake may lead to smaller required doses of drugs or therapies sufficient for clinical effects, thereby reducing the toxicity of administered substances.

A common point of concern in drug delivery with internalization processes is the ability to escape the acidic and degradative environment of late-stage phagosomes and lysosomes. Interestingly, internalization via the mannose receptor may bypass or delay phagosome maturation. It has been shown that Hck may serve as a useful marker for phagosomal maturation after the fusion with LAMP-1 vesicles. CD206-dependent phagocytosis of mannosylated particles led to fusion with LAMP-1 but not Hck-carrying vesicles and CD206 did not trigger activation of

Hck. This most likely meant that particles taken up via CD206 did not allow maturation of phagosomes to proceed to fusion with Hck-positive vesicles[74]. Another study demonstrated similar results, such that silica beads coated with glycopeptidolipids for CD206 internalization showed limited acidification and delayed recruitment of late endosomal and lysosomal markers. Beads not coated with carbohydrates failed to delay phagosome-lysosome fusion[75]. These results provide exciting motivation for the development of CD206 targeted drug delivery systems.

1.D. Bioengineering glycopolymer drug delivery systems to combat intracellular pathogens

Owing to the fact that receptor-saccharide interactions are significantly amplified by the increase of sugar density via multivalent interactions, or the "glyco-cluster" effect, various well-defined glycopolymers and glycosylated carriers have been a major focus towards achieving biologically functional drug delivery systems. Monomeric interactions with receptors are generally weak due to weak interactions including hydrogen bonds, hydrophobic interactions, and electrostatic interactions[76]. Lee and Lee reported one of the first results of the glycoside cluster effect, in which a lectin with clustered sugar binding sites and a multivalent ligand that presents proper orientation and spacing are required for the strong cluster effect to occur[77]. Various divalent and trivalent complex-type N-acetylgalactosamine oligosaccharide structures were tested to bind to hepatic lectins. Divalent oligosaccharide K_d values were in the range of 1-40μM and those of trivalent structures were in the range of 10-100nM[78]. Not only do glycosylated carriers exhibit biological functionality, but these synthetic materials are generally water-soluble, highly polar, and biocompatible[79].

1.D.1 Reversible addition-fragmentation chain transfer (RAFT) polymerization

Polymers have been of critical importance in the advancement and development of drug delivery technologies. Low drug solubility, drug degradation, drug toxicity, and rapid-clearance

from the body are some of the obstacles encountered; however, synthetic polymer techniques have thus allowed researchers to overcome these limitations. Modern advances in drug delivery entail rational design of polymers tailored for specific biological functions and environments. Some of the advancements made via polymer chemistry include controlled release of therapeutic agents in constant doses over long periods of time, cyclic dosages, tunable release of both hydrophilic and hydrophobic drugs, polymer-therapeutic conjugates, and molecular recognition and intracellular delivery[80].

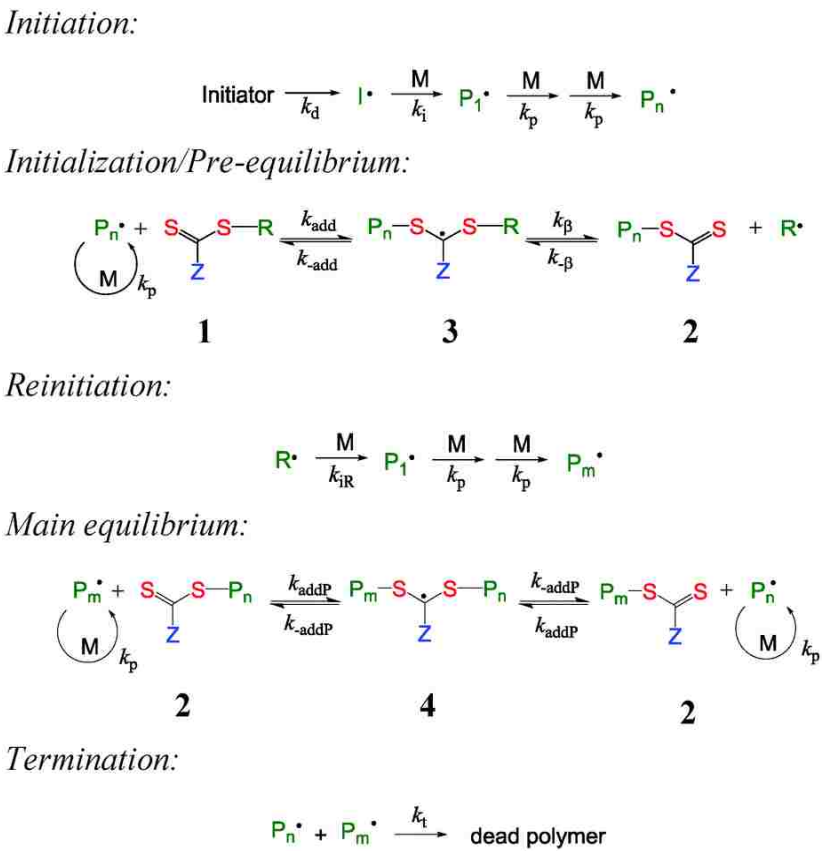

Figure 1-6 Mechanism for reversible addition-fragmentation chain transfer (RAFT) depicting the equilibria of the CTA.

Traditional chain-growth polymerization is capable of utilizing a wide array of vinyl-containing monomers with unique chemical functionalities, but is limited to a broad range of molecular weight distributions, making it unsuitable for conditions needing more precisely

controlled polymers. Controlled, or "living" radical polymerization enables control over the polymer architecture, which includes molecular weight, polydispersity, functionality, and composition. The occurrence of premature termination is also minimized, and molecular weight proceeds linearly with time until monomers are consumed[81]. One fundamental "living" polymerization technique is reversible addition-fragmentation chain transfer (RAFT) polymerization, which has very high versatility and compatibility with a wide range of monomers and reaction conditions[82]. What distinguishes RAFT polymerization from other techniques is the use of a chain transfer agent (CTA) which allows for reversible deactivating propagating radicals and rapid equilibria between active and dormant chains, thereby maintaining the living character of the polymerization[81]. In brief, the CTA, which typically contains a thiocarbonylthio group, facilitates uniform polymer chain growth by forming intermediate radicals equally shared between two propagating polymer chains. This intermediate can fragment in either direction causing chains to have equal opportunities for growth and ultimately narrow polydispersity[83,84].

1.D.2 Glycopolymers in drug delivery

A myriad of glycosylated drug carriers have been designed for a variety of therapeutic applications. In extensive reviews covered by multiple researchers, the majority of glycosylated delivery systems involve liposomal constructs[85,86]. Despite their promising clinical relevance, liposomal delivery systems have displayed several limitations, such as low drug loading efficiencies, burst release of drug content, stability issues, batch to batch irreproducibility, and poor sterilization methods for manufacturing[87,88]. Glycopolymers provide an alternative to liposomes as promising drug delivery carriers. Various polymerization techniques have been developed to synthesize glycopolymers, such as living ionic polymerization, ring opening polymerization, ring opening metathesis polymerization, click chemistry, post-polymerization glycoconjugation, ATRP, NMP, and RAFT[76,79]. Recent advances in synthetic polymer chemistry, such as living polymerization, have encouraged the synthesis of precise and complex

glycopolymers. Glycopolymers are prepared by direct polymerization of saccharide derived monomers with polymerizable functional groups such as vinyl, or a two-step reaction occurs, such that polymerization with reactive functional groups is first synthesized and a post-glycan conjugation step occurs[76]. Most polymerization techniques involve protective carbohydrate chemistry in which a post-polymerization deprotection step is required. RAFT polymerization enables polymerization in aqueous conditions, thereby bypassing protective chemistry[89,90]. Utilizing RAFT polymerization, various polymer architectures have been synthesized such as block copolymers for micellar constructs. For example, a double-hydrophilic hydroxyethylmethacrylate and N-acetylglucosamine diblock was synthesized to form homogenous self-assembled spherical micelles in water[91]. Star polymers, nanocarbon conjugates, and polymer brushes are some of the many complex architectures synthesized[76].

1.D.3 Prodrug-based nanoparticle systems

Approximately 5-7% of all approved drugs worldwide are classified as prodrugs[92]. Prodrugs are biologically inert derivatives of drug molecules that undergo chemical or enzymatic reactions to release the active parent drug. Over the years, prodrugs have become an established strategy to improve physiochemical, biopharmaceutical, and pharmacokinetic properties of otherwise promising drug candidates. They have shown to overcome challenging barriers in drug formulation and delivery such as poor aqueous solubility, chemical instability, rapid systemic metabolism, toxicity, and drug targeting[93].

More recently, integration of prodrug strategies with nanotechnology strategies have become notable. Current prodrug-based carrier systems can be categorized into three types: nanosystems based on polymer-drug conjugates in which drug molecules are covalently conjugated to polymers, small amphiphilic self-assembly molecular weight prodrugs, and prodrug-encapsulated nanosystems[94]. The common polymers utilized in the synthesis of polymer-drug conjugates include block copolymers, dendritic polymers, and comb-like polymers. Several

polymer-drug conjugates have undergone clinical trials, such as a Phase I study with SN-38, a chemotherapeutic drug, conjugated to PEG-poly(glutamic acid) copolymers[95]. The prodrug-polymer micelles demonstrated sustained release and exhibited linear pharmacokinetics. A similar Phase I study was conducted with doxorubicin conjugated PEG-poly(aspartic acid) copolymers[96]. Recently, polymerizable ciprofloxacin and norfloxacin prodrug monomers have been synthesized bypassing the need for post polymerization conjugation reactions[97,98]. Both studies demonstrated antibacterial efficacy *in vitro* and sustained drug release. These initial results provide exciting room for improvement or modifications, such as the addition of targeting moieties.

1.E. Chapter 1 References

1. Cossart, P. & Sansonetti, P. J. Bacterial Invasion: The Paradigms of Enteroinvasive Pathogens. *Science (80-.).* **304,** 242–248 (2004).
2. Haas, A. The phagosome: Compartment with a license to kill. *Traffic* **8,** 311–330 (2007).
3. Ray, K., Marteyn, B., Sansonetti, P. J. & Tang, C. M. Life on the inside: the intracellular lifestyle of cytosolic bacteria. *Nat. Rev. Microbiol.* **7,** 333–340 (2009).
4. Kumar, Y. & Valdivia, R. H. Leading a Sheltered Life: Intracellular Pathogens and Maintenance of Vacuolar Compartments. *Cell Host Microbe* **5,** 593–601 (2009).
5. General FAQ's about select agents and toxins. *Federal Select Agent Program* (2014).
6. Cheng, A. C. & Currie, B. J. Melioidosis: epidemiology, pathophysiology, and management. *Clin. Microbiol. Rev.* **18,** 383–416 (2005).
7. West, T. E., Myers, N. D., Liggitt, H. D. & Skerrett, S. J. Murine pulmonary infection and inflammation induced by inhalation of Burkholderia pseudomallei. *Int. J. Exp. Pathol.* **93,** 421–428 (2012).
8. White, N. J. Melioidosis. *Lancet* **361,** 1715–1722 (2003).
9. Centers for Disease Control and Prevention. Melioidosis: Treatment. Available at: https://www.cdc.gov/melioidosis/treatment.html.
10. Wiersinga, W. J., van der Poll, T., White, N. J., Day, N. P. & Peacock, S. J. Melioidosis: insights into the pathogenicity of Burkholderia pseudomallei. *Nat. Rev. Microbiol.* **4,** 272–82 (2006).
11. Jones, A. L., Beveridge, T. J. & Woods, D. E. Intracellular survival of Burkholderia pseudomallei. *Infect.Immun.* **64,** 782–790 (1996).
12. Mohamed, R., Nathan, S., Embi, N., Razak, N. & Ismail, G. Inhibition of macromolecular synthesis in cultured macrophages by Pseudomonas pseudomallei exotoxin. *Microbiol. Immunol.* **33,** 811–820 (1989).
13. Dejsirilert, S., Kondo, E., Chiewsilp, D. & Kanai, K. Growth and survival of *Pseudomonas pseudomallei* in acidic environments. *Japanese J. Med. Sci. Biol.* **44,** 63–74 (1991).
14. Harley, V. S., Dance, D. A., Drasar, B. S. & Tovey, G. Effects of Burkholderia pseudomallei and other Burkholderia species on eukaryotic cells in tissue culture. *Microbios* **96,** (1998).
15. Kespichayawattana, W., Rattanachetkul, S., Wanun, T., Utaisincharoen, P. & Sirisinha, S.

Burkholderia pseudomallei induces cell fusion and actin-associated membrane protrusion: A possible mechanism for cell-to-cell spreading. *Infect. Immun.* **68,** 5377–5384 (2000).
16. *Health Aspects of Chemical and Biological Weapons*. *World Helath Organization* (1970).
17. Morner, T. The ecology of tularemia. *Rev. Sci. Tech.* **11,** 1123–1130 (1992).
18. Evans, M. E., Gregory, D. W., Schaffner, W. & McGee, Z. A. Tularemia: a 30-year experience with 88 cases. *Med.* **64,** 251–269 (1985).
19. Dienst, J. F. T. Tularemia — a perusal of three hundred thirty-nine cases. *J. La State Med. Soc.* **115,** 114–127 (1963).
20. Anthony, L. S. D., Burke, R. D. & Nano, F. E. Growth of Francisella spp. in rodent macrophages. *Infect. Immun.* **59,** 3291–3296 (1991).
21. Clemens, D. L., Lee, B. Y. & Horwitz, M. A. Virulent and avirulent strains of Francisella tularensis prevent acidification and maturation of their phagosomes and escape into the cytoplasm in human macrophages. *Infect. Immun.* **72,** 3204–3217 (2004).
22. Golovliov, I., Baranov, V., Krocova, Z., Kovarova, H. & Sjöstedt, A. An attenuated strain of the facultative intracellular bacterium Francisella tularensis can escape the phagosome of monocytic cells. *Infect. Immun.* **71,** 5940–5950 (2003).
23. Thomas, L. & Schaffner, W. Tularemia pneumonia. *Infect Dis Clin North Am* **24,** 43 (2010).
24. Tärnvik, A. & Chu, M. C. New approaches to diagnosis and therapy of tularemia. *Ann N Y Acad Sci* **1105,** 378–404 (2007).
25. Enderlin, G., Morales, L., Jacobs, R. & Cross, J. Streptomycin and alternative agents for the treatment of tularemia: review of the literature. *Clin. Infect. Dis.* **19,** 42 (1994).
26. Gardner, J. C. *et al.* Familial streptomycin ototoxicity in a South African family: a mitochondrial disorder. *J. Med. Genet.* **34,** 904–906 (1997).
27. Hepburn, M. J. & Simpson, A. J. H. Tularemia: current diagnosis and treatment options. *Expert Rev. Anti. Infect. Ther.* **6,** 231–240 (2008).
28. Meric, M. *et al.* Evaluation of clinical, laboratory, and therapeutic features of 145 tularemia cases: the role of quinolones in oropharyngeal tularemia. *APMIS* **116,** 66 (2008).
29. Limaye, A. P. & Hooper, C. J. Treatment of tularemia with fluoroquinolones: two cases and review. *Clin. Infect. Dis.* **29,** 922 (1999).
30. Chocarro, A., Gonzalez, A. & Garcia, I. Treatment of tularemia with ciprofloxacin. *Clin. Infect. Dis.* **31,** 623 (2003).
31. Johansson, A., Berglund, L., Gothefors, L., Sjostedt, A. & Tarnvik, A. Ciprofloxacin for treatment of tularemia in children. *Pediatr. Infect. Dis. J.* **19,** 449–453 (2000).
32. Perez-Castrillon, J. L., Bachiller-Luque, P., Martin-Luquero, M., Mena-Martin, F. J. & Herreros, V. Tularemia epidemic in northwestern Spain: clinical description and therapeutic response. *Clin. Infect. Dis.* **33,** 573–576 (2001).
33. Tärnvik, A. & Berglund, L. Tularemia. *Eur. Respir. J.* **21,** 361–373 (2003).
34. Eliasson, H., Broman, T., Forsman, M. & Bäck, E. Tularemia: current epidemiology and disease management. *Infect Dis Clin North Am* **20,** 289–311 (2006).
35. Dennis, D. T. *et al.* Tularemia as a biological weapon: medical and public health management. *JAMA* **285,** 2763–2773 (2001).
36. Oyston, P. C., Sjostedt, A. & Titball, R. W. Tularaemia: bioterrorism defence renews interest in Francisella tularensis. *Nat Rev Microbiol* **2,** 967–978 (2004).
37. CIPRO® (ciprofloxacin hydrochloride) Tablets. Drug Fact Sheet. *Bayer Pharmaceuticals Corporation* (2004). Available at: http://www.fda.gov/downloads/Drugs/EmergencyPreparedness/BioterrorismandDrugPreparedness/UCM130802.pdf.
38. Revoir, W. H. & Bien, C.-T. Respiratory Protection Handbook. *CRC Press* (1997).

39. Kopf, M., Schneider, C. & Nobs, S. P. The development and function of lung-resident macrophages and dendritic cells. *Nat Immunol* **16,** 36–44 (2015).
40. Holt, P. G., Strickland, D. H., Wikström, M. E. & Jahnsen, F. L. Regulation of immunological homeostasis in the respiratory tract. *Nat. Rev. Immunol.* **8,** 142–152 (2008).
41. Rawlins, E. L., Ostrowski, L. E., Randell, S. H. & Hogan, B. L. M. Lung development and repair: contribution of the ciliated lineage. *Proc. Natl. Acad. Sci. U. S. A.* **104,** 410–7 (2007).
42. Bedoret, D. *et al.* Lung interstitial macrophages alter dendritic cell functions to prevent airway allergy in mice. *J. Clin. Invest.* **119,** 3723–3738 (2009).
43. MacLean, J. a *et al.* Sequestration of inhaled particulate antigens by lung phagocytes. A mechanism for the effective inhibition of pulmonary cell-mediated immunity. *Am. J. Pathol.* **148,** 657–666 (1996).
44. Westphalen, K. *et al.* Sessile alveolar macrophages communicate with alveolar epithelium to modulate immunity. *Nature* **506,** 503–506 (2014).
45. Gardai, S. J. *et al.* By binding SIRPα or calreticulin/CD91, lung collectins act as dual function surveillance molecules to suppress or enhance inflammation. *Cell* **115,** 13–23 (2003).
46. Snelgrove, R. J. *et al.* A critical function for CD200 in lung immune homeostasis and the severity of influenza infection. *Nat. Immunol.* **9,** 1074–1083 (2008).
47. Aderem, A. & Underhill, D. M. Mechanisms of phagocytosis in macrophages. *Annu. Rev. Immunol.* **17,** 593–623 (1999).
48. Underhill, D. & Ozinsky, A. Phagocytosis of Microbes: Complexity in Action. *Annu. Rev. Immunol.* **20,** 825–852 (2002).
49. Mosser, D. M. & Edwards, J. P. Exploring the full spectrum of macrophage activation. *Nat. Rev. Immunol.* **8,** 958–69 (2008).
50. Benoit, M., Desnues, B. & Mege, J.-L. Macrophage polarization in bacterial infections. *J. Immunol.* **181,** 3733–3739 (2008).
51. Lopez-Bojorquez, L. N. *et al.* Molecular Mechanisms Involved in the Pathogenesis of Septic Shock. *Arch. Med. Res.* **35,** 465–479 (2004).
52. Bozza, F. a *et al.* Cytokine profiles as markers of disease severity in sepsis: a multiplex analysis. *Crit. Care* **11,** R49 (2007).
53. Patton, J. S. & Byron, P. R. Inhaling medicines: delivering drugs to the body through the lungs. *Nat Rev Drug Discov* **6,** 67–74 (2007).
54. Patton, J. S. Mechanisms of macromolecule absorption by the lungs. *Adv. Drug Deliv. Rev.* **19,** 3–36 (1996).
55. Brown, R. A. J. & Schanker, L. S. Absorption of aerosolized drugs from the rat lung. *Drug Metab. Dispos.* **11,** 355–360 (1983).
56. Schanker, L. S., Mitchell, E. W. & Brown, R. A. J. Species comparison of drug absorption from the lung after aerosol inhalation or intratracheal injection. *Drug Metab. Dispos.* **14,** 79–88 (1986).
57. Tronde, A. *et al.* Pulmonary Absorption Rate and Bioavailability of Drugs in Vivo in Rats: Structure–Absorption Relationships and Physicochemical Profiling of Inhaled Drugs. *J. Pharm. Sci.* **92,** 1216–1233 (2003).
58. Patton, J. S., Fishburn, C. S. & Weers, J. G. The Lungs as a Portal of Entry for Systemic Drug Delivery. *Proc. Am. Thorac. Soc.* **1,** 338–344 (2004).
59. Byron, P. R. Determinants of drug and polypeptide bioavailability from aerosols delivered to the lung. *Adv. Drug Deliv. Rev.* **5,** 107–132 (1990).
60. Byron, P. R. Physiochemical effects on lung disposition of pharmaceutical aerosols. *Aerosol Sci. Tech.* **18,** 223–229 (1993).
61. Taylor, P. R. *et al.* Macrophage receptors and immune recognition. *Annu. Rev. Immunol.*

23, 901–44 (2005).
62. Akira, S., Takeda, K. & Kaisho, T. Toll-like receptors: critical proteins linking innate and acquired immunity. *Nat Immunol* **2,** 675–680 (2001).
63. Inohara, N. & Nuñez, G. NODs: intracellular proteins involved in inflammation and apoptosis. *Nat. Rev. Immunol.* **3,** 371–82 (2003).
64. Taylor, M., Bezouska, K. & Drickamer, K. Contribution to ligand binding by multiple carbohydrate-recognition domains in the macrophage mannose receptor. *J Biol Chem* **267,** 1719–1726 (1992).
65. Taylor, M. E. & Drickamer, K. Structural requirements for high affinity binding of complex ligands by the macrophage mannose receptor. *J. Biol. Chem.* **268,** 399–404 (1993).
66. Martinez-Pomares, L., Linehan, S. a, Taylor, P. R. & Gordon, S. Binding properties of the mannose receptor. *Immunobiology* **204,** 527–535 (2001).
67. Stahl, P. D. & Ezekowitz, R. a. The mannose receptor is a pattern recognition receptor involved in host defense. *Curr. Opin. Immunol.* **10,** 50–55 (1998).
68. Stein, M., Keshav, S., Harris, N. & Gordon, S. Interleukin 4 potently enhances murine macrophage mannose receptor activity: a marker of alternative immunologic macrophage activation. *J. Exp. Med.* **176,** 287–292 (1992).
69. Maródi, L. *et al.* Enhancement of macrophage candidacidal activity by interferon-γ: Increased phagocytosis, killing, and calcium signal mediated by a decreased number of mannose receptors. *J. Clin. Invest.* **91,** 2596–2601 (1993).
70. Martínez-Pomares, L. *et al.* Fc chimeric protein containing the cysteine-rich domain of the murine mannose receptor binds to macrophages from splenic marginal zone and lymph node subcapsular sinus and to germinal centers. *J. Exp. Med.* **184,** 1927–37 (1996).
71. Gabius, H.-J. *The Sugar Code: Fundamentals of Glycosciences*. (2009).
72. Lee, R. T. & Lee, Y. C. Affinity enhancement by multivalent lectin-carbohydrate interaction. *Glycoconj. J.* **17,** 543–551 (2000).
73. Stahl, P., Schlesinger, P. H., Sigardson, E., Rodman, J. S. & Lee, Y. C. Receptor-mediated pinocytosis of mannose glycoconjugates by macrophages: characterization and evidence for receptor recycling. *Cell* **19,** 207–215 (1980).
74. Astarie-Dequeker, C. *et al.* The mannose receptor mediates uptake of pathogenic and nonpathogenic mycobacteria and bypasses bactericidal responses in human macrophages. *Infect. Immun.* **67,** 469–477 (1999).
75. Sweet, L. *et al.* Mannose receptor-dependent delay in phagosome maturation by Mycobacterium avium glycopeptidolipids. *Infect. Immun.* **78,** 518–526 (2010).
76. Miura, Y. Design and synthesis of well-defined glycopolymers for the control of biological functionalities. *Polym. J.* **44,** 679–689 (2012).
77. Lee, Y. C. & Lee, R. T. Carbohydrate-Protein Interactions: Basis of Glycobiology. *Acc. Chem. Res.* **28,** 321–327 (1995).
78. Lee, Y. C. *et al.* Binding of synthetic oligosaccharides to the hepatic Gal/GalNAc lectin. *J. Biol. Chem.* **258,** 199–202 (1983).
79. Stenzel, M. H. RAFT polymerization: an avenue to functional polymeric micelles for drug delivery. *Chem. Commun. (Camb).* 3486–3503 (2008). doi:10.1039/b805464a
80. Liechty, W. B., Kryscio, D.R., Slaughter, B. V. and Peppas, N. A. Polymers for drug delivery systems. *Annu. Rev. Chem. Biomol. Eng.* **1,** 149–173 (2010).
81. *Controlled Radical Polymerization Guide: ATRP, RAFT, NMP*. *Sigma-Aldrich* (2012).
82. Chiefari, J. *et al.* Living Free-Radical Polymerization by Reversible Addition - Fragmentation Chain Transfer : The RAFT Process. *Macromolecules* **31,** 5559–5562 (1998).
83. Moad, G. *et al.* Living free radical polymerization with reversible addition – fragmentation chain transfer (the life of RAFT). *Polym. Int.* **49,** 993–1001 (2000).
84. Keddie, D. J. A guide to the synthesis of block copolymers using reversible-addition

fragmentation chain transfer (RAFT) polymerization. *Chem. Soc. Rev.* **43,** 496–505 (2014).
85. Zhang, H., Ma, Y. & Sun, X.-L. Recent developments in carbohydrate decorated targeted drug/gene delivery. *Med. Res. Rev.* **30,** 270–289 (2009).
86. Jain, K., Kesharwani, P., Gupta, U. & Jain, N. K. A review of glycosylated carriers for drug delivery. *Biomaterials* **33,** 4166–4186 (2012).
87. Sharma, A. & Sharma, U. S. Liposomes in drug delivery: Progress and limitations. *Int. J. Pharm.* **154,** 123–140 (1997).
88. Toh, M.-R. & Chiu, G. N. C. Liposomes as sterile preparations and limitations of sterilisation techniques in liposomal manufacturing. *Asian J. Pharm. Sci.* **8,** 88–95 (2013).
89. Lowe, A. B., Sumerlin, B. S. & McCormick, C. L. The direct polymerization of 2-methacryloxyethyl glucoside via aqueous reversible addition-fragmentation chain transfer (RAFT) polymerization. *Polymer (Guildf).* **44,** 6761–6765 (2003).
90. Albertin, L., Stenzel, M. H., Barner-Kowollik, C., Foster, L. J. R. & Davis, T. P. Well-defined diblock glycopolymers from RAFT polymerization in homogeneous aqueous medium. *Macromolecules* **38,** 9075–9084 (2005).
91. Park, H. *et al.* Micelles from self-assembled Double-Hydrophilic PHEMA-Glycopolymer-Diblock Copolymers as multivalent Scaffolds for Lectin Binding. *Polym. Chem.* 878–886 (2015). doi:10.1039/C5PY00797F
92. Stella, V. J. Prodrugs as therapeutics. *Expert Opin. Ther. Pat.* **14,** 277–280 (2004).
93. Rautio, J. *et al.* Prodrugs: design and clinical applications. *Nat. Rev. Drug Discov.* **7,** 255–270 (2008).
94. Luo, C., Sun, J., Sun, B. & He, Z. Prodrug-based nanoparticulate drug delivery strategies for cancer therapy. *Trends Pharmacol. Sci.* **35,** 556–566 (2014).
95. Hamaguchi, T. *et al.* Phase I study of NK012, a novel SN-38-incorporating micellar nanoparticle, in adult patients with solid tumors. *Clin. Cancer Res.* **16,** 5058–5066 (2010).
96. Matsumura, Y. *et al.* Phase I clinical trial and pharmacokinetic evaluation of NK911, a micelle-encapsulated doxorubicin. *Br. J. Cancer* **91,** 1775–1781 (2004).
97. Dizman, B., Elasri, M. O. & Mathias, L. J. Synthesis, characterization, and antibacterial activities of novel methacrylate polymers containing norfloxacin. *Biomacromolecules* **6,** 514–520 (2005).
98. Das, D. *et al.* RAFT polymerization of ciprofloxacin prodrug monomers for the controlled intracellular delivery of antibiotics. *Polym. Chem.* **7,** 826–837 (2015).

2. Chapter 2: Investigation of carbohydrate receptor-mediated targeting via nano-structured glycopolymer functional liposomes

Reprinted, slightly modified, with permission from Chen *et al.*, Nanomedicine: Nanotechnology, Biology and Medicine 12(7), 2016, 2031-2041.

2.A. Graphical Abstract

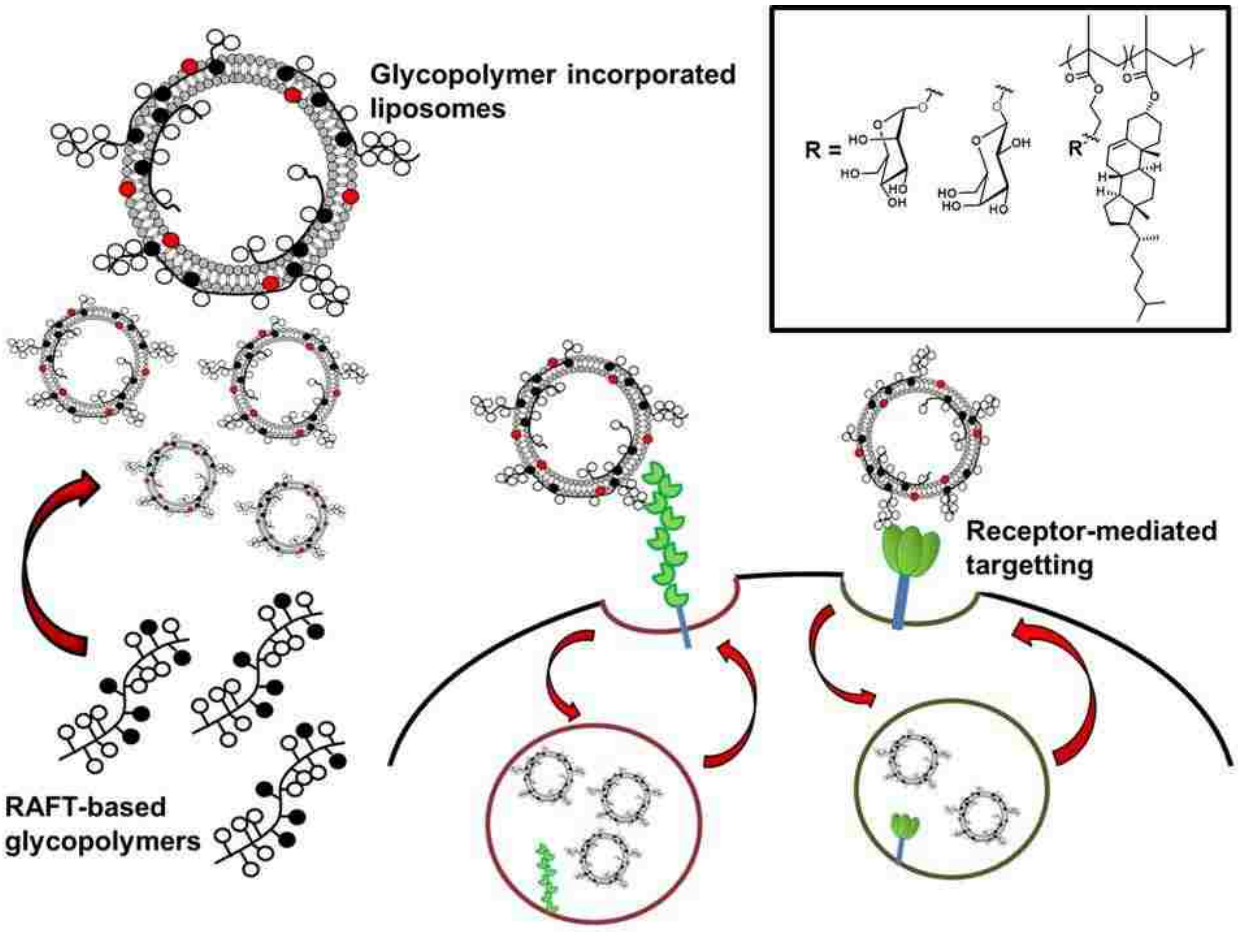

In this study, we employed reversible addition fragmentation chain transfer (RAFT) polymerization to synthesize neoglycopolymers, consisting of mannose- and galactose methacrylate-based monomers copolymerized with cholesterol methacrylate for use in functional liposome studies. We elucidate the carbohydrate receptor-targeting paradigm for nanoparticle binding and delivery in *in vitro* alveolar macrophage models and demonstrate specific receptor-

mediated uptake in a manner dependent on carbohydrate receptor expression. These results establish a platform capable of probing endogenous carbohydrate receptor-mediated targeting via glycofunctional nanomaterials.

2.B. Abstract

Carbohydrate receptors on alveolar macrophages are attractive targets for receptor-mediated delivery of nanostructured therapeutics. In this study, we employed reversible addition fragmentation chain transfer polymerization to synthesize neoglycopolymers, consisting of mannose- and galactose methacrylate-based monomers copolymerized with cholesterol methacrylate for use in functional liposome studies. Glycopolymer-functional liposomes were employed to elucidate macrophage mannose receptor (CD206) and macrophage galactose-type lectin (CD301) targeting in both primary macrophage and immortal macrophage cell lines. Expression of CD206 and CD301 were observed to vary significantly between cell lines (murine alveolar macrophage, murine bone marrow-derived macrophage, RAW264.7, and MH-S), which has significant implications in *in vitro* targeting and uptake studies. Synthetic glycopolymers and glycopolymer augmented liposomes demonstrated specific receptor-mediated uptake in a manner dependent on carbohydrate receptor expression. These results establish a platform capable of probing endogenous carbohydrate receptor-mediated targeting via glycofunctional nanomaterials.

2. C. Introduction

Airborne transmission of infectious agents can severely debilitate the respiratory system, contributing to the public health threat posed by aerosolizable pathogens such as influenza, tuberculosis, and weaponized biothreat agents. Innate immunity plays a critical role in defending the host upon the first minutes or hours post exposure to such pathogens[1,2]. Alveolar macrophages (AMs) resident to the lung are the predominant effector cells of the pulmonary

innate immune response. AMs express high levels of the mannose receptor, a C-type lectin pattern-recognition receptor, that enables them to recognize pathogen-associated glycans, localize and isolate infectious events, and trigger adaptive immunity [3–5].

The calcium-dependent carbohydrate recognition domain (CRD) of the C-type lectins allows for high affinity carbohydrate binding[5,6]. Consequently the mannose receptor on AMs recognizes a number of pulmonary pathogens, including but not limited to, *M. tuberculosis, B. pseudomallei, F. tularensis, Streptococci,* and *S. pneumonia,* via their cognate carbohydrate ligands[7–9]. The macrophage's ability to bind and internalize microorganisms via endocytosis and phagocytosis in the absence of opsonins make them favorable cells not only for host defense, but paradoxically for pathogen inhabitation and infection[10]. Therefore, strategies that utilize carbohydrate receptor-mediated uptake to improve cellular targeting by nanomedicines and therapeutics have received significant attention[11–14].

Mannose receptors highly expressed on AMs are favorable targets for receptor-mediated delivery strategies. However, in-depth *in vitro* carbohydrate receptor-mediated studies in alveolar macrophages are complicated by limited access to primary alveolar macrophages. As a result, most studies are conducted using alternative primary cells or cell lines, even though cells obtained from disparate anatomical sites or cell lines differ phenotypically from one another[10,15]. The implications of cell phenotype on carbohydrate receptor expression and subsequent targeting are poorly understood and require further elaboration. To this end, we have synthesized and formulated multivalent mannose and galactose glycopolymer augmented liposomes to investigate and compare receptor-mediated uptake in various macrophage cell lines. The objective of this study is to explore and elucidate the carbohydrate receptor-targeting paradigm for molecular and nanomaterial delivery systems in *in vitro* alveolar macrophage models.

Previous work conducted on mannosylated liposomes have employed monomeric forms of the carbohydrate for augmentation, including synthetic cetylmannoside[16], p-aminophenyl-alpha-mannoside[17], mannosylated cholesterol derivative, cholesten-5- yloxy-N-(4-((1-imino-2-b-

D-thiomannosyl-ethyl)amino)butyl) formamid[18], and 4-aminophenyl-a-D-mannopyranoside[19,20]. However, it is well established that monosaccharides exhibit only modest affinities towards lectins. Multivalent interactions have been shown to lead to a significant increase in avidity[21–23]. The precise control in reversible addition fragmentation chain transfer (RAFT) polymerization allows the synthesis of multivalent glycopolymers with predictable molecular weights, narrow molecular weight distribution, and complex polymer architectures displaying pendant carbohydrates[24]. To our knowledge this is the first synthesis of a RAFT-based glycopolymer that enables anchorage onto liposomes and the formulation of multivalent carbohydrate stealth liposomes for cellular targeting.

2. D. Materials and methods

2.D.1. Materials

Materials were purchased from Sigma–Aldrich unless otherwise specified. 1,2-Distearoyl-*sn*- glycero-3-phosphocholine (DSPC) and 1,2-distearoyl-*sn*-glycero-3-phosphoethanolamine-N-[methoxy(polyethylene glycol)-2000] (ammonium salt) (DSPE-mPEG(2000)) were purchased from Avanti Polar Lipids (Alabaster, AL, USA). Rhodamine B 1,2-Dihexadecanoyl-*sn*-Glycero-3-Phosphoethanolamine was purchased from Life Technologies (Grand Island, NY USA). 4,4′-Azobis(4-cyanovaleric acid) (V501) was obtained from Wako Chemicals USA. Alexa Fluor 488-conjugated anti-mouse MMR/CD206 antibody was purchased from R&D Systems (Polyclonal Goat IgG, Minneapolis, MN, USA). APC-conjugated anti-mouse CD301 (MGL1/MGL2) antibody was purchased from BioLegend (Rat IgG2b Isotype, Clone LOM-14, San Diego, CA, USA). Rat anti-mouse CD16/CD32 antibody was purchased from BD Biosciences (Rat IgG2b isotype, Clone 2.4G2, San Jose, CA, USA).

2.D.2. Synthesis of monomers

2.D.2.1. Synthesis of 2-O-((2',3',4',6' –tetra-*O*-acetyl)-α-D-mannosyl or -β-D-galactose) ethyl methacrylate

Acetylation of carbohydrate hydroxyl groups

To a mixture of mannose or galactose (50 g, 0.28 mol) and acetic anhydride (500 mL), iodine was added (5 g, 39.4 mmol). The reaction mixture was stirred at room temperature overnight. DCM was added to the reaction mixture prior to washing steps. Iodine was quenched by mixing the reaction mixture with aqueous sodium thiosulfate. The organic phase was washed with H_2O, then with saturated aqueous sodium bicarbonate. Granule sodium sulfate is added to the organic phase to remove remaining aqueous solvents. The product was obtained after removal of solvent under reduced pressure. Methods stated below were also carried out to synthesize 2-O-(β-D-galactosyl)hydroxyethyl methacrylate.

Procedure for anomeric deacetylation (1)

Glacial acetic acid (22.8 mL, 0.398 mol) was added dropwise and with stirring to a solution of hydrazine (22.87 mL, 0.341 mol) in THF (400mL), resulting in immediate formation of a precipitate which remained present until aqueous work-up. The starting peracetate (110.98 g, 0.284 mol) dissolved in minimal THF was added and the mixture was stirred 16-24 h. TLC (1:2 hexane—ethyl acetate) then showed absence of the starting material and presence of a product which, in most cases, appeared as two poorly separated spots representing a mixture of anomers (NMR). DCM (25mL) was added to the mixture to allow for extraction. The mixture was washed with H_2O (5x), 1M HCl (3x), saturated sodium bicarbonate (3x) and dried with granule sodium

sulfate. The product was obtained after removal of solvent under reduced pressure (52.31g, 53% yield).

Synthesis of (2', 3', 4', 6' –tetra-O-acetyl) –α-D-mannopyranosyl) trichloroacetimidate) and (2', 3', 4', 6' –tetra-O-acetyl) –β-D-galactopyranosyl) trichloroacetimidate) (2)

Cesium carbonate (9.8 g, 0.03 mol) and trichloroacetonitrile (30.135 mL, 0.3 mol) were added to a solution of the anomeric deacetylated carbohydrate monomer (52.31 g, 0.15 mol) dissolved in minimal DCM. Completion of the reaction was confirmed via TLC. The mixture was concentrated under reduced pressure. The product was obtained by purification through silica column chromatography using a gradient running solvent of 5:1, 4:1, 3:1, 2:1 hexane: ethyl acetate (39.86g, 54% yield).

Synthesis of 2-O-((2',3',4',6' –tetra-O-acetyl)-α-D-mannopyranosyl) ethyl methacrylate and 2-O-((2',3',4',6' –tetra-O-acetyl)-β-D-galactopyranosyl) ethyl methacrylate (3)

Hydroxyethyl methacrylate (12.23 mL, 0.097 mol) was added to a solution of (2', 3', 4', 6', -tetra-O-acetyl)-α –D-mannosyl trichloroacetimidate or (2', 3', 4', 6' –tetra-O-acetyl) –β-D-galactosyl) trichloroacetimidate) (39.86 g, 0.0812 mol) dissolved in minimal DCM. To this mixture, TMSOTf (0.397 mL, 2.19 mmol) was added at room temperature. The reaction mixture was stirred at room temperature for 20 minutes and then quenched by the addition of triethylamine. The product was obtained after removal of solvent under reduced pressure followed by purification through silica column chromatography using a gradient running solvent of 4:1, 3:1, 2:1 hexane: ethyl acetate (18.99g, 80% yield).

2.D.2.2. Synthesis of cholesterol methacrylate

Cholesterol methacrylate (CMA) monomer was synthesized according to a modified procedure to the literature[25]. In brief, cholesterol (2.0 g, 0.02 mol) was dissolved in a mixture of toluene containing triethylamine (5 mL, 23% v/v triethylamine/toluene) in a 100 mL round bottom flask with a stir bar. The solution was left under N_2 gas for 1 hour at 60 °C. Methacryloyl chloride (3.3 ml, 0.60 mol) along with the remaining triethylamine–toluene mixture (11.25 ml, 23% v/v) was added drop wise over a period of 30 minutes and the solution was stirred at 60 °C under a bed of N_2 gas overnight. The reaction was cooled to room temperature, and the product was purified by precipitating in 1.6 N HCl–methanol from toluene. The white colored precipitate, CMA, was dried under vacuo overnight (7.27g, 80% yield).

2.D.2.3. Synthesis of rhodamine B-ethyl methacrylate

To rhodamine B 5.26 g (11 mmol), N,N'-dicyclohexylcarbodimide 2.88 g (14 mmol) and 4-dimethylaminopyridine 134 mg (1.1 mmol) in CH_2Cl_2 (75 mL), was added 2-hydroxyethyl methacrylate 1.82 g (14 mmol) at 0 °C. After 30 min, the ice bath was removed and the reaction mixture was stirred at room temperature for 16 h. After filtering off the byproduct dicyclohexylurea, the solvent was evaporated under reduced pressure. The residue was redissolved in 30 mL acetonitrile and the insoluble materials were filtered off. The crude product obtained after evaporating acetonitrile was purified by flash column chromatography using 6 % methanol in chloroform (5.89g, 91% yield).

2.D.3. Synthesis of glycopolymers

The glycopolymers were synthesized via RAFT polymerization[24,26,27]. The RAFT copolymerization of protected per-O-acetylated mannose ethyl methacrylate (ManEMA-OAc) or per-O-acetylated galactose ethyl methacrylate (GalEMA-OAc) and cholesterol methacrylate (CMA) was conducted in inhibitor free dioxane (See supplemental information for monomer synthesis). 4-cyano-4-(phenylcarbonothioylthio)pentanoic acid (CTP) and 4,4′-azobis(4-

cyanovaleric acid) (V501) were used as the chain transfer agent (CTA) and radical initiator, respectively. A stock solution of V501 (2.7 mg, 9.56 mM) dissolved in dioxane was added to per-O-acetylated mannose or galactose ethyl methacrylate monomer (1 g, 2.17 mmol), cholesterol methacrylate monomer (CMA; 108 mg, 0.217 mmol), and CTP (13 mg, 0.0478 mmol). The initial monomer to CTA molar ratio ($[M]_0$:$[CTA]_0$) was 50:1 and the initial CTA to initiator molar ratio ($[CTA]_0$:$[I]_0$) was 5:1. The molar ratio of sugar to CMA ($[sugar]_0$: $[CMA]_0$) was 10:1. For fluorophore labeled glycopolymers, following the addition of V501, 25 mg of methacrylate rhodamine B dissolved in DMSO was added. The solution was purged in nitrogen for 30 min and allowed to react at 70°C for 24 h. The resulting copolymer was purified via dialysis in acetone for 48 h and then precipitated via dialysis in deionized H_2O for 24 h.

The mannose and galactose copolymers were deprotected to reveal the pendant sugars (the resulting deprotected glycopolymers are denoted poly(ManEMA-*co*-CMA) and poly(GalEMA-*co*-CMA)). Deprotected copolymers were dissolved in DCM (50 mg/mL) and 25 wt% sodium methoxide in methanol was added to obtain a 1 wt% sodium methoxide solution. The resulting solution was stirred at room temperature for 1 h and quenched with excess acetic acid. The deprotected copolymer solution was dialyzed against acetone for 48 h followed by dialysis against H_2O for 24 h and dried *in vacuo* overnight.

2.D.4. Glycopolymer characterization

Monomer incorporation was determined by ^{1}H NMR (Bruker AV-500, $CDCl_3$). Copolymer composition was calculated from terminal methyl protons (-CH-(CH_3)$_2$) on CMA (δ 0.88, 0.84) and the protons on C6 of the sugar monomer (δ 5.32-5.44). Molecular weights (M_n) and polydispersity indices ($Đ$) were determined by gel permeation chromatography (GPC) using an Agilent 1200 series (Agilent Technologies, Santa Clara, CA) and refractometer Optilab-TrEX and triple-angle static light scattering detector miniDAWN TREOS (Wyatt Technology, Dernbach, Germany) with SEC TSK-GEL α-3000 and α-e4000 columns (Tosoh Bioscience, Montgomeryville, PA). HPLC-

grade DMF containing 0.1 wt% LiBr was used as the eluent at a flow rate of 1 ml/min while column temperature was maintained at 50 °C. Absolute number average molecular weights were calculated from dn/dc values that were determined for each glycopolymer (p(HAM-*co*-CMA): 0.0647, p(HAG-*co*-CMA): 0.0656)

2.D.5. Glycopolymer augmented liposome preparation and characterization

Liposomes were prepared according to the film-method[28]. In brief, stock solutions of DSPC (5 mg/mL), cholesterol(5 mg/mL), and Rhodamine DHPE (1 mg/mL) dissolved in chloroform were added to a beaker at a molar ratio of 60:25:0.05 respectively, and the organic phase was allowed to evaporate overnight. For liposomes with DSPE-mPEG(2000), a molar ratio of DSPC: cholesterol: Rhodamine DHPE: DSPE-mPEG(2000) of 60:25:0.05:5 was used. The lipid film was hydrated at 60°C in an aqueous solution of glycopolymers (5.41 mg/ml, 60:25:0.05:15 molar ratio) dissolved in 10 mM pH 7.4 phosphate buffered saline at a phospholipid and cholesterol concentration of 10 mg/ml with stirring. To ensure homogeneity in the fluidity and packing of the lipids, the molar ratios of lipid and cholesterol were held constant (including the cholesterol contributed by the glycopolymer-cholesterol copolymer); the total ratio of DSPC lipid to cholesterol was maintained at 60:40 regardless of the amount of polymer added. The liposome suspensions were sonicated for 15 min, and subsequently extruded at 60 °C eleven times through each of the following polycarbonate filters: 800, 400, 200, and 100 nm (Whatman, GE Healthcare, Pittsburgh, PA USA). As an independent study to confirm that copolymer was integrating into the liposomes (figure shown in Supplementary Information), ethyl methacrylated rhodamine B copolymerized with galEMA and CMA were used in rehydrating the lipid film and subsequently rhodamine DHPE was omitted. Fluorescent liposomes were detected via excitation at 532 nm with a 565 nm long pass filter on the Malvern NanoSight NS300 (Malvern Instruments, UK). The mean particle size was determined by dynamic light scattering (DLS) with a Malvern Zetasizer Nano ZS (Malvern

Instruments, UK). For studies with Concanavalin A-binding, a total concentration of 1 μM ConA was added to 0.5mg/ml polymer incorporated liposomes. Size was measured by DLS (n=3).

2.D.6. Fluorescence microscopy

Binding and uptake of liposomes on BMDM were observed using a Nikon Ti-E live-cell fluorescence microscope. After dosing with liposomes, cells were collected, and fixed with 10% formaldehyde solution onto Lab-Tek II chambered coverglass slides (NUNC, Rochester, NY). Antifade reagent with DAPI (Molecular Probes, Thermo Fisher Scientific, Grand Island, NY) was added to the cells. Cells were imaged with a mercury lamp and a 100x objective lens.

2.D.7. Cryo-EM sample preparation

Cryo-EM samples were imaged by the Tecnai G2 F20 transmission electron microscope (FEI Co., Hillsboro, OR) at 200 kV and equipped with a field emission gun. Images were recorded under low-dose conditions (30 e/Å^2) at a magnification of 50,000 and a pixel spacing of 2.2 Å on a Gatan camera (Gatan, Inc., Pleasanton, CA). The freeze-plunging method was used for the cryo-immobilization of the samples. Approximately 5 μl of the liposome samples were applied on holey carbon film supported TEM copper grids (Electron Microscopy Sciences, Hatfield, PA). The samples were allowed to adhere to the grids before removing the excess solution by blotting the sample with filter paper (Whatman, Pittsburgh, PA). The samples were then immediately plunge-frozen via immersion into liquid ethane cooled by liquid nitrogen. The sample grids were then kept under liquid nitrogen and transferred to a Gatan 626 cryo-holder (Gatan, Inc., Pleasanton, CA). During cryo-imaging, the temperature was maintained below −179 °C at all times to minimize formation of amorphous ice.

2.D.8. Cell isolation and culture

All protocols for animal handling were approved by the University of Washington

Institutional Animal Care and Use Committee. To isolate mouse alveolar macrophage, lungs of BALB/c mice were lavaged with 3.4 ml of DPBS containing 1 mM EDTA. The bronchoalveolar lavage cells were centrifuged, rinsed, and resuspended in RPMI-1640 medium containing 10 % FBS. Bone marrow-derived macrophages (BMDMs) were generated as previously described using mouse macrophage colony-stimulating factor[29]. BMDMs were cultured in RPMI-1640 medium containing 20% horse serum (Gibco, Grand Island, NY) and 20 ng/ml M-CSF (Shenandoah Biotech, Warwick, PA USA). RAW 264.7 cells and MH-S cells were cultured in RPMI-1640 medium containing 10% FBS. HeLa cells were cultured in DMEM medium containing 10% FBS with 4.5 mg/ml glucose. All cells were cultured in medium containing 100 U/ml penicillin and 100 µg/ml streptomycin in a 37°C, 5% CO_2 incubator.

2.D.9. Determination of CD206 and CD301 expression

For analysis of cell surface expression of the macrophage mannose receptor and macrophage galactose type lectin on macrophage cells, AM, BMDM, RAW 264.7, and MH-S were cultured with or without interleukin (IL)-4 (Gibco). The cells (10^6 cells/100µl) were blocked with anti-mouse CD16/CD32 antibody (BD Biosciences) to reduce non-specific Fc receptor binding and subsequently incubated with primary antibodies, Alexa Fluor 488-conjugated anti-mouse MMR/CD206 (R&D Systems) and APC-conjugated anti-mouse CD301 (MGL1/MGL2) (BioLegend). All antibody incubations were conducted according to the protocol of each antibody data sheet. Alexa Fluor 488-conjugated anti-mouse CD206 Ab was titrated at 100 ng/ml and APC-conjugated anti-mouse CD301 was titrated at a 300 ng/ml. Flow cytometry was performed on an LSRII flow cytometer (BD Biosciences) and analyzed using FlowJo software (Tree Star, Inc.). For flow analysis, the percent of cells positive for carbohydrate receptor staining was determined by including cell samples that were not incubated with antibody. The background fluorescent signals generated by the unstained cells were gated as having 0% cells positive for the receptors. Cells that were stained with antibody were gated to the same background signals. Percent of cells

positive was therefore measured as the percent of cells out of the cell population displaying fluorescence signals above the negative gate.

2.D.10. *In vitro* and *ex vivo* uptake studies

BMDM, RAW 264.7, and HeLa cells were suspended at a density of 1 x 10^6 cells/ml and blocked with growth media containing 10% FBS for 30 min at 37˚C. The cells were subsequently treated with 20 μg/ml of rhodamine B conjugated polymers or 25, 50, 100, 200, and 400 μg/ml of rhodamine B-DHPE liposomes for designated times of 3 h and 30 min, respectively, at 37°C. Studies with competitors, 20 mg/ml of D-mannose and D-galactose monosaccharides were added 10 min prior to polymer or liposome treatment. For AM cells, liposomes were dosed at 400 μg/ml for 3 h in IL-4 stimulated AMs. The cells were centrifuged for 3 min at 2500 rpm and washed and resuspended with cold PBS containing 0.2 % FBS to remove excess polymers or liposomes in solution that were not bound or internalized. The uptake level was detected via the intensity of rhodamine B under a PE filter on the BD LSRII flow cytometer (BD Biosciences) and analyzed using FlowJo software (Tree Star, Inc.).

2.D.11. *In vitro* binding studies

Cell suspensions of BMDM and RAW 264.7 were collected at a density of 0.5 X 10^6 cells/ml and blocked with PBS pH7.4 containing 2% FBS. The cells were treated with increasing concentrations of rhodamine B-DHPE mannose and galactose liposomes for 30 min at 4˚C to minimize internalization. Binding levels were detected via rhodamine B using a PE filter on the BD LSRII flow cytometer (BD Biosciences). Analysis was conducted using FlowJo software.

2.D.12. Statistics

Statistical analysis was performed by Student's paired *t* test. (*) denotes a p-value of < 0.05. (**) denotes a p-vaue of < 0.005. Error bars are reported as SDs. All samples were

performed in triplicate unless noted otherwise.

2.E. Results

2.E.1 CD206 & CD301 receptor expression in mouse primary macrophage cells and macrophage cell lines

Cell surface expression of two C-type lectins, mannose receptor (CD206) and galactose-type lectin (CD301), were investigated in primary macrophage cells and commonly used macrophage cell lines, including mouse alveolar macrophages (AMs), bone marrow derived macrophages (BMDMs), RAW264.7, and MH-S. Cells were cultured with or without 20 ng/ml IL-4. The expression of CD206 and CD301 was observed by flow cytometry (**Figure 2.1**) and represented as percent of cells in the population positive for receptor staining. There was a distinct difference between the two cell groups investigated, macrophage primary cells and macrophage cell lines. The primary cells, including AMs and BMDMs, showed higher percent of cells positive for the expression of the mannose receptor, whereas mouse macrophage cell lines, RAW264.7 and MH-S, showed significantly greater percent of cells expressing the macrophage galactose-type lectin relative to the mannose receptor. IL-4 treatment for M2 macrophage activation increased the percent of cells expressing both the mannose and galactose receptors; however, IL-4 treatment for AMs only significantly increased the percent of cells expressing CD206 whereas there was no significant change in the percent cells positive for CD301 expression

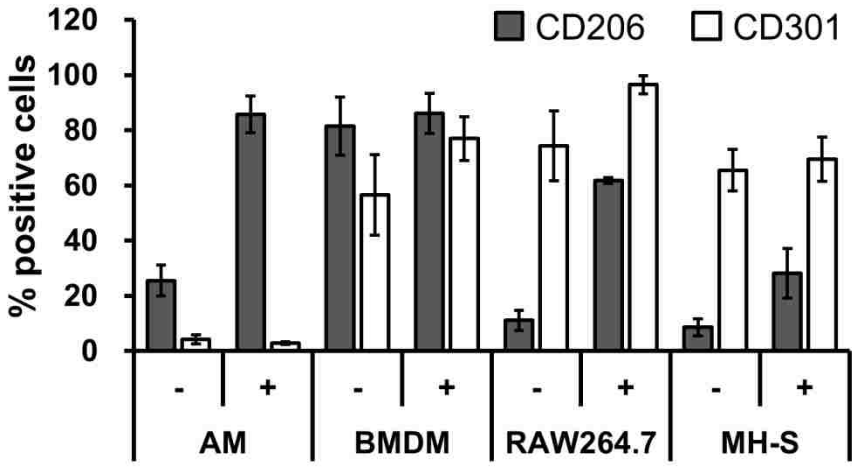

Figure 2.1.
Comparison of macrophage mannose receptor (CD206) and macrophage galactose-type lectin (CD301) expression levels on various macrophage cells. Primary cells, including isolated mouse alveolar macrophages (AMs) and BMDMs, and macrophage cell lines, including RAW264.7 and MH-S, were cultured with (**+**) or without (**-**) 20 ng/ml IL-4, and stained with Alexa 488 conjugated anti-CD206 and APC conjugated anti-CD301 antibodies.

2.E.2 Preparation and characterization of glycopolymers

Prior to synthesis of the glycopolymers, monomers were synthesized per methods described, and subsequently characterized with ^{1}H NMR **(Figure 2.2-2.4).** To formulate liposomes capable of targeting the mannose receptor (CD206) or the macrophage galactose lectin (CD301), we synthesized glycopolymers capable of augmenting bare liposomes. Leveraging the ability of cholesterol to anchor into the hydrophobic lipid bilayer, we copolymerized anomeric ethyl methacrylate functionalized per-*O*-acetylated mannose (ManEMA-OAc) or galactose (GalEMA-OAc) with cholesterol methacrylate (CMA), forming the well-defined glycopolymer-co-cholesterol copolymers ManEMA-OAc-*co*-CMA and GalEMA-OAc-*co*-CMA, respectively. Owing to the solubility mismatch between the CMA monomer and the glycomonomers, we chose a molar feed ratio glycan:CMA of 10:1 facilitating solubility in organic solvent during polymerization and aqueous solvent (following deprotection) during liposome formulation. Ethyl methacrylate

functionalized rhodamine B was conjugated to the glycopolymers for copolymer uptake studies. Results of 10:1 glycan:CMA glycopolymer characterization are summarized in **Table 2.1**. The glycopolymers synthesized via RAFT polymerization displayed low M_w/M_n values of 1.1 with M_n = 24.8 kDa and 24.3 kDa for p(ManEMA-OAc-*co*-CMA) and p(GalEMA-OAc-*co*-CMA), respectively. ^{1}H NMR results indicated a final copolymer composition of 90.2% ManEMA-OAc and 9.8% CMA, and 88% GalEMA-OAc and 12% CMA. To display the native pendant glycomoieties on the glycopolymers, protective acetyl groups were removed via base-catalyzed hydrolysis as demonstrated by the absence of the ^{1}H NMR acetyl singlet peaks (δ 2.0-2.2) shown in **Figure 2.5**.

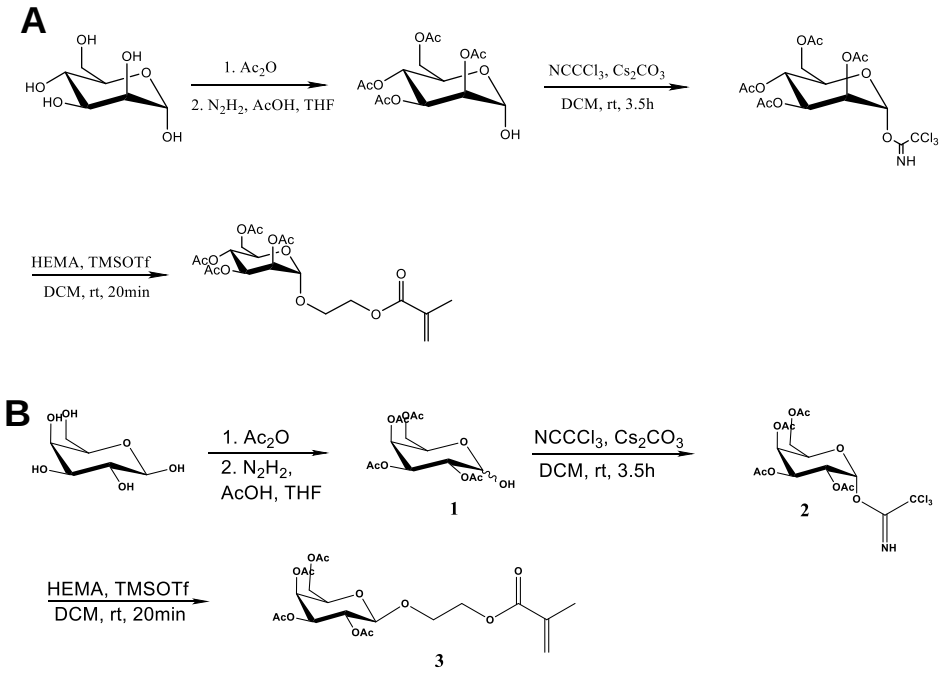

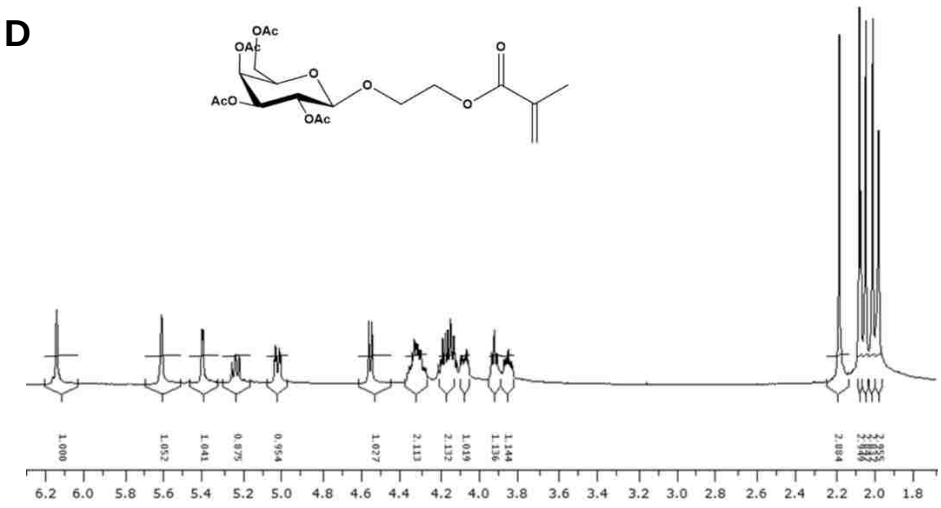

Figure 2.2.
Schematic of the synthesis of **(A)** 2-O-((2',3',4',6' –tetra-O-acetyl)-α-D-mannosyl) ethyl methacrylate and **(B)** 2-O-((2',3',4',6' –tetra-O-acetyl)-β-D-galactosyl) hydroxyethyl methacrylate. **(C)** ^{1}H NMR (500 MHz, $CDCl_3$) 2-O-(2',3',4',6' –tetra-O-acetyl)-α-D-mannosyl) ethyl methacrylate. **(D)** ^{1}H NMR (500 MHz, $CDCl_3$ solvent) 2-O-(2',3',4',6' –tetra-O-acetyl)-β-D-galactosyl) ethyl methacrylate.

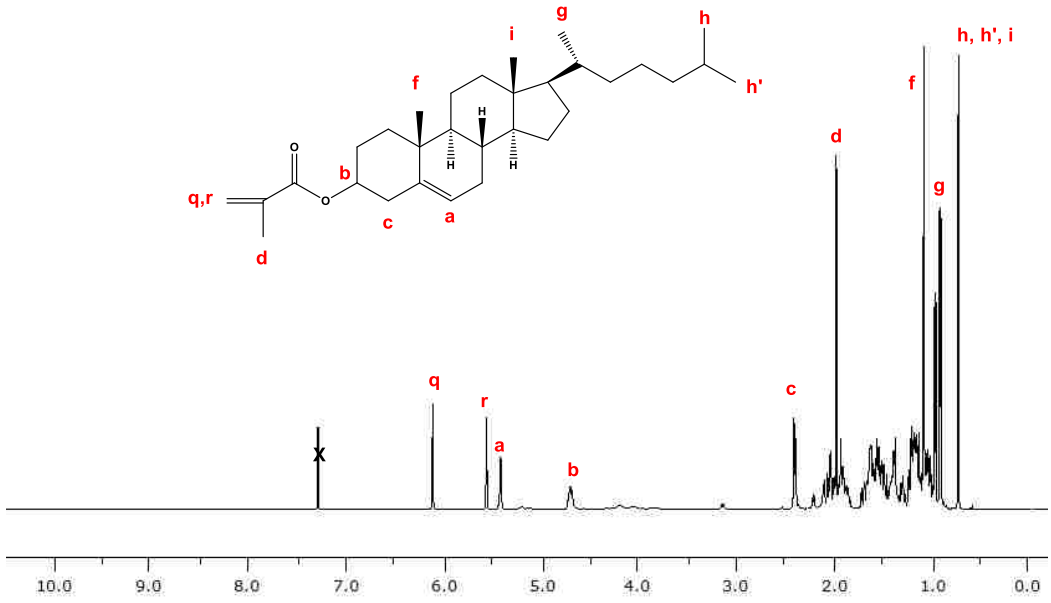

Figure 2.3.
^{1}H NMR (500 MHz, $CDCl_3$) Cholesterol methacrylate monomer

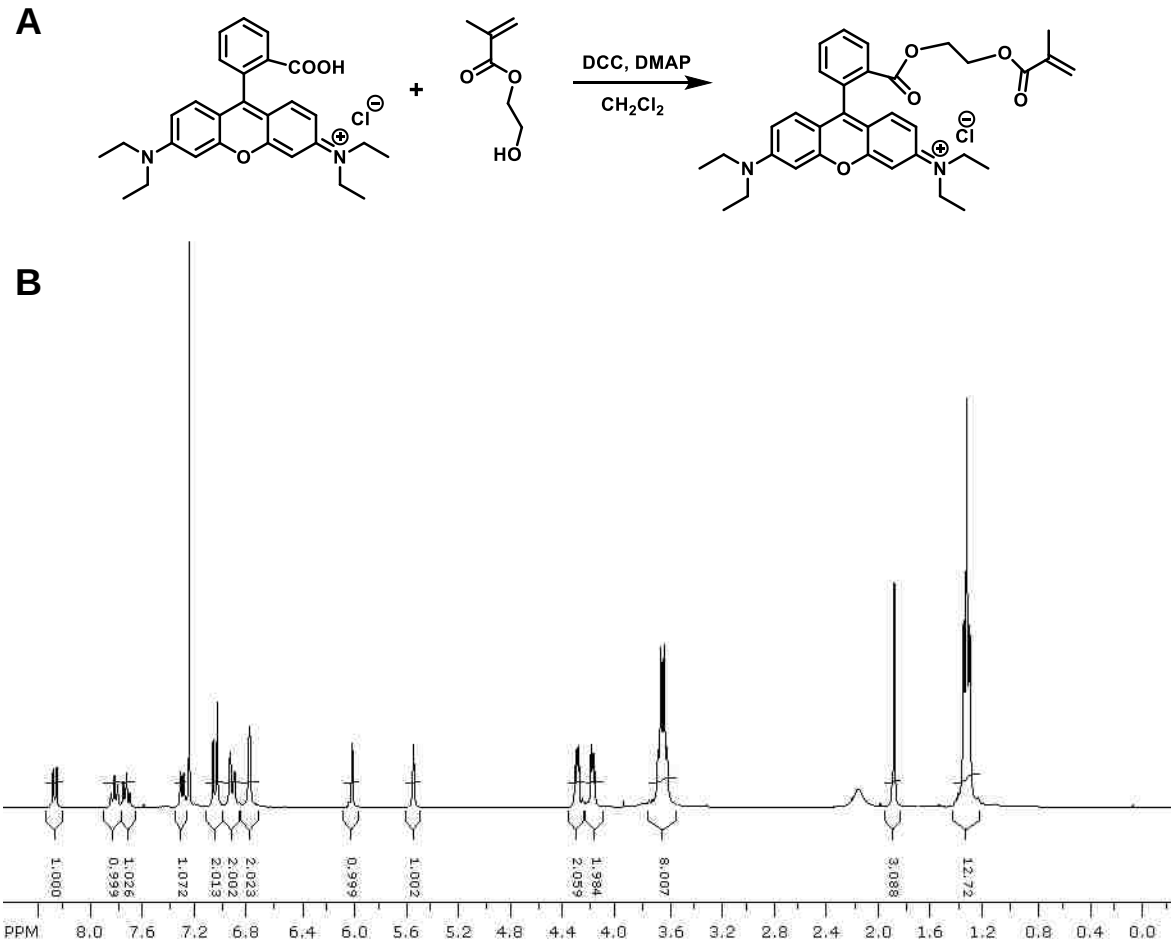

Figure 2.4.
(A) Schematic of rhodamine B-ethyl methacrylate synthesis. **(B)** ^{1}H NMR (300 MHz, $CDCl_3$) rhodamine B-ethyl methacrylate

Polymer	*[monomer]₀/[CTA]₀*	Sugar Exp. mol %[a]	Chol. Exp. mol %[a]	Sugar Theo. mol %	Chol. Theo. mol %	*Đ* [b]	*Mn (kD)*[b]	*Mn (kD)* Deprotected
OAcMan-*co*-chol	50	90.2	9.8	91	9	1.109	24.8	16.6
OAcGal-*co*-chol	50	88	12	91	9	1.091	24.3	16.3

Table 2.1.
Summary of theoretical and experimentally determined molecular weights and *Đ* values for cholesterol copolymers synthesized
a As determined by ^{1}H NMR in $CDCl_3$ by comparison of the methyl resonances in cholesterol between δ= 0.88, 0.84 to the protons on C6 of the sugar monomer resonances between δ=5.32-5.44 ppm.
b As determined by size exclusion chromatography (see methods).

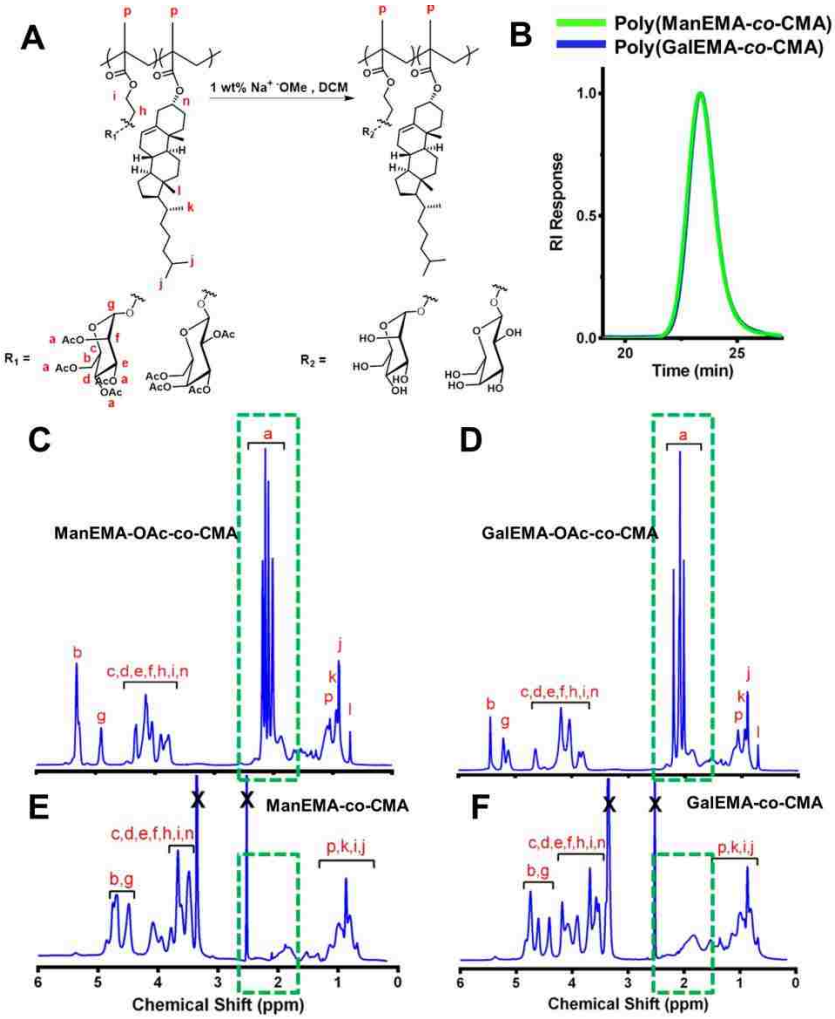

Figure 2.5.
Characterization of copolymers containing ManEMA-OAc or GalEMA-OAc and CMA prepared by RAFT and subsequent deprotection of the *O*-acetyl protecting groups displayed on the glycans. **(A)** Schematic of pre- and post- base-catalyzed deprotection of the glycopolymers. **(B)** Gel permeation chromatography molecular weight distributions for the protected glycopolymers at a molar ratio of 10:1 glycan:cholesterol. Validation of deprotection of glycopolymers demonstrated with NMR analysis. ^{1}H-NMR (500 MHz) of **(C)** poly(ManEMA-OAc-*co*-CMA) and **(D)** poly(GalEMA-OAc-*co*-CMA) in $CDCl_3$ and **(E)** poly(ManEMA-*co*-CMA) and **(F)** poly(GalEMA-*co*-CMA) in DMSO. Resonances associated with the acetyl groups are in the range of δ=~1.8-2.2. 'X' denotes solvent peaks DMSO and trace H_2O.

2.E.3 Receptor-mediated uptake of deprotected glycopolymers

To investigate the bioactivity of the deprotected glycopolymers, we measured the uptake of free polymer (20 μg/m) in either CD206 or CD301 dominant expressing cell lines, BMDM and RAW264.7, respectively. Cells were cultured with 20 ng/ml IL-4 48 h prior to polymer dosing to

mimic conditions found in chronic inflammation during respiratory infection caused by airborne transmission of infectious agents[30,31]. In order to investigate whether the glycopolymers were selectively taken up via surface receptors, cells were competitively dosed with excess (20mg/ml) free D-mannose or D-galactose (**Figure 2.6**). By normalizing to the mean fluorescence intensity of cells dosed with glycopolymers without inhibitors, we compared the effectiveness of mannose and galactose as competitors of glycopolymer uptake between BMDMs, RAW264.7, and HeLa cells. HeLa cells were used as a negative control against both mannose and galactose receptors.

In BMDM, mannose glycopolymer uptake was significantly inhibited by about 80% in the presence of D-mannose, compared to the untreated condition. Statistical significance comparing mean uptake levels of mannose glycopolymer in the presence of D-mannose and D-galactose were compared ($p<0.005$) to illustrate that D-mannose led to significant inhibition of the glycopolymer compared to D-galactose. (**Figure 2.6, *A***). Galactose polymer uptake in BMDM, however, had little or no effect upon treatment with competitors **(Figure 2.6, *B*)**. We also investigated uptake in RAW264.7 cells treated with IL-4, which yielded a high percentage of cells expressing CD301 and moderate percentage of cells expressing CD206 compared to BMDM, as shown in **Figure 2.1.** The galactose glycopolymers showed a significant decrease in uptake level by up to about 30% with D-galactose competition compared to the uninhibited condition, whereas uptake was unaffected with the addition of D-mannose **(Figure 2.6, *B*)**. Comparing mean uptake levels of the galactose glycopolymer in the presence of D-mannose and D-galactose ($p<0.05$) confirmed that D-galactose led to significant inhibition of the glycopolymer compared to D-mannose. HeLa cells showed negligible change in uptake levels for both poly(ManEMA-*co*-CMA) and poly(GalEMA-*co*-CMA) with the addition of competitors, free D-mannose and D-galactose.

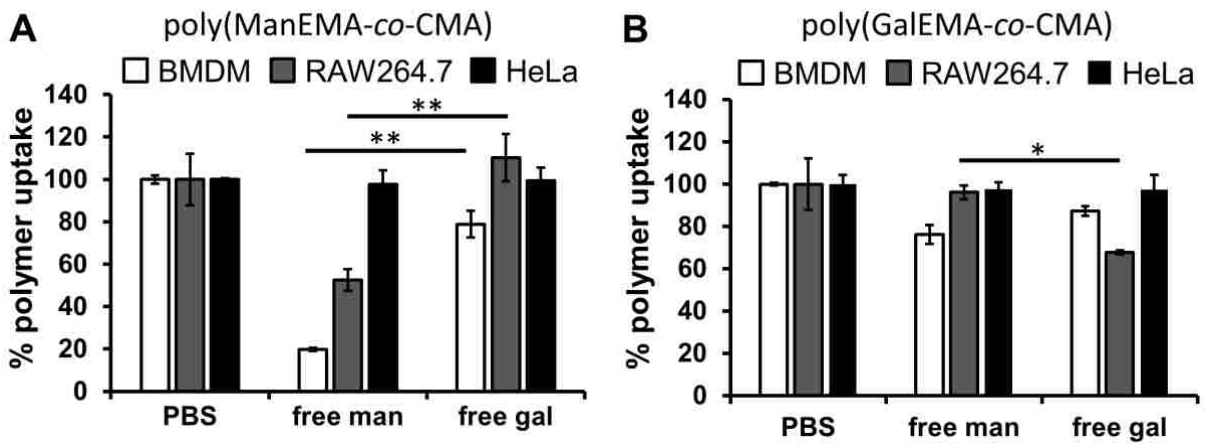

Figure 2.6.
In vitro uptake and inhibition of glycopolymers by highly expressed CD206 BMDM, highly expressed CD301 RAW264.7 cells, and negative control HeLa cells. Cells were cultured with 20 ng/ml IL-4 for 48 h prior to polymer dosing. BMDM were incubated with 20μg/ml poly(ManEMA-*co*-CMA) **(A)** or poly(GalEMA-*co*-CMA) **(B)** glycopolymers in the presence of 20mg/ml free D-mannose or D-galactose. Uptake levels were normalized to the median fluorescence intensity of glycopolymer treated cells without the addition of competitors. The addition of D-mannose inhibited the mannose glycopolymer uptake significantly (~80%) compared to the addition of D-galactose (~20%). Neither D-mannose nor D-galactose significantly inhibited the galactose glycopolymer uptake. RAW264.7 cells were also incubated with 20μg/ml poly(ManEMA-*co*-CMA) **(A)** or poly(GalEMA-*co*-CMA) **(B)** in the presence of 20mg/ml free D-mannose or D-galactose. The addition of D-galactose inhibited the galactose glycopolymer uptake considerably compared to the addition of D-mannose. None of the competitors affected polymer uptake in HeLa cells.

2.E.4 Preparation and characterization of glycopolymer incorporated liposomes

Augmented DSPC liposomes were formulated with PEGylated lipid, poly(ManEMA-*co*-CMA), or poly(GalEMA-*co*-CMA). Liposomes were prepared by the thin-film method and rehydrated in PBS pH 7.4 to a final concentration of 10 mg/ml total lipid and cholesterol **(Figure 2.7, *A*).** To formulate the augmented liposomes, glycopolymers dissolved in PBS were added during rehydration of the lipid thin film to allow the cholesterol to anchor itself into the hydrophobic lipid bilayer. DLS was used to characterize the hydrodynamic size and polydispersity in each preparation following extrusion of the augmented liposomes (see methods). Augmented liposomes ranged in size from 120-170 nm with polydispersity index (PDI) of 0.08-0.22,

demonstrating homogenous liposomes. Cryo-TEM images of the PEGylated- and glycopolymer augmented liposomes show that incorporation of the glycopolymers did not affect or disrupt the morphology of the liposomes **(Figure 2.7, *C*)**. To determine whether the glycopolymers were incorporated onto the liposomes, glycopolymers with methacrylate rhodamine B monomers were also synthesized and formulated with liposomes in the absence of rhodamine DHPE lipids. Only fluorescently labeled particles were detected using a 532 nm excitation laser and 565 nm long pass filter on the Malvern NanoSight NS300 **(Figure 2.8)**. Particles ranging from 90-155nm were detected indicating that fluorescently labeled polymers were associated with the liposomes. To further confirm whether the glycopolymers were anchored onto the liposomes during rehydration of the lipids, an agglutination assay with Concanavalin A (ConA), a plant lectin that binds specifically to terminal α-D-mannosyl and α-D-glucosyl groups[32], was conducted. ConA was added to liposome preparations (1 μM ConA final concentration) and particle size was immediately measured via DLS **(Figure 2.7, *B*).** As expected, the mannose liposomes showed statistically significant ($p < 0.005$) increase in particle size upon incubation with ConA, whereas the PEG and galactose liposomes showed negligible change in particle size **(Figure 2.7, *B*)**. These data demonstrate that the mannose polymer incorporated liposomes display bioactivity on the liposome surface.

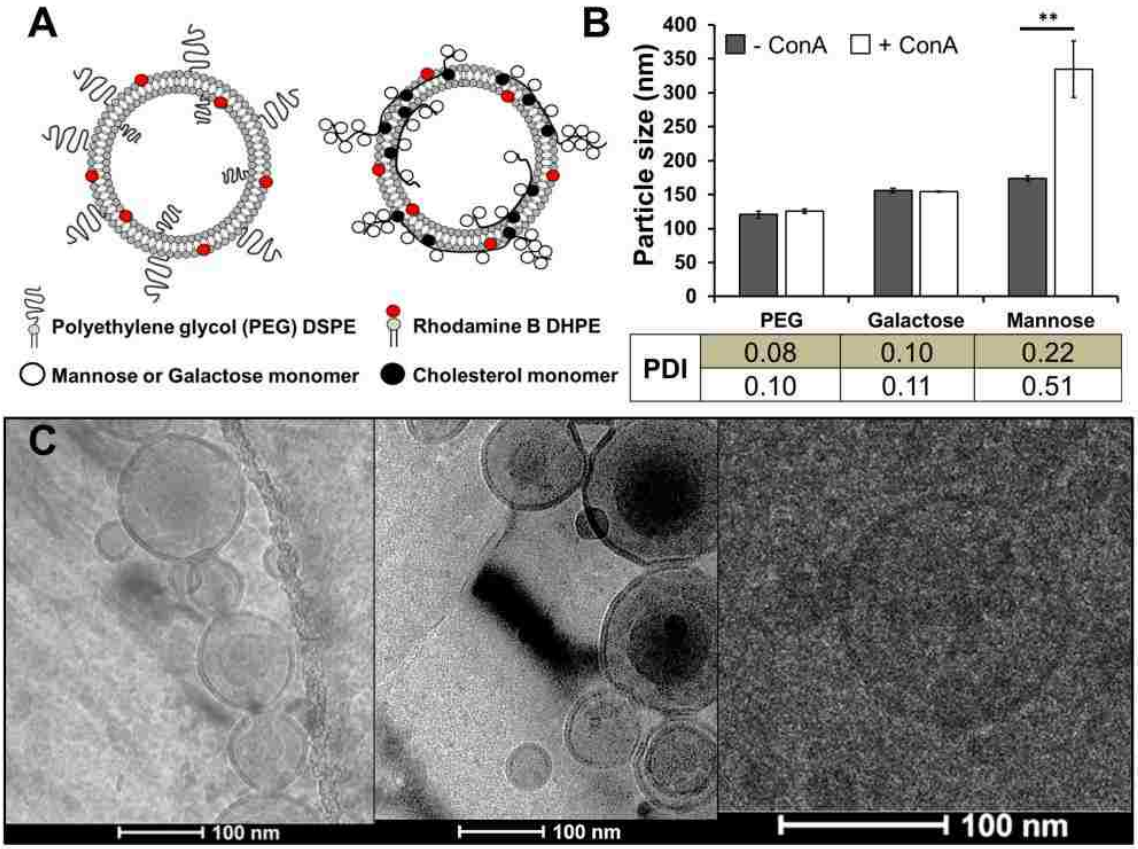

Figure 2.7.
(A) Illustration of conventional PEGylated "stealth" liposomes (left) and the glycopolymer-incorporated liposomes (right). **(B)** Particle size determination of liposomes via DLS. Mannose, galactose, and PEG liposomes show similar particle sizes ranging from 120-170 nm. All liposome groups were resuspended with 1 μM ConA solution and particle size was measured by DLS. A significant increase in particle size was observed for the mannose augmented liposomes, but negligible size change for the PEG liposomes and galactose liposomes. All values are expressed as mean ± SD (n = 3). **P<0.005. **(C)** Cryo-EM images of PEG (left) and galactose glycopolymer incorporated liposomes (middle and right). The incorporation of polymers did not alter the shape of the liposomes.

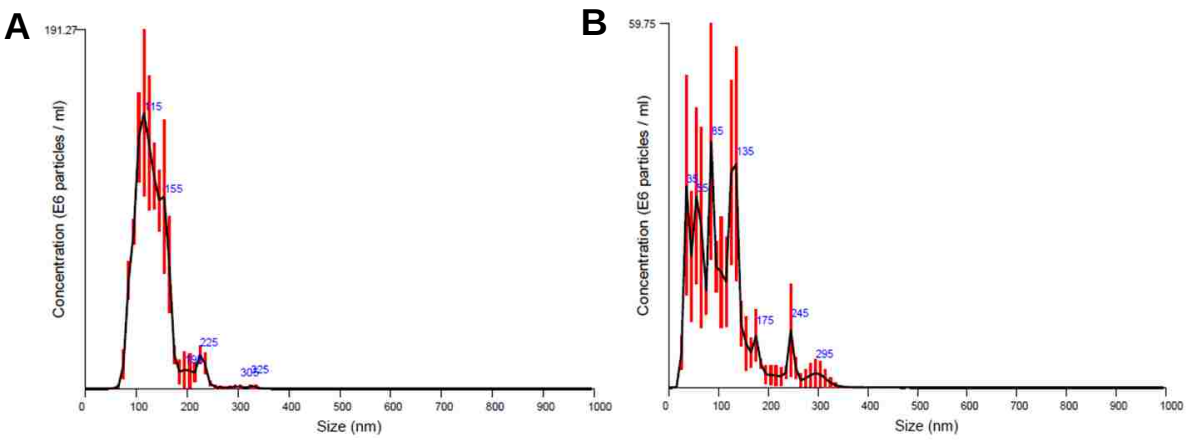

Figure 2.8.
An independent measurement of size distribution of liposomes was made using the Malvern NanoSight NS300 as a means to identify whether the glycopolymers were incorporating onto the liposomes. Liposomes of 10mg/ml were diluted 10,000x in PBS. Non-fluorescently labelled glycopolymer incorporated liposomes **(A)** were measured and showed a mean particle size of 127.5 ± 1.5nm (whereas no measurements could be made under fluorescent detection filters). Glycopolymers with rhodamine B-ethyl methacrylate were formulated with non-fluorescently labelled lipids **(B)** and detected via excitation at 532 nm with a 565 nm long pass filter on the Malvern NanoSight NS300. The fluorescent glycopolymer incorporated liposomes showed a mean particle size of 104.5 ± 9.3 nm. The results provide a strong indication that the polymers are incorporating onto the liposomes.

2.E.5 Relationship between CD206 and CD301 receptor expression and in vitro uptake and binding of glycosylated liposomes in primary macrophage and macrophage cell lines

We next investigated the bioactivity of the glycopolymer augmented liposomes as determined by the targeted uptake levels of PEG, mannose, and galactose liposomes in association with the receptor expression in BMDM and RAW264.7 cells. As shown in Fig. 1, BMDM have the greatest percentage of cells expressing CD206 relative to CD301 and RAW264.7 have high CD301 expression. Cells were incubated with 400 μg/ml of the PEG stealth liposomes and the poly(ManEMA-*co*-CMA) and poly(GalEMA-*co*-CMA) incorporated stealth liposomes for 30 min at 37℃. Uptake of both mannose and galactose glycopolymer incorporated liposomes were significantly greater ($p<0.005$) than that of the PEG liposome in BMDM and RAW264.7 **(Figure 2.9, *A, B*)**. Additionally, BMDM uptake of the mannose and galactose liposomes was

similar, whereas in RAW264.7 uptake of the galactose liposomes was significantly greater ($p<0.005$) than that of the mannose liposomes; these results correspond to the receptor expression observed in **Figure 2.1**. Punctate stains in fluorescence microscopy images **(Figure 2.10)** demonstrate that uptake mediated by the macrophage mannose receptor lead to cytosolic delivery of the liposomes.

Liposomes were also dosed in a concentration dependent manner. For both BMDM and RAW 264.7, PEG liposomes showed the least concentration-dependent uptake **(Figure 2.9 *C, D*)**. In BMDM cells, where both CD206 and CD301 are highly expressed, both mannose and galactose liposomes had similar uptake levels **(Figure 2.9, *C*)** whereas in RAW264.7, which predominantly express CD301, mannose liposomes have lower influx per increase in concentration compared to galactose liposomes **(Figure 2.9, *D*)**. We then dosed bronchoalveolar lavaged murine AMs with the liposomes to determine whether there was an association between receptor expression and uptake **(Figure 2.9, *E*)**. The lavaged AMs were first stimulated with 20 ng/ml IL-4 for 24 h prior to the addition of liposomes. Uptake for the mannose liposomes in AMs was the greatest compared to PEG and galactose liposomes, in which the mannose liposome uptake was approximately 1.6-fold greater than that of the PEG liposomes and about 1.4-fold greater than that of the galactose liposomes.

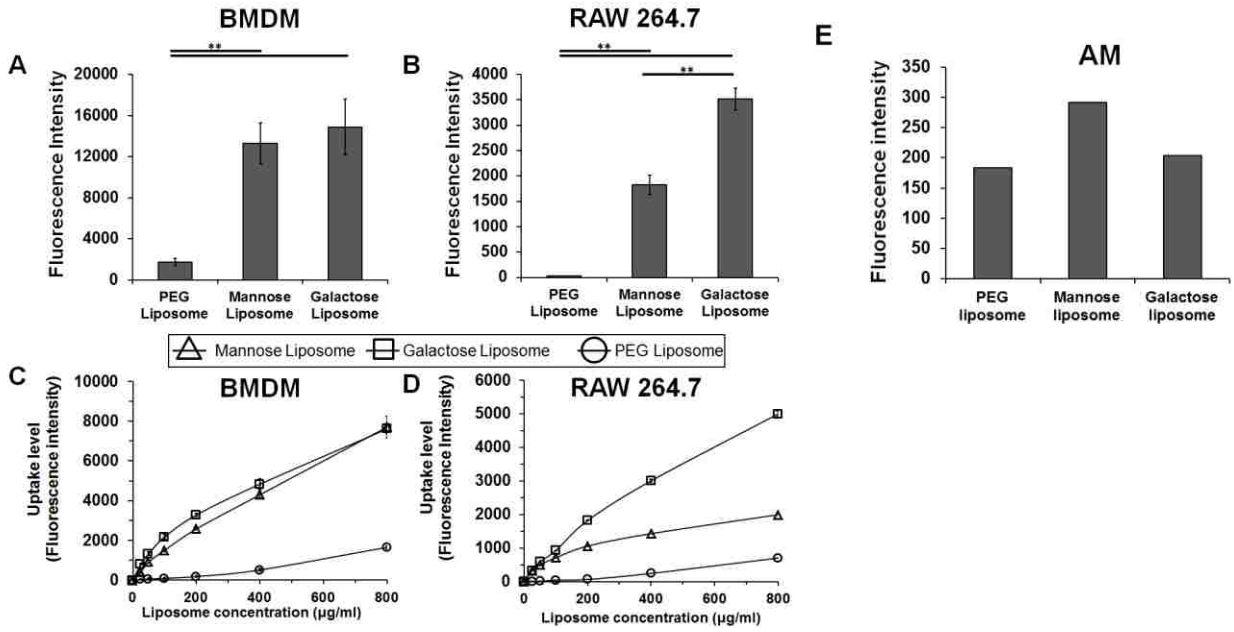

Figure 2.9.
In vitro uptake of glycopolymer incorporated liposomes by BMDM, RAW264.7 cells, and AM. BMDM and RAW264.7 cells were incubated with 400 µg/ml of the PEG stealth liposomes and the mannose- and galactose-liposomes for 30 min at 37 ℃. Uptake of both glycopolymer incorporated liposomes were significantly greater ($p<0.005$) than that of the PEG liposome. In BMDM cells **(A)**, uptake levels of the mannose and galactose liposomes were similar, whereas in RAW264.7 cells **(B)** uptake level of the galactose liposomes was significantly greater ($p<0.005$) than that of the mannose liposomes, which corresponds to the different receptor expression levels observed on the two cell lines. The liposomes were also dosed in a concentration dependent manner. In BMDM cells **(C)**, where both CD206 and CD301 are highly expressed, both mannose and galactose liposomes had similar uptake levels whereas in RAW264.7 **(D)**, which predominantly express CD301, mannose liposomes have lower uptake compared to galactose liposomes. Uptake levels were also observed in bronchoalveolar lavaged mouse AM stimulated with IL-4, which express predominantly CD206 **(E).** Uptake for the mannose liposomes was the greatest compared to PEG and galactose liposomes. (n=1 for AM uptake; n=3 for all other samples).

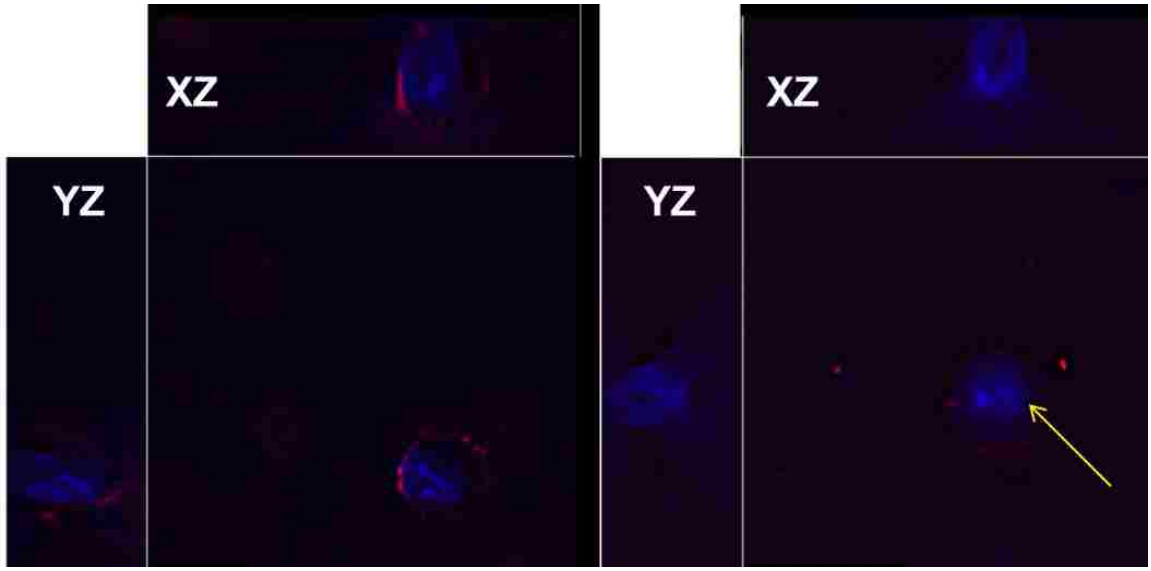

Figure 2.10.
Fluorescence microscopy to differentiate between binding and uptake experiments. The binding (A) image shows rhodamine labeled liposomes binding externally to BMDM cells, whereas for uptake (B), punctate stains of the liposomes can be observed (shown by the arrow).

To further demonstrate receptor-mediated interaction between the glycopolymer incorporated liposomes and CD206 and CD301, binding interactions were investigated by incubating BMDM and RAW264.7 with increasing concentration of liposomes **(Figure 2.11)**. The cells were incubated with the liposomes for 30 min. on ice to minimize internalization. Saturation of the receptor-mediated binding were unmet with BMDM due to high receptor expression; however, saturation of the mannose liposomes with RAW264.7 cells corresponded to the low percent of cells expressing CD206 (**Figure 2.1**). Binding studies of the glycopolymer incorporated liposomes was compared to binding of non-specific PEGylated liposomes, and minimal binding was observed for the PEG control liposome **(Figure 2.12)**.

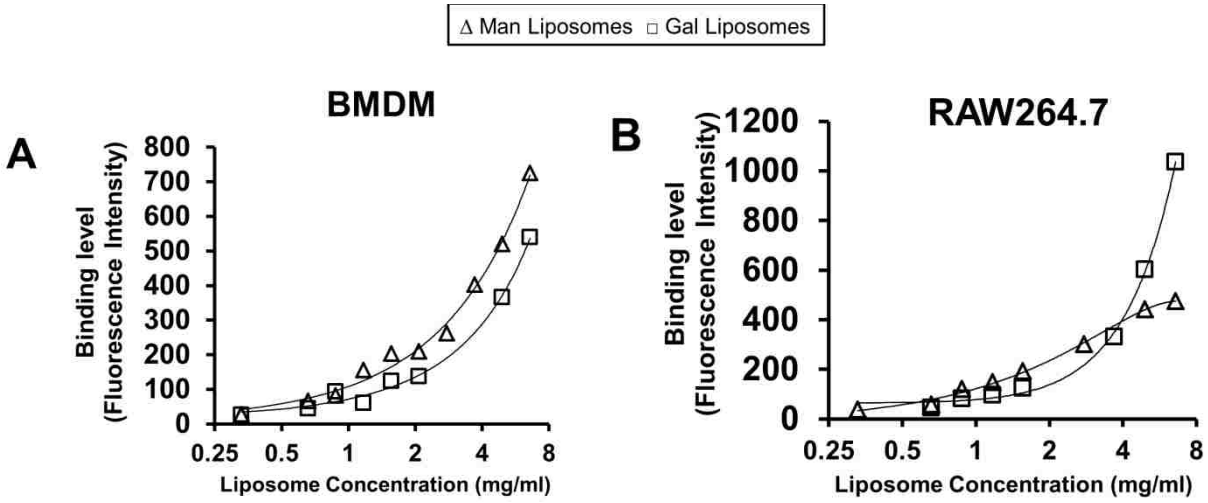

Figure 2.11.
In vitro binding of glycopolymer incorporated liposomes with CD206 and CD301 on BMDM and RAW264.7. Binding studies were conducted in **(A)** BMDM and **(B)** RAW264.7 cells in a liposome concentration dependent manner. The cells were incubated with the liposomes for 30 min at 0℃.

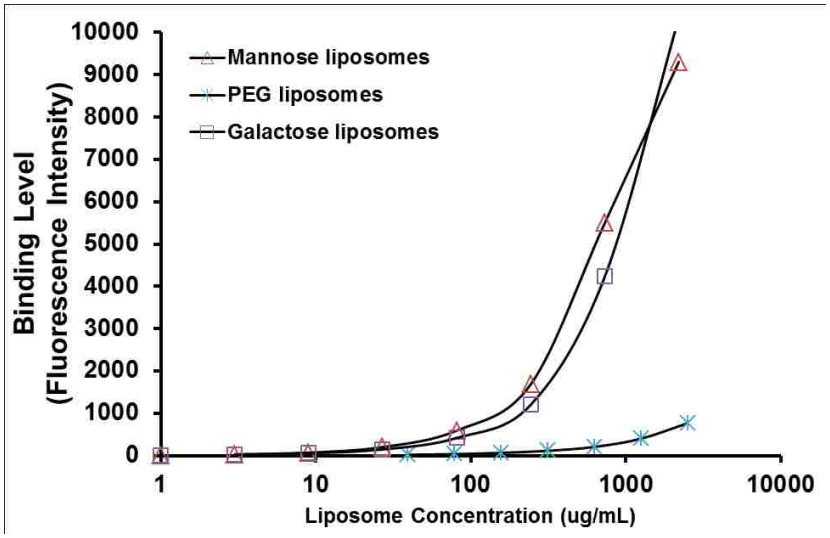

Figure 2.12.
Binding studies of glycopolymer augmented liposomes and PEG liposomes. Minimal binding of the PEGylated liposomes was observed.

2. F. Discussion

Alveolar macrophages play an important role in the phagocytic clearance of inhaled microorganisms in the distal airways and the alveoli[10,33,34]. The inability to clear persistent foreign stimuli and to repair cellular damage can result in chronic pulmonary disease[30,35]. Under chronic inflammatory conditions, AMs undergo phenotypic changes representing alternative (M2) polarization and an overexpression of the macrophage mannose receptor of these cells occurs[4,30,31]. For these reasons, targeting AMs via their mannose receptor has been widely sought after for antibiotic, vaccine, and therapeutic applications, showing promising results both *in vitro* and *in vivo*[19,36,37]. One of the challenges in studying alveolar macrophages for targeted delivery of therapeutics is the difficulty in procuring sufficient quantities of cells via bronchoalveolar lavage for extensive studies. As a result, it has become common practice for alternative primary cells, such as BMDM, or immortalized cell lines, such as RAW264.7, to be used as a surrogate for AMs in *in vitro* studies.

Carbohydrates and glycoconjugates have received significant attention for their specificity for molecular recognition and the myriad of roles they play in biological processes[38]. Chemical synthesis enables precise and scalable formulation of oligosaccharides and glycoconjugates, providing access to this important class of biomolecules. This strategy leverages cell-surface display of receptors that interact and bind with carbohydrates that decorate cells, viruses, and bacteria, enabling cellular adhesion and cell signaling[39]. The presence of receptor CD206, the macrophage mannose receptor, on alveolar macrophage[40,41], is just one such example of a cell surface receptor that mediates AM interactions with host tissues and pathogens. However, due to the differences in observed receptor expression levels for the disparate macrophage cells, it is difficult to translate the overall contribution of carbohydrate receptors on macrophage targeting and uptake to various primary macrophage cells and cell lines.

We first investigated CD206 and CD301 expression levels in AMs isolated by bronchoalveolar lavage, in addition to common AM surrogate cell lines, BMDM, RAW264.7, and MH-S[42–46]. While alveolar macrophage were found to predominantly express the mannose receptor (CD206), as has been demonstrated in the literature[41,47], it is worth noting that CD206 and CD301 expression levels differed widely between macrophage cell lines, in which RAW264.7 and MH-S expressed high levels of the galactose-type lectin. These observations have significant implications regarding the translation of results from *in vitro* cell models to *in vivo* experiments, as carbohydrate-mediated targeting and uptake varies by receptor expression levels.

To examine the effect of cell phenotype on receptor expression, we activated primary macrophage and macrophage cell lines with IL-4 to represent chronic inflammation of tissues and cells observed during respiratory infection[48–53]. Macrophages acquire diverse functional phenotypes of classically (M1) and alternatively activated (M2) macrophages depending on the microenvironmental stimuli such as pathogen invasion, damaged cells, and cytokines[54]. M2 macrophages are activated by IL-4 or IL-13 and characterized by high expression of scavenger receptors, such as mannose and galactose receptors, for phagocytic functions[55–57].Our results support this hypothesis, finding that IL-4 upregulated both CD206 and CD301 carbohydrate receptors. Consequently, these macrophages can be targeted to facilitate receptor-mediated uptake and delivery of therapeutics during respiratory infection. It is worth noting that isolated AM cells had very low CD301 expression level pre- and post- activation with IL-4 while displaying a significant increase of CD206 expression. This supports the assertion that surrogate cells from disparate anatomical sites (e.g. BMDM) or immortal cell lines behave differently and do not necessarily approximate the physiology of the target cell population.

To evaluate CD206 and CD301 binding and uptake in macrophage, we utilized RAFT polymerization to synthesize well-controlled multivalent glycopolymers. Lectins have been shown to rely on molecular recognition and binding events that benefit from multivalent interactions, motivating our strategy to employ multivalency for cell targeting[23]. Lectins have only modest

affinities for monovalent ligands; however, multivalency dramatically increases the effective affinity and selectivity[58]. The synthetic glycopolymers were found to be bioactive via receptor-mediated uptake with IL-4 activated BMDM and RAW264.7 cells. In both RAW264.7 and BMDM cells, mannose glycopolymer uptake was significantly inhibited ($p<0.005$) in the presence of D-mannose, compared to both non-treatment and D-galactose treatment (**Figure 2.3, *A***). The galactose glycopolymers in RAW264.7 cells showed a significant ($p<0.05$) decrease in uptake level with D-galactose competition, whereas uptake was unaffected by the addition of D-mannose **(Figure 2.3, *B*)**. Interestingly, galactose glycopolymer uptake in IL-4 activated BMDM was unaffected by treatment with free D-galactose despite high expression levels of CD301 **(Figure 2.3, *B*)**. This observation may be explained by the overall complexity of the biological system such that different mechanisms of interactions are concurrent[23,58]. Also, subsite association may be occurring such that a second unknown binding site with different affinity and specificity can associate with our multivalent ligands of interest[59]. While the overall results show that glycopolymers are taken-up specifically via receptor-mediated pathways that are dependent on receptor expression level, not surprisingly there are also alternative uptake pathways that deem further exploration.

The corresponding uptake and binding results of the glycopolymer-functionalized nanoparticle liposomes further support the hypothesis that our delivery is carbohydrate receptor-mediated. Of course, some level of non-specific phagocytosis by macrophages is inevitable, as demonstrated by the PEG liposome control. However, glycofunctional liposome uptake is dose dependent **(Figure 2.5 *C, D*)**, suggesting a promising route for more effective intracellular nanoparticle delivery. The results show that despite the presence of non-specific uptake, receptor-mediated targeting allows for a greater influx of particles, while providing the advantages of selectivity and specificity. We further wanted to demonstrate the associated relationship between receptor expression level and liposomal uptake in our ultimate cell of interest, alveolar macrophages. Despite having higher non-specific uptake compared to the surrogate macrophage

cells, the poly(ManEMA-*co*-CMA) decorated liposomes had the greatest uptake level. We also observed uptake of the poly(GalEMA-*co*-CMA) decorated liposomes; however, the uptake level was similar to that of the non-specific PEG liposomes. These initial findings show promise in utilizing glycopolymer incorporated liposomes as nano-delivery carriers for therapeutics.

2.G. Conclusion

Carbohydrate-mediated targeting of functional nanomaterials for therapeutic and diagnostic applications remains an area of active pursuit among the delivery community. We feel that this study yields insight into the role of macrophage phenotype on targeting and uptake of glycofunctional nanomaterials, particularly as it relates to the selection of specific cell lines versus primary cells for use in *in vitro* studies. The RAFT-based synthetic strategy described affords access to material compositions that can be readily tuned, opening the door to additional studies capable of elaborating the roles played by glycan density and conformation on functional nanoparticle bioactivity.

2.H. Acknowledgements

We would like to thank Dr. Liguo Wang and Lige Tonggu for technical support with Cryo-EM imaging and Julia Swanson and Fiona Brown for assisting in carbohydrate monomer synthesis. This work was supported by the Defense Threat Reduction Agency [grant number HDTRA1-13-1-0047]; and by the National Science Foundation Graduate Research Fellowship [DGE-0718124 and DGE-1256082].

2.I. References

1. Medzhitov, R. & Janeway, C. A. J. Innate Immunity: The Virtues of a Nonclonal System of Recognition. *Cell* **91,** 295–298 (1997).
2. Martin, T. R. Recognition of Bacterial Endotoxin in the Lungs. *Am. J. Respir. Cell Mol.*

Biol. **23,** 128–132 (2000).
3. Zhang, J. *et al.* Negative regulatory role of mannose receptors on human alveolar macrophage proinflammatory cytokine release in vitro. *J. Leukoc. Biol.* **78,** 665–74 (2005).
4. Gordon, S. Alternative activation of macrophages. *Nat. Rev. Immunol.* **3,** 23–35 (2003).
5. Fraser, I. P., Koziel, H. & Ezekowitz, R. A. B. The serum mannose-binding protein and the macrophage mannose receptor are pattern recognition molecules that link innate and adaptive immunity. *Semin. Immunol.* **10,** 363–372 (1998).
6. Stahl, P. D. The mannose receptor and other macrophage lectins. *Curr. Opin. Immunol.* **4,** 49–52 (1992).
7. Schlesinger, L. S., Kaufman, T. M., Iyer, S., Hull, S. R. & Marchiando, L. K. Differences in mannose receptor-mediated uptake of lipoarabinomannan from virulent and attenuated strains of Mycobacterium tuberculosis by human macrophages. *J. Immunol.* **157,** 4568–4575 (1996).
8. Schulert, G. S. & Allen, L.-A. H. Differential infection of mononuclear phagocytes by Francisella tularensis: role of the macrophage mannose receptor. *J. Leukoc. Biol.* **80,** 563–571 (2006).
9. Zamze, S. *et al.* Recognition of Bacterial Capsular Polysaccharides and Lipopolysaccharides by the Macrophage Mannose Receptor. *J. Biol. Chem.* **277,** 41613–41623 (2002).
10. Murray, P. J. & Wynn, T. a. Protective and pathogenic functions of macrophage subsets. *Nat. Rev. Immunol.* **11,** 723–737 (2011).
11. Yamazaki, N. *et al.* Endogenous lectins as targets for drug delivery. *Adv. Drug Deliv. Rev.* **43,** 225–244 (2000).
12. Davis, B. G. & Robinson, M. a. Drug delivery systems based on sugar-macromolecule conjugates. *Curr. Opin. Drug Discov. Devel.* **5,** 279–288 (2002).
13. Shriver, Z., Raguram, S. & Sasisekharan, R. Glycomics: a pathway to a class of new and improved therapeutics. *Nat. Rev. Drug Discov.* **3,** 863–873 (2004).
14. Fuster, M. M. & Esko, J. D. The sweet and sour of cancer: glycans as novel therapeutic targets. *Nat. Rev. Cancer* **5,** 526–542 (2005).
15. Gordon, S. & Taylor, P. R. Monocyte and macrophage heterogeneity. *Nat. Rev. Immunol.* **5,** 953–964 (2005).
16. Matsuo, H., Funato, K., Harashima, H. & Kiwada, H. The Complement- but not Mannose Receptor- Mediated Phagocytosis is Involved in the Hepatic Uptake of Cetylmannoside-Modified Liposomes In Situ The Complement- but not Mannose Receptor-Mediated Phagocytosis is Involved in the Hepatic Uptake of Cetylmannosi. *J. Drug Target.* **2,** 141–146 (2008).
17. Umezawa, F. & Eto, Y. Liposome targeting to mouse brain: Mannose as a recognition marker. *Biochem. Biophys. Res. Commun.* **153,** 1038–1044 (1988).
18. Kawakami, S., Sato, A., Nishikawa, M., Yamashita, F. & Hashida, M. Mannose receptor-mediated gene transfer into macrophages using novel mannosylated cationic liposomes. *Gene Ther.* **7,** 292–299 (2000).
19. Chono, S., Tanino, T., Seki, T. & Morimoto, K. Efficient drug targeting to rat alveolar macrophages by pulmonary administration of ciprofloxacin incorporated into mannosylated liposomes for treatment of respiratory intracellular parasitic infections. *J Control Release* **127,** 50–58 (2008).
20. Chono, S. *et al.* Effect of surface-mannose modification on aerosolized liposomal delivery to alveolar macrophages. *Drug Dev. Ind. Pharm.* **36,** 102–107 (2010).
21. Lee, R. T. & Lee, Y. C. Affinity enhancement by multivalent lectin-carbohydrate interaction. *Glycoconj. J.* **17,** 543–551 (2000).
22. Lepenies, B., Lee, J. & Sonkaria, S. Targeting C-type lectin receptors with multivalent

carbohydrate ligands. *Adv. Drug Deliv. Rev.* **65,** 1271–1281 (2013).
23. Gestwicki, J. E., Cairo, C. W., Strong, L. E., Oetjen, K. A. & Kiessling, L. L. Influencing Receptor-Ligand Binding Mechanisms with Multivalent Ligand Architecture. *J. Am. Chem. Soc.* **124,** 14922–14933 (2002).
24. Chiefari, J. *et al.* Living Free-Radical Polymerization by Reversible Addition - Fragmentation Chain Transfer : The RAFT Process. *Macromolecules* **31,** 5559–5562 (1998).
25. Sevimli, S., Sagnella, S., Kavallaris, M., Bulmus, V. & Davis, T. P. Synthesis, self-assembly and stimuli responsive properties of cholesterol conjugated polymers. *Polym. Chem.* **3,** 2057 (2012).
26. Moad, G. *et al.* Living free radical polymerization with reversible addition – fragmentation chain transfer (the life of RAFT). *Polym. Int.* **49,** 993–1001 (2000).
27. Chiefari, J. *et al.* Thiocarbonylthio Compounds (S d C (Z) S - R) in Free Radical Polymerization with Reversible Addition-Fragmentation Chain Transfer (RAFT Polymerization). Effect of the Activating Group Z. *Macromolecules* **36,** 2273–2283 (2003).
28. Hope, M. J., Bally, M. B., Webb, G. & Cullis, P. R. Production of large unilamellar vesicles by a rapid extrusion procedure. Characterization of size distribution, trapped volume and ability to maintain a membrane potential. *Biochim. Biophys. Acta - Biomembr.* **812,** 55–65 (1985).
29. Weischenfeldt, J. & Porse, B. Bone Marrow-Derived Macrophages (BMM): Isolation and Applications. *CSH Protoc.* **2008,** pdb.prot5080 (2008).
30. Redente EF, Higgins DM, Dwyer-Nield LD, Orme IM, Gonzalez-Juarrero M, M. Differential polarization of alveolar macrophages and bone marrow-derived monocytes following chemically and pathogen-induced chronic lung inflammation. *J Leukoc Biol* **88,** 159–168 (2010).
31. Mills, C. D., Kincaid, K., Alt, J. M., Heilman, M. J. & Hill, A. M. M-1/M-2 macrophages and the Th1/Th2 paradigm. *J Immunol* **164,** 6166–6173 (2000).
32. Baenziger, J. U. & Fiete, D. Structural determinants of concanavalin A specificity for oligosaccharides. *J. Biol. Chem.* **254,** 2400–2407 (1979).
33. Green, G. M. & Kass, E. H. The role of the alveolar macrophage in the clearance of bacteria from the lung. *J. Exp. Med.* **119,** 167–176 (1964).
34. Goldstein, E., Lippert, W. & Warshauer, D. Pulmonary alveolar macrophage. Defender against bacterial infection of the lung. *J. Clin. Invest.* **54,** 519–528 (1974).
35. Kobzik, L. *et al.* Nitric oxide synthase in human and rat lung: immunocytochemical and histochemical localization. *Am J Respir Cell Mol Biol* **9,** 371–377 (1993).
36. Wijagkanalan, W. *et al.* Efficient targeting to alveolar macrophages by intratracheal administration of mannosylated liposomes in rats. *J Control Release* **125,** 121–130 (2008).
37. Irache, J. M., Salman, H. H., Gamazo, C. & Espuelas, S. Mannose-targeted systems for the delivery of therapeutics. *Expert Opin. Drug Deliv.* **5,** 703–724 (2008).
38. Bertozzi, C. R. & Kiessling, L. L. Chemical glycobiology. *Science (80-.).* **291,** 2357–2364 (2001).
39. Zhao, Y.-Y. *et al.* Functional roles of N-glycans in cell signaling and cell adhesion in cancer. *Cancer Sci.* **99,** 1304–1310 (2008).
40. Misharin, A. V., Morales-Nebreda, L., Mutlu, G. M., Budinger, G. R. S. & Perlman, H. Flow cytometric analysis of macrophages and dendritic cell subsets in the mouse lung. *Am. J. Respir. Cell Mol. Biol.* **49,** 503–510 (2013).
41. Hussell, T. & Bell, T. J. Alveolar macrophages: plasticity in a tissue-specific context. *Nat. Rev. Immunol.* **14,** 81–93 (2014).
42. Matsunaga, K., Klein, T. W., Friedman, H. & Yamamoto, Y. Alveolar macrophage cell line

MH-S is valuable as an in vitro model for Legionella pneumophila infection. *Am. J. Respir. Cell Mol. Biol.* **24,** 326–331 (2001).
43. Xu, G. *et al.* Hemolytic phospholipase Rv0183 of Mycobacterium tuberculosis induces inflammatory response and apoptosis in alveolar macrophage RAW264.7 cells. *Can. J. Microbiol.* **56,** 916–924 (2010).
44. Saito, Y., Azuma, A., Takizawa, H. & Sugawara, I. Effects of diesel exhaust on murine alveolar macrophages and a macrophage cell line. *Exp Lung Res.* **28,** 201–217 (2002).
45. Guidi-Rontani, C., Weber-Levy, M., Labruyère, E. & Mock, M. Germination of Bacillus anthracis spores within alveolar macrophages. *Mol. Microbiol.* **31,** 9–17 (1999).
46. Xu, Y. *et al.* Toll-like Receptor 4 Is a Sensor for Autophagy Associated with Innate Immunity. *Immunity* **27,** 135–144 (2007).
47. Stephenson, J. D. & Shepherd, V. L. Purification of the human alveolar macrophage mannose receptor. *Biochem. Biophys. Res. Commun.* **148,** 883–889 (1987).
48. Stein, M., Keshav, S., Harris, N. & Gordon, S. Interleukin 4 potently enhances murine macrophage mannose receptor activity: a marker of alternative immunologic macrophage activation. *J. Exp. Med.* **176,** 287–292 (1992).
49. Feghali, C. a & Wright, T. M. Cytokines in acute and chronic inflammation. *Front. Biosci.* **2,** d12–d26 (1997).
50. Aaron, S. D. *et al.* Granulocyte inflammatory markers and airway infection during acute exacerbation of chronic obstructive pulmonary disease. *Am. J. Respir. Crit. Care Med.* **163,** 349–355 (2001).
51. Nathan, C. & Ding, A. Nonresolving Inflammation. *Cell* **140,** 871–882 (2010).
52. Papi, A. *et al.* Infections and airway inflammation in chronic obstructive pulmonary disease severe exacerbations. *Am. J. Respir. Crit. Care Med.* **173,** 1114–1121 (2006).
53. Sethi, S. Bacterial infection in chronic obstructive pulmonary disease in 2000 : a state-of-the-art review. *Clin. Microbiol. Rev.* **14,** 336–363 (2001).
54. Stout, R. D. *et al.* Macrophages sequentially change their functional phenotype in response to changes in microenvironmental influences. *J. Immunol.* **175,** 342–349 (2005).
55. Sica, A. & Mantovani, A. Macrophage plasticity and polarization: in vivo veritas. *J. Clin. Invest.* **122,** 787–795 (2012).
56. Benoit, M., Desnues, B. & Mege, J.-L. Macrophage polarization in bacterial infections. *J. Immunol.* **181,** 3733–3739 (2008).
57. Gordon, S. & Martinez, F. O. Alternative activation of macrophages: Mechanism and functions. *Immunity* **32,** 593–604 (2010).
58. Lis, H. & Sharon, N. Lectins: Carbohydrate-Specific Proteins that Mediate Cellular Recognition. *Chem. Rev.* **98,** 637–674 (1998).
59. Mammen, M., Choi, S.-K. & Whitesides, G. M. Polyvalent Interactions in Biological Systems: Implications for Design and Use of Multivalent Ligands and Inhibitors. *Angew. Chemie Int. Ed.* **37,** 2754–2794 (1998).

3. Chapter 3: Evaluation of glycopolymer ciprofloxacin prodrugs towards targeting host alveolar macrophages

3.A. Abstract

Alveolar macrophages resident to the lung are the predominant effector cells of the pulmonary innate immune response. The macrophages' defensive phagocytic functions make them favorable cells not only for host defense, but paradoxically for pathogen invasion, inhabitation, and infection. Consequently, facultative intracellular bacteria, such as *F. tularensis* and *B. pseudomallei*, lead to severe systemic disease and sepsis, with high morbidity and mortality associated with pulmonary infection. Current clinical treatment involves prolonged antibiotic therapy generally administered orally or intravenously; however, these methods of administration have limitations of systemic dissemination of the antibiotics, leading to exhaustive dosing and unwanted side effects. Pulmonary administration is an efficient method for delivering antibiotics directly to the lung and represents a promising alternative to oral administration. Ciprofloxacin, a fluoroquinolone, is one of the antibiotics orally administered to treat tularemia; however, due to poor solubility in aqueous solutions, ciprofloxacin cannot be delivered via inhalation. Here, we have synthesized mannosylated ciprofloxacin prodrug neoglycopolymers using aqueous RAFT polymerization for efficient pulmonary delivery, targeting, and subsequent internalization in alveolar macrophages. The ciprofloxacin prodrugs have been designed such that sustained antibiotic release occurs via hydrolysis mechanisms. We demonstrate that targeting and enhanced internalization of drug carrier systems is critical for efficient removal of intracellular pathogens.

3.B. Introduction

The severity of public threat posed by certain pathogens requires the Department of Health and Human Services to establish and regulate a list of biological agents and toxins that have potential to harm public health and safety (www.selectagents.gov). Within this list, select agents and toxins are further subcategorized as Tier 1 agents, in which they present the greatest risk of deliberate misuse with significant potential for mass casualties or may present devastating effects to the economy[1]. Two facultative intracellular bacteria, *Burkholderia pseudomallei* and *Francisella tularensis*, are classified as Tier 1 select agents. They are the causative agents of tropical disease melioidosis and tularemia, respectively. Aerosol sprays of select agents are the most likely and effective means of widespread dissemination as infectious material could be easily dispersed, are invisible, and silent[2]. This ultimately highlights the importance for efficacious pulmonary-administered antimicrobial treatments. Fluoroquinolones, particularly ciprofloxacin, have shown excellent microbiological and clinical success in treating *F. tularensis* infections in both children and adults[3–7]. Ciprofloxacin, however, presents several limitations, such as poor aqueous solubility properties and short circulations times[8].

Cells of the innate immune system are the first to encounter and recognize foreign pathogens via pathogen-associated molecular patterns and pattern recognition receptors. In the presence of aerosolized pathogens, alveolar macrophages (AMs) are the first line of innate cellular defense in the lower airways. They are found in the alveoli and constitute 90% of the cellular content in steady state[9]. AMs encounter microbes that are transported to the alveoli via alveolar liquid flow[10]. The key roles that AMs play in immunity are defending against pathogens via their phagocytic ability and immunological homeostasis after infection-mediated damage[11,12]. Both *B. pseudomallei* and *F. tularensis* utilize the cytosol as a niche for replication and to evade the host innate immune response. The ability of many pathogenic bacteria to survive intracellularly

after the invasion of host eukaryotic cells is crucial as the intracellular niche provides protection from several aspects of host immunity, such as antibodies and the complement. Provided that the primary function of innate immune cells is to destroy pathogens, the survival of intracellular pathogens in the cytosol remains a paradox. Their complexity is why intracellular pathogens are a major cause of global morbidity and mortality, and as a result, they establish immediate medical precedence.

In recent years, advances in living polymerization techniques have encouraged the synthesis of precise and complex glycopolymers. Glycopolymers have raised interest as potential drug carriers largely due to their ligand binding ability to carbohydrate receptors, their water soluble properties, polarity, and biocompatibility[13]. Glycopolymers are prepared by direct polymerization of saccharide derived monomers with polymerizable functional groups such as vinyl, or a two-step reaction occurs, such that polymerization with reactive functional groups is first synthesized and a post-glycan conjugation step occurs[14]. Most polymerization techniques involve protective carbohydrate chemistry in which a post-polymerization deprotection step is required. RAFT polymerization enables polymerization in aqueous conditions, thereby bypassing protecting group chemistry[15,16]. Utilizing RAFT polymerization, various polymer architectures have been synthesized such as block copolymers for micellar constructs.

Over the years, prodrugs have become an established strategy to improve physiochemical, biopharmaceutical, and pharmacokinetic properties of otherwise promising drug candidates. They have shown to overcome challenging barriers in drug formulation and delivery such as poor aqueous solubility, chemical instability, rapid systemic metabolism, toxicity, and drug targeting[17]. Recently, polymerizable ciprofloxacin and norfloxacin prodrug monomers have been synthesized bypassing the need for post polymerization conjugation reactions[18,19]. Das *et al*. showed that phenolic ester linkages hydrolyzed significantly faster (~10 days) than aliphatic esters (>35 days). They further demonstrated the ability of the ciprofloxacin monomers to be polymerized into both statistical and block copolymers via RAFT polymerization. Both studies

demonstrated antibacterial efficacy *in vitro* and sustained drug release. These initial results provide exciting room for improvement or modifications, such as the addition of targeting moieties

The mannose receptor presents a promising route for targeted drug delivery. Aside from its non-opsonic phagocytic properties and the fact that CD206 is expressed at high levels on macrophage cells, several other functions and abilities of CD206 allow for an encouraging and relatively new route of targeted drug delivery. The macrophage mannose receptor is a pattern recognition receptor that has high affinity for multivalent mannosylated oligosaccharides, or pathogen-associated molecular patterns, which make it a phagocytic receptor with broad pathogen specificity.

Drawing inspiration from pathogen associated interactions, we have engineered a synthetic multivalent mannose ciprofloxacin prodrug neoglycopolymer for efficient pulmonary delivery, targeting, and subsequent internalization in alveolar macrophage cells. We demonstrate that targeting and enhanced internalization of drug prodrug systems is critical for efficient removal of intracellular pathogens. These results demonstrate a promising modular platform that can be fine-tuned and altered to synthesize a combination of antibiotics and targeting monomers to treat infectious diseases.

3.C. Materials and Methods

Materials were purchased from Sigma-Aldrich unless otherwise specified. All solvents were Fisher HPLC grade.

3.C.1. Ethics statement

All animal procedures and handling were conducted under a protocol approved by the Institutional Animal Care and Use Committee at the University of Washington. C57bl/6 mice were purchased from The Jackson Laboratory.

3.C.2. Cell and bacterial culture

All *in vitro* experiments were conducted using MPI cells, which were generously obtained from Dr.Gyorgy Fejer, Plymouth University and cultured according to previously published methods[20]. In brief, cells were cultured in RPMI media (Gibco) supplemented with 10% fetal bovine serum (FBS), 100 U/ml penicillin, 100 µg/ml streptomycin, and 30ng/ml murine GM-CSF in a 37°C, 5% CO_2 incubator. All *in vitro* infection experiments were done with *Burkholderia thailandensis* E264 cultured in LB media.

3.C.3. Synthesis of monomers

3.C.3.1. Synthesis of 2-(α-D-mannosyloxy)ethyl methacrylate and 2-(β-D-galactosyloxy) ethyl methacrylate

Synthesis of 2-(2',3',4',6'-tetra-*O*-acetyl-α-D-mannosyloxy)ethyl methacrylate and 2-(2',3',4',6'-tetra-*O*-acetyl-β-D-galactosyloxy)ethyl methacrylate

Synthesis was slightly modified from methods described in literature[21]. In Brief, α-D-mannose pentaacetate or β-D-galactose pentaacetate (Sigma-Aldrich) (5.0 g, 12.8 mmol) and 2-hydroxyethyl methacrylate (Sigma-Aldrich) (1.4 ml, 1.5g, 11.5 mmol) were dissolved in anhydrous dichloromethane (20 ml) and sonicated under a blanket of anhydrous N_2 for 5 min. BF_3Et_2O (Sigma-Aldrich) (5.0 ml, 5.75 g, 40.5 mmol) was subsequently added and the solution was sonicated for a further 45 min. The reaction mixture was washed with brine (30 ml), in which the organic layer was then dried over $MgSO_4$ and butylhydroxytoluene was added as an inhibitor. The solvent was removed under reduced pressure to yield crude product.

Synthesis of 2-(α-D-mannosyloxy)ethyl methacrylate and 2-(β-D-galactosyloxy) ethyl methacrylate

Crude 2-(2',3',4',6'-tetra-*O*-acetyl-α-D-mannosyloxy)ethyl methacrylate or 2-(2',3',4',6'-tetra-*O*-acetyl-β-D-galactosyloxy)ethyl methacrylate (2.5 g, 5.5 mmol) was stirred in damp MeOH (20 ml). K_2CO_3 (1.0 g, 7.2 mmol) was added and the reaction was monitored by TLC (9:1, MeCN-H_2O). When the product of methacrylate ester cleavage was seen on TLC (R_f 0.15, approximately 15 min reaction time) the reaction was neutralized by filtering into a flask containing DOWEX 50WX4-200 (Sigma-Aldrich) cation exchange resin and the mixture was stirred for 15 min. The resin was removed via filtration and the solvent was subsequently removed under reduced pressure. The resulting oil was purified by a gradient elution ($CHCl_3$-MeOH) using column chromatography to yield a colorless oil. LR-MS (ES^+) *m/z* requires 315.3, found 314.9 ($M + Na^+$) or 607.56, found 607.0 ($2M + Na^+$).

3.C.3.2. Synthesis of CTM

Synthesis of butanoic acid, 4-[(4-hydroxyphenyl)ethylamino]-4-oxo, 1-(2-methacryloyloxy)ethyl ester (1)

To an ice cold solution of mono-2-(methacryloyloxy)ethyl succinate 9.2 g (40 mmol) in 150 mL CH_2Cl_2, were added *N*-hydroxysuccinimide 4.72 g (41 mmol) and *N*-*N'*-dicyclohexylcarbodimide 9.06 g (44 mmol). After 15 min, the ice bath was removed and the reaction mixture was stirred at room temperature for 16 h. The byproduct dicyclohexylurea was filtered off, and the filtrate was concentrated to 40 mL by evaporating the solvent under reduced pressure. This solution containing the activated NHS ester was directly added to 6.85 g (50 mmol) of 4-(aminoethyl)phenol pre-dissolved in 30 mL *N*,*N*-dimethylformamide, followed by 13.94 mL (0.1 mol) trimethylamine. After stirring for 6 h at RT, the reaction mixture was diluted with 200 mL CH_2Cl_2, and washed with water (2 X 100 mL). The organic layer was dried over anhydrous sodium sulfate and concentrated under reduced pressure. The thick residue obtained was treated with

100 mL diethyl ether, and vigorously stirred for 15 min. Then 75 mL hexane was added, and again stirred well for 10 min. The solvent was carefully decanted and the process was repeated one more time. The product obtained was further purified by flash silica gel column chromatography using 5 % methanol in chloroform. Overall yield for two steps: 11.2 g (80.1 %).

Synthesis of 7-(4-(*tert*-Butoxycarbonyl)piperazin-1-yl)-1-cyclopropyl-6-fluoro-4-oxo-1,4-dihydroquionoline-3-carboxylic acid (Boc ciprofloxacin 2)

To 20 g (60 mmol) of ciprofloxacin in 350 mL of dioxane:water (1:1) was added 90 mL 1N NaOH, followed by 20 g (91.6 mmol) of di-tert-butyl dicarbonate. The reaction mixture was stirred at room temperature for 17 h. The white precipitate obtained was filtered, washed with water and then with acetone. The product was dried under high vacuum overnight. Yield = 25.14 g (96.5 %).

Synthesis of BocCTM

Boc protected ciprofloxacin (**2**) 4.3 g (10 mmol) and N,N-dimethylpyridin-4-amine (DMAP) 1.22 g (10 mmol) were taken in 350 mL of CH_2Cl_2 and cooled to 4 ºC. To this solution, N,N,N',N'-tetramethyl-O-(1*H*-benzotriazol-1-yl)uronium hexafluorophosphate (HBTU) 9.48 g (25 mmol) was added, followed by N,N-diisopropylethylamine 7.0 mL (40 mmol). After 10 min at 4 ºC, the reaction mixture was stirred at RT for 30 min, and then cooled back to 4 ºC. Phenolic monomer **1** 3.49 g (10 mmol) was introduced and the reaction was continuously stirred at 4 ºC for 20 min, and then at RT for 16 h. The reaction mixture was filtered and the filtrate was washed with water (150 mL) and brine (150 mL). The organic phase was dried over anhydrous sodium sulfate and the solvent was evaporated under reduced pressure. The residue was precipitated in diethyl ether, and then purified by silica gel column chromatography using 30 % tetrahydrofuran in chloroform containing 0.1 % triethylamine. Yield = 5.76 g (75.5 %).

Synthesis of CTM

BocCTM 2.29 g (3 mmol) was treated with 25 % trifluoroacetic acid in CH_2Cl_2 (60mL) at 4 ºC, and the resulting solution was stirred at 4 ºC for 5 min, and then at RT for 2h. After evaporating solvent under reduced pressure, oily crude product was triturated with diethyl ether and the insoluble residue was dried under high vacuum to afford CTM. Yield = 2.31 g (99.1%).

3.C.3.3. Synthesis of rhodamine B-ethyl methacrylate

To rhodamine B 5.26 g (11 mmol), N,N'-dicyclohexylcarbodimide 2.88 g (14 mmol) and 4-dimethylaminopyridine 134 mg (1.1 mmol) in CH_2Cl_2 (75 mL), was added 2-hydroxyethyl methacrylate 1.82 g (14 mmol) at 0 °C. After 30 min, the ice bath was removed and the reaction mixture was stirred at room temperature for 16 h. After filtering off the byproduct dicyclohexylurea, the solvent was evaporated under reduced pressure. The residue was redissolved in 30 mL acetonitrile and the insoluble materials were filtered off. The crude product obtained after evaporating acetonitrile was purified by flash column chromatography using 6 % methanol in chloroform (5.89g, 91% yield).

3.C.4 Synthesis of copolymers

3.C.4.1 Aqueous RAFT copolymerization of OHManEMA (Man)/OHGalEMA (Gal) and CTM

The aqueous copolymerization of poly(Man-co-CTM) and poly(Gal-co-CTM) was conducted in 150 mM acetate buffer, pH 5.5. Prior to polymerization, CTM was incubated in the buffer at room temperature for 6 hours to evaluate possible hydrolysis. TLC results indicated that no hydrolysis was occurring (results not shown). Copolymerization proceeded, in which 4-cyano-4-(phenylcarbonothioylthio)pentanoic acid (CTP) and 4,4′-azobis(4-cyanovaleric acid) (V501) were used as the chain transfer agent (CTA) and radical initiator, respectively. CTP (10.76 mg, 0.385M) and V501 (2.16mg, 0.154M) were dissolved in ethanol in separate glass vials. OHManEMA/OHGalEMA (500mg, 0.964M), CTM (167mg, 0.121M), CTP stock, V501 stock, and acetate buffer (1.775mL) were added to a 5mL round bottom flask. The initial monomer to CTA

molar ratio ($[M]_0$:$[CTA]_0$) was 50:1 and the initial CTA to initiator molar ratio ($[CTA]_0$:$[I]_0$) was 5:1. The molar ratio of sugar to CTM ($[sugar]_0$: $[CTM]_0$) was 8:1. For fluorescently labeled polymers, rhodamine B ethyl methacrylate (4.55mg, 4.34mM) was also added into the round bottom flask. The solution was purged in nitrogen for 20 minutes and allowed to react for 3 hours at 70ºC. The resulting copolymer was purified via dialysis at 4ºC in 100mM phosphate buffer, pH 7 with repeated buffer changes (2-3x) daily over a span of 48 hours then dialysate was changed to 4ºC DI water (with repeated changes) for another 48 hours. The polymers were then flash frozen with LN_2 and lyophilized prior to further purification *via* PD-10 desalting columns (GE Life Sciences). The resulting purified copolymers were flash frozen, lyophilized, and stored at -18ºC.

3.C.4.2. RAFT copolymerization of carboxybetaine methacrylate (CBM) and CTM

Copolymerization of tert-butyl protected carboxybetaine methacrylate (tCBM) and CTM was conducted in DMSO at 70 ºC for 18 h in the presence of CTP and ABCVA. The initial molar feed composition by mole was 17.8 % CTM and 82.2 % tCBM (33.33 wt % CTM, 66.66 wt % tCBM). The $[M]_o$:$[CTA]_o$:$[I]_o$) was 25:1:0.2 at an initial monomer concentration of 20 wt. %. To a 10 mL round bottom flask was added tCBM (2.00 g, 5.91 mmol), CTM (1.00 g, 1.29 mmol), CTP (80.5 mg, 0.288 mmol), ABCVA (16.1 mg, 0.0567 mmol), and DMSO (12 mL). The round bottom flask was then sealed with a rubber septa and purged with nitrogen for 1 hour. After this time the polymerization solution was transferred to a preheated water bath at 70 ºC and allowed to react for 18 hours. After this time the solution was precipitated into a 50 times excess of diethyl ether. The precipitate was then redissolved in minimal methanol and then precipitated once more into diethyl ether. This process was repeated five additional times after which the copolymer was dried under high vacuum for 48 hours. The dry polymer was then dissolved in trifluoracetic acid at a polymer concentration of 50 mg/mL for 8 hours. After this time the polymer was precipitated into diethyl ether and dried overnight under high vacuum. The copolymer was then dissolved in phosphate buffer (pH 7.4, 200 mM) at a concentration of 50 mg/ml and dialyzed against 20 mM

phosphate buffer pH 7.4 at 5 ^{o}C. The copolymer was then further purified via PD-10 desalting columns followed by lyophilization. Complete removal of the tBoc protect group was confirmed by ^{1}H NMR.

3.C.5. Polymer characterization

Monomer incorporation was determined by ^{1}H NMR (Bruker AV-500, ($(CD_3)_2S=O$)). Poly(Man-co-CTM) composition was calculated from the resonance of the protons adjacent to the secondary amine on CTM (-NH-(CH_2) (δ 2.73-2.74, peak 8 of Fig. 2), resonance of the protons from the ethyl group between the two ester groups on CTM (-O-(CH_2)-(CH_2)-O-) (δ 4.08, peak 10,11,12 of Fig. 2), and resonance of the protons adjacent to the ester group of the sugar monomers (δ 4.08, peak 10,11,12 of Fig. 2 for poly(Man-*co*-CTM). Poly(Gal-co-CTM) composition was calculated by comparing resonances from protons adjacent to the secondary amine on CTM (-NH-(CH_2) (δ 2.73-2.74, peak 8 of Fig. 2) and resonances from the proton on the anomeric carbons (δ 3.90). Copolymer characterization was further confirmed via ^{19}F NMR. In brief, 5µl of a 2mg/ml solution sodium tri-fluoroacetate ($C_2F_3NaO_2$) was doped as an internal standard into 1ml of a 10 mg/ml polymer solution in C_2D_6OS. Molar composition was determined by comparing the three fluorine resonances from the internal standard (δ -73.3) and the single fluorine resonances from the ciprofloxacin drugs (δ 123.92) polymerized onto the glycopolymers. Molecular weights (M_n), polydispersity indices ($Đ$), and *dn/dc* values were determined by gel permeation chromatography (GPC). Aqueous SEC-MALLS was performed in 150 mM acetate buffer pH 4.4 on a Shodex (Kawasaki, Japan) SB-804 HQ column connected to a Shimadzu (Kyoto, Japan) LC-20AD liquid chromatography pump and Wyatt (Santa Barbara, CA) MiniDawn Treos and Optilab rEX system.

3.C.6. *In vitro* time dependent uptake study of MPI cells

MPI cells were suspended at a density of 10^6 cells/ml and blocked with growth media containing 10% FBS for 30 min at 37˚C. The cells were subsequently treated with 1 μM of rhodamine B fluorescently labeled polymers: poly(Man-co-CTM), poly(Gal-co-CTM), poly(CBM-co-CTM). To ensure identical fluorescence intensity was dosed within all treatment groups, standard curves were created as a function of molarity. Respective non-fluorescently labeled polymers were added to each polymer solution to match the fluorescence intensity of the lowest FI polymer such that the total concentration dosed was 1 μM (thereby ensuring similar FIs at equal concentrations of polymer). Cells were treated with the copolymers for 0.25, 0.5, 1, 2, and 4 hours at 37°C. The cells were centrifuged for 10 min at 400xg at 4°C, washed, and resuspended with cold PBS containing 0.2 % FBS to remove excess polymers in solution that were not bound or internalized. Samples were kept on ice and uptake level was detected via the intensity of rhodamine B under a 586/15 nm Y1 channel on a MACSQuant Analyzer 10 flow cytometer (MACS Miltenyi Biotec) and analyzed using FlowJo software (Tree Star, Inc.).

3.C.7. *In vitro* competition study

MPI and HeLa cells were suspended at a density of 2.5 x 10^5 cells/ 400μl and blocked with growth media containing 10% FBS for 30 min at 37˚C. The cells were subsequently treated with a total of 4mg/ml mannan or 18mg/ml of D-Galactose for 15 minutes at 37°C. The cells were then treated with 1, 5, or 10μg of polymer and allowed to incubate for 3 hours at 37°C. Cells were centrifuged for 10 min at 400xg at 4°C. Supernatant was aspirated and cells were washed with 500 μl cold PBS containing 0.2% FBS. Cells were centrifuged again for 10 min at 400xg at 4°C. Supernatant was aspirated and each sample was resuspended with cold PBS containing 0.2% FBS. Samples were kept on ice and uptake level was detected via the intensity of rhodamine B under a 586/15 nm Y1 channel on a MACSQuant Analyzer 10 flow cytometer (MACS Miltenyi Biotec) and analyzed using FlowJo software (Tree Star, Inc.).

3.C.8. *In vitro* intracellular killing assay

To assess intracellular killing with targeted poly(Man-*co*-CTM), MPI cells were seeded overnight into 24-well plates at 5 x 10^5 cells $well^{-1}$. The macrophage cells were treated with 0.5mg $well^{-1}$ of total ciprofloxacin from the treatment groups (poly(Man-*co*-CTM), poly(Gal-*co*-CTM), poly(CBM-*co*-CTM), and ciprofloxacin HCl (Alfa Aesar) for 4 hours at 37ºC to allow internalization. Cells were subsequently washed 3x with serum-free RPMI media to remove non-internalized drug or polymers and replenished with media. *Burkholderia thailandensis* E264 was taken from an exponentially growing curve (OD_{600} =0.2-0.25). MPI cells were infected with *B. thailandensis* at an MOI of 0.5. After 1 hour, the infected cells were washed 3x with serum-free RPMI media and replaced with 500μg ml^{-1} kanamycin to kill remaining extracellular bacteria. After 1 hour, cells were washed once and replaced with 50 μg ml^{-1} kanamycin to prevent growth of extracellular bacteria. At the end of the incubation period (6 or 24 hours), the macrophages were washed with PBS 3x, and the cells were lysed with 100μl $well^{-1}$ of 0.1% Triton X-100 in PBS. Serial dilutions of the lysate were made in LB media and the total number of surviving intracellular bacteria was determined by plating on LB agar plates (in triplicates). Data is represented as CFU $well^{-1}$. All treatment groups were conducted in triplicate wells.

3.C.9. *In vivo* alveolar macrophage targeting

Eight- to ten- week old female C57bl/6 mice were anesthesized using 5% isoflurane flowed with 1 liter min^{-1} O_2 for 4 minutes. Fluorescently labeled polymer suspension dissolved in PBS, or blank PBS were intratracheally administered to the mice at 50μl doses of 2μM polymer per mouse via a MicroSprayer Aerosolizer (Penn-Century, Inc). After 3 hours, mice were euthanized via CO_2 and bronchoalveolar lavage was conducted with 3.4 ml of DPBS containing 0.1 mM EDTA to extract lung resident macrophages. Lavage fluid was kept on ice, centrifuged at 400xg for 15 minutes, and resuspended in cold PBS with 0.2% FBS. Samples were kept on ice and uptake

level was detected via a 586/15 nm Y1 channel on a MACSQuant Analyzer 10 flow cytometer (MACS Miltenyi Biotec) and analyzed using FlowJo software (Tree Star, Inc.).

3.D. Results

3.D.1. Design of ciprofloxacin prodrug glycoplymers, poly(Man-*co*-CTM) and poly(Gal-*co*-CTM)

Therapies aimed at eliminating intracellular bacteria may improve clinical success. We designed a synthetic glycopolymer containing ciprofloxacin prodrug monomers that selectively internalize in macrophage cells via CD206 and enable cleavage of ciprofloxacin antibiotic via hydrolysis methods. The prodrug glycopolymer consists of carbohydrate monomers **(Figure 3.1-3.7)**, mannose ethyl methacrylate, which result in a multivalent display of the carbohydrate moieties, and phenolic ester ciprofloxacin. This approach allowed for targeted delivery to the macrophage mannose receptor displayed on lung resident macrophages and enabled solubility in aqueous conditions for pulmonary delivery (**Figure 3.8**).

A

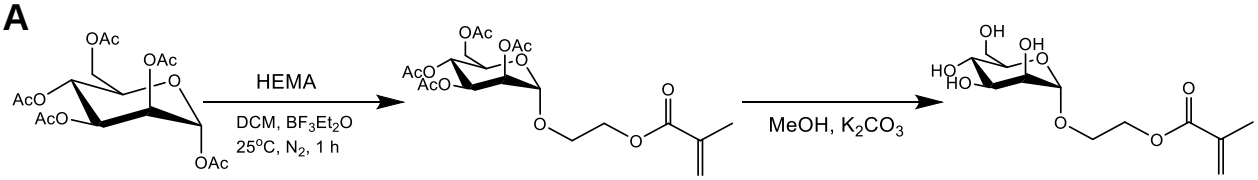

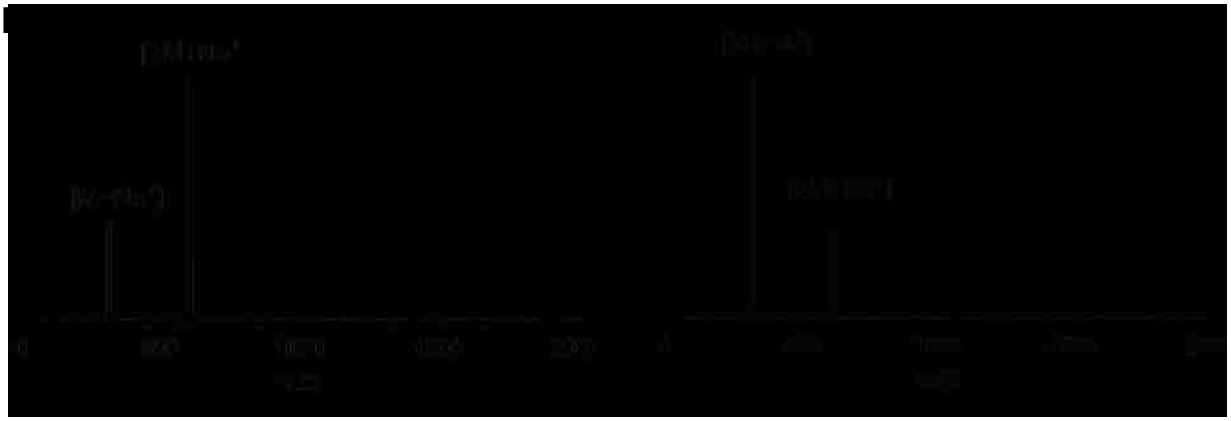

Figure 3.1.
(A) Schematic of the synthesis of OHManEMA and **(B)** ESI-MS of OHManEMA (left) and OHGalEMA (rght).

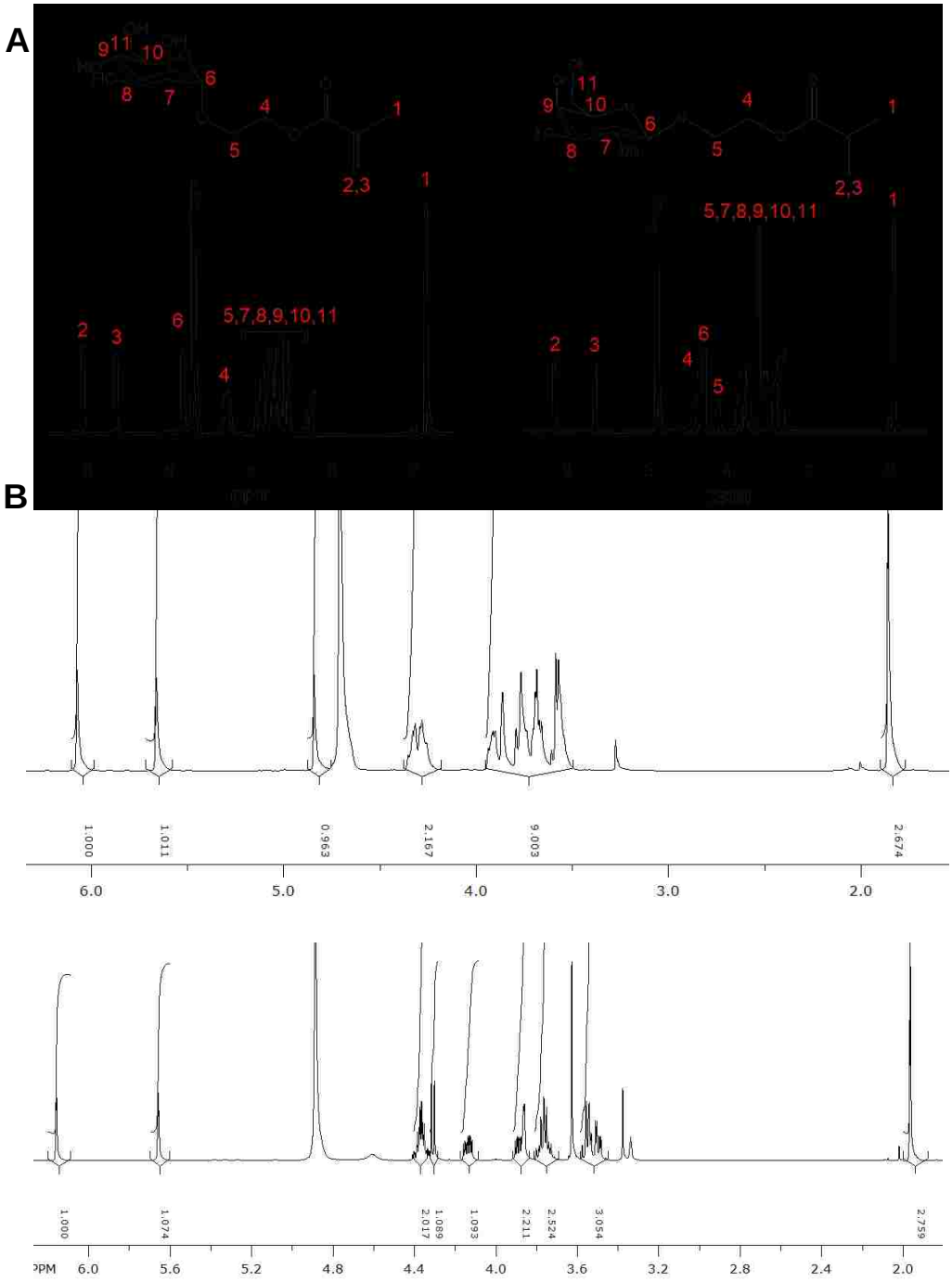

Figure 3.2.
(A) Labeled ^{1}H-NMR spectrum of OHManEMA (left) and OHGalEMA (right) and **(B)** ^{1}H-NMR spectrum peak integration of OHManEMA (top) and OHGalEMA (bottom).

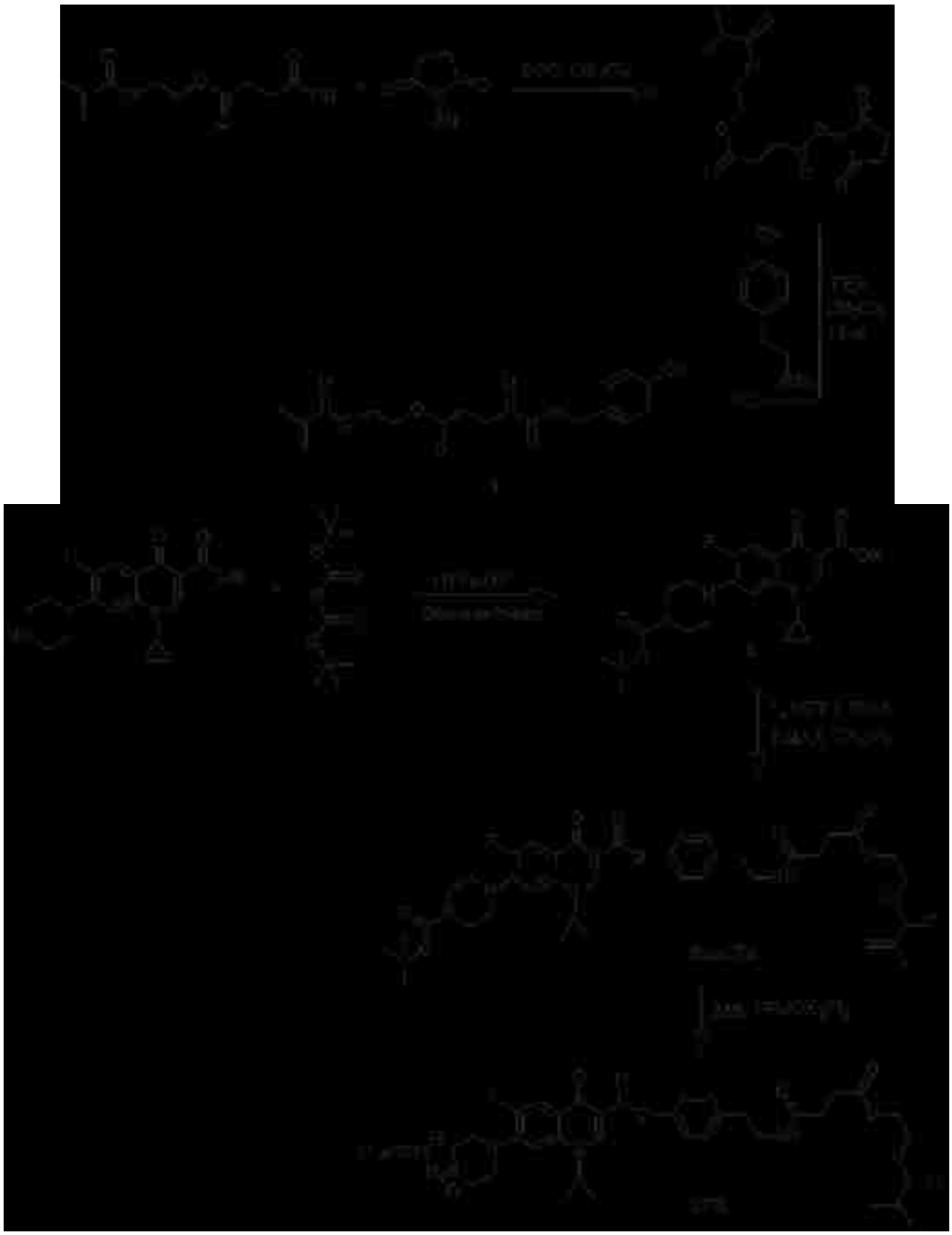

Figure 3.3.
Schematic of the synthesis of butanoic acid, 4-[(4-hydroxyphenyl)ethylamino]-4-oxo, 1-(2-methacryloyloxy)ethyl ester (1), boc ciprofloxacin (2), BocCTM and CTM

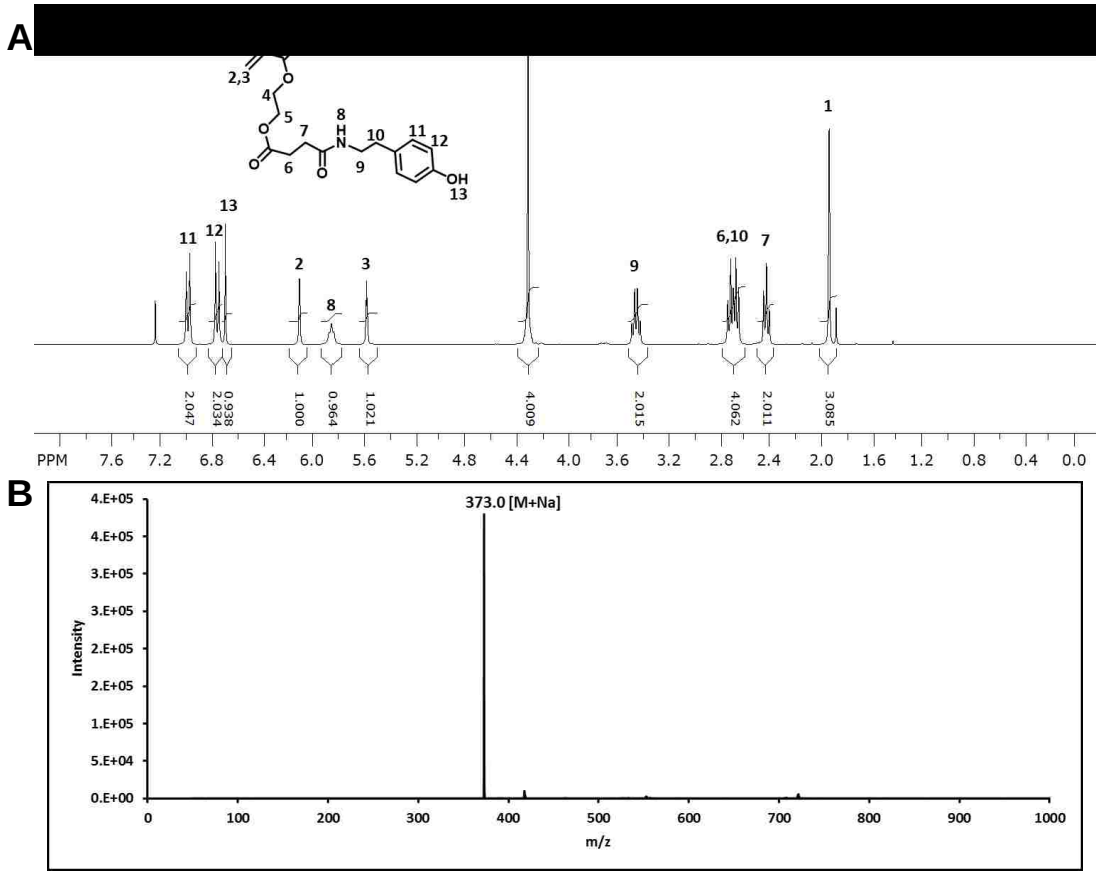

Figure 3.4.
(A) ^{1}H-NMR spectrum of butanoic acid, 4-[(4-hydroxyphenyl)ethylamino]-4-oxo, 1-(2-methacryloyloxy)ethyl ester (1) and **(B)** ESI-Mass spectrum of butanoic acid, 4-[(4-hydroxyphenyl)ethylamino]-4-oxo, 1-(2-methacryloyloxy)ethyl ester (**1**).

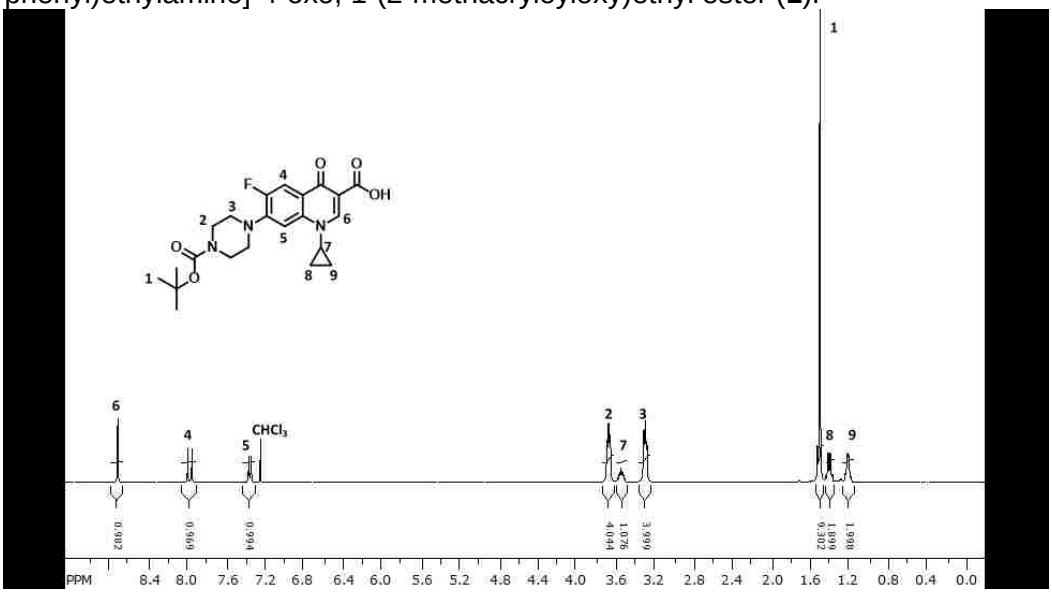

Figure 3.5.
^{1}H-NMR spectrum of boc ciprofloxacin (2).

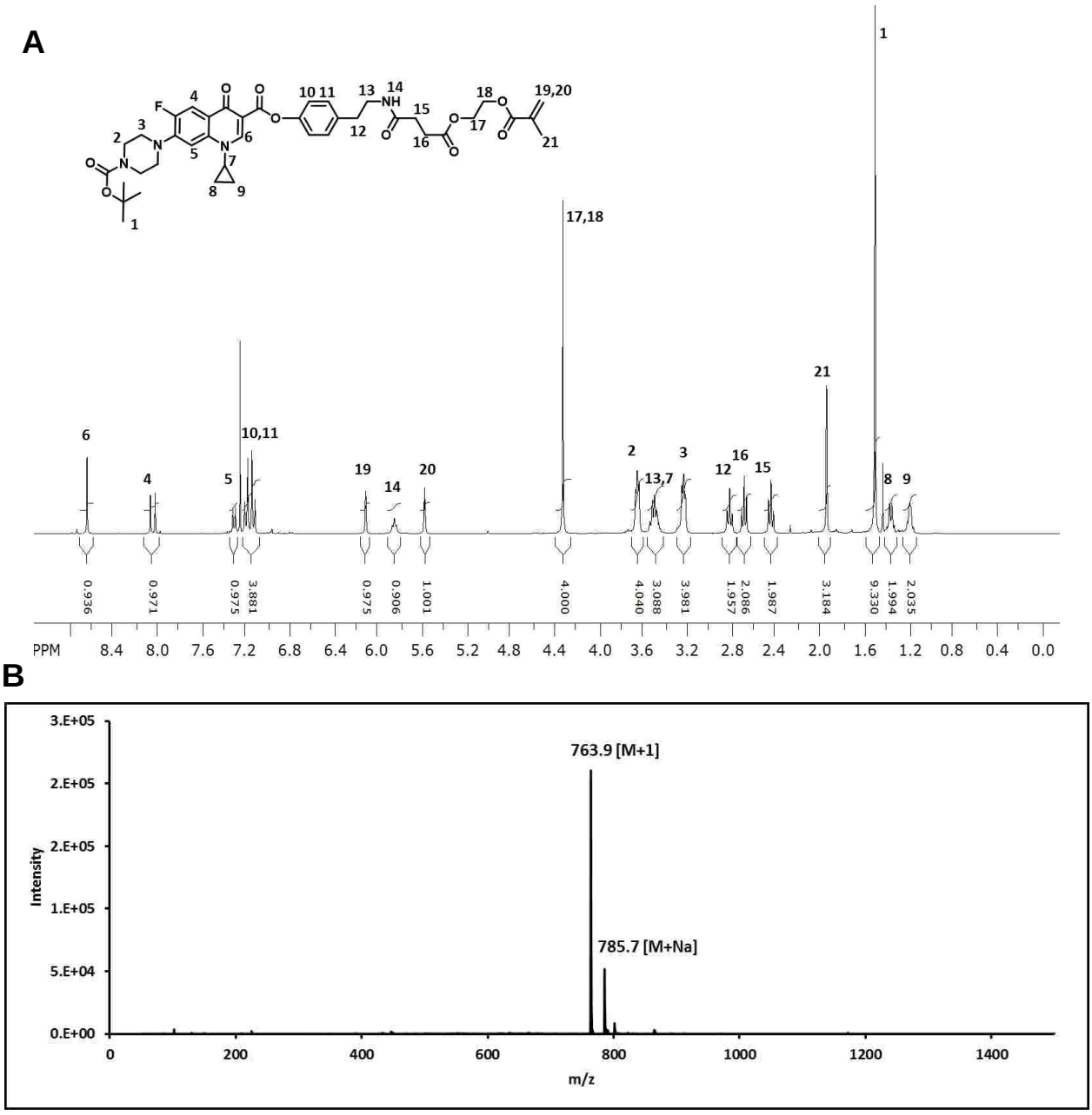

Figure 3.6.
(A) ^{1}H-NMR spectrum of BocCTM and **(B)** ESI-Mass spectrum of BocCTM.

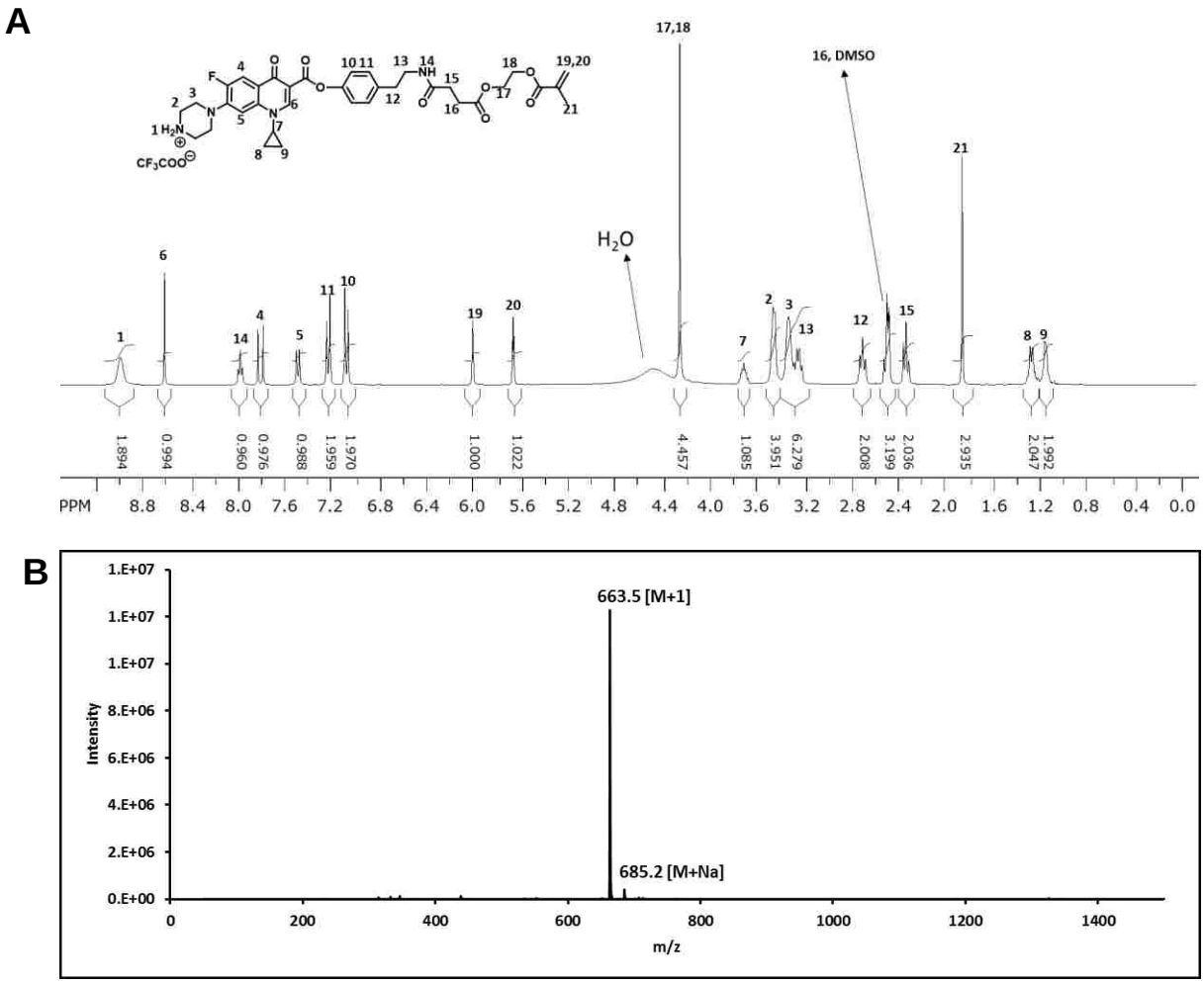

Figure 3.7.
(A) ^{1}H-NMR spectrum of CTM and **(B)** ESI-Mass spectrum of CTM.

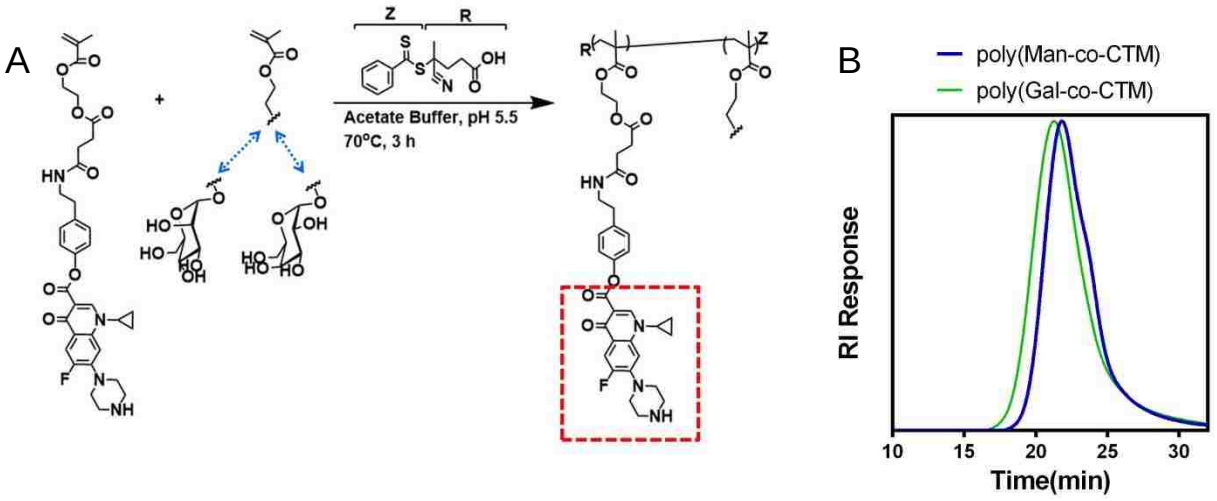

Fig. 3.8 Aqueous RAFT polymerization as a synthetic strategy for the intracellular delivery of ciprofloxacin antibiotics. **(A)** A scheme of the polymerization strategy for the incorporation of OHManEMA, OHGalEMA, and CTM to make the resulting glycopolymer prodrug systems, poly(Man-*co*-CTM) and poly(Gal-*co*-CTM). The resulting copolymers contain phenolic ester functionalized ciprofloxacin monomers that may be cleaved in the presence of esterases and strong acidic environments. (B) The RI traces obtained from SEC equipped with light scattering detectors show narrow molecular weight distributions of both glycopolymers.

Fluoroquinolone classes were chosen since they are broad based antibiotics and have shown promising microbiological and clinical success in treating *F. tularensis* infections in both children and adults[3–7]. Ciprofloxacin, in particular, allowed functionalization for enabling polymerization through the carboxylic acid group. Recently, it was shown that ciprofloxacin linked via phenolic esters showed faster hydrolysis rates (~7 days) than corresponding aliphatic ester linkages (>30 days), therefore, we adopted the phenolic ester linkage into our system.

Poly(Man-*co*-CTM) and non-macrophage targeting poly(Gal-*co*-CTM) were synthesized by aqueous RAFT polymerization, which bypassed harsh deprotection chemistry conditions. Owing to the solubility mismatch between the hydrophobic ciprofloxacin monomer and the glycomonomers, we chose a molar feed ratio glycan:CTM of 8:1 to prevent the hydrophobic CTM from self-assembling into nanoparticles under physiological conditions and allowing multivalent targeting. Ethyl methacrylate functionalized rhodamine B was also polymerized to the

glycopolymers for copolymer uptake studies. Results of glycopolymer characterization are summarized in **Table 3.1**. The glycopolymers synthesized via RAFT polymerization displayed low M_w/M_n values of 1.01 and 1.04 with M_n = 25.5 kDa and 20.7 kDa for poly(ManEMA- *co*-CTM) and poly(GalEMA- *co*-CTM), respectively, as determine by GPC. ^{1}H NMR results indicated a final copolymer composition of 88% ManEMA and 12% CTM, and 86% GalEMA and 14% CTM (**Figure 3.9A-B**). The total ciprofloxacin weight percent was 12% and 14% for mannose and galactose prodrug systems, resulting in approximately 9 ciprofloxacin molecules per polymer. F^{19} NMR was conducted as a secondary measure of ciprofloxacin content as well as a determinant for remnant TFA salts **(Figure 3.9C)**.

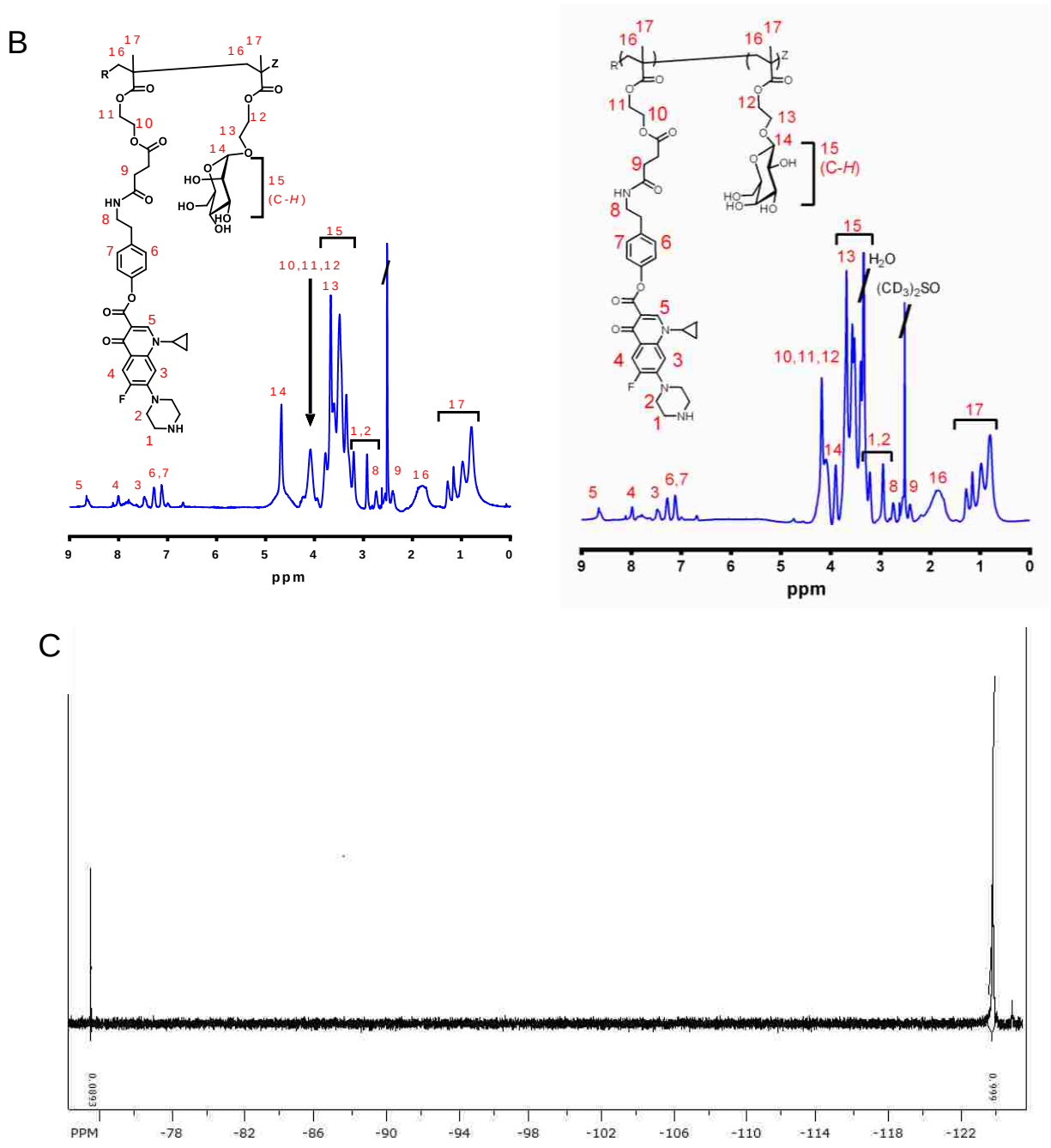

Fig. 3.9 Representative ^{1}H NMR (500 MHz) of **(A)** poly(OHManEMA-*co*-CTM) and **(B)** poly(OHGalEMA-*co*-CTM) with assignment of characteristic resonances associated with the comonomers. Poly(Man-*co*-CTM) composition was calculated from the resonance of the protons adjacent to the secondary amine on CTM (-NH-(CH_2) (δ 2.73-2.74, peak 8), resonance of the protons from the ethyl group between the two ester groups on CTM (-O-(CH_2)-(CH_2)-O-) (δ 4.08, peak 10,11,12), and resonance of the protons adjacent to the ester group of the sugar monomers (δ 4.08, peak 10,11,12). Poly(Gal-*co*-CTM) composition was calculated by comparing resonances from protons adjacent to the secondary amine on CTM (-NH-(CH_2) (δ 2.73-2.74, peak 8) and resonances from the proton on the anomeric carbon (δ 3.90, peak 14). **(C)** F^{19} NMR of poly(Gal-*co*-CTM) to demonstrate internal standard peak and ciprofloxacin peak.

Polymer	Sugar (feed)		Sugar[a] (exp)		CTM (feed)		CTM[a] (exp)		Đ [b]	M_n[b] (kDa)	Drug %	
	wt.	*mol.*	*wt.*	*mol.*	*wt.*	*mol.*	*wt.*	*mol.*			*wt.*	*mol.*
(OHManEMA-*co*-CTM)	75	89	76	88	25	11	24	12	1.01	25.5	13.4	12
(OHManEMA-co-CTM)-•	75	89	78	89	25	11	22	11	1.04	25.5	12.3	11
(OHGalEMA-co-CTM)	75	89	73	86	25	11	27	14	1.04	20.7	15.5	14
(OHGalEMA-co-CTM)-•	75	89	73	86	25	11	27	14	1.06	20.7	15.5	14

Table 3.1.
Summary of feed and experimental composition, molecular weights, and Đ values for statistical glycopolymers of mannose and galactose with CTM. "•" denotes glycopolymers labelled with rhodamine b.
a As determined by ^{1}H NMR in C_2D_6SO as described in Fig. 2
b As determined by size exclusion chromatography (see methods).

3.D.2 Enhanced intracellular delivery of ciprofloxacin with poly(Man-*co*-CTM)

To confirm that poly(Man-*co*-CTM) targeted alveolar macrophages and thereby increased the rate of internalization of prodrug polymers, a time dependent uptake study was conducted with nontransformed murine macrophages, Max Planck Institute (MPI) cells. Fejer et al. generated this relatively new cell line and demonstrated that MPI cells reflected the innate immune characteristics of alveolar macrophages and closely resembled AMs. MPI cells were stained for CD206 and showed high percent of cells positive for the receptor. The cells were dosed with either 20 μg ml^{-1} of fluorescently labelled poly(Man-co-CTM), non-targeted poly(Gal-co-CTM), or non-targeted/non-carbohydrate poly(CBM-co-CTM), in which CBM is a zwitterionic carboxybetaine monomer of similar molecular weight and hydrophilicity as carbohydrate monomers for varying time points of 0.25, 0.5, 1, 2, and 4 hours at 37°C. Polymer prodrug uptake, as measured by cellular fluorescence via a flow cytometer, showed that poly(Man-co-CTM) polymers had approximately 7 times greater rate of intake compared to both non-specific polymers **(Figure 3.10)**. At 4 hours, the total amount of poly(Man-co-CTM) taken up by macrophage cells was almost 8 times greater than poly(CBM-co-CTM) and 3.5 times greater than poly(Gal-co-CTM).

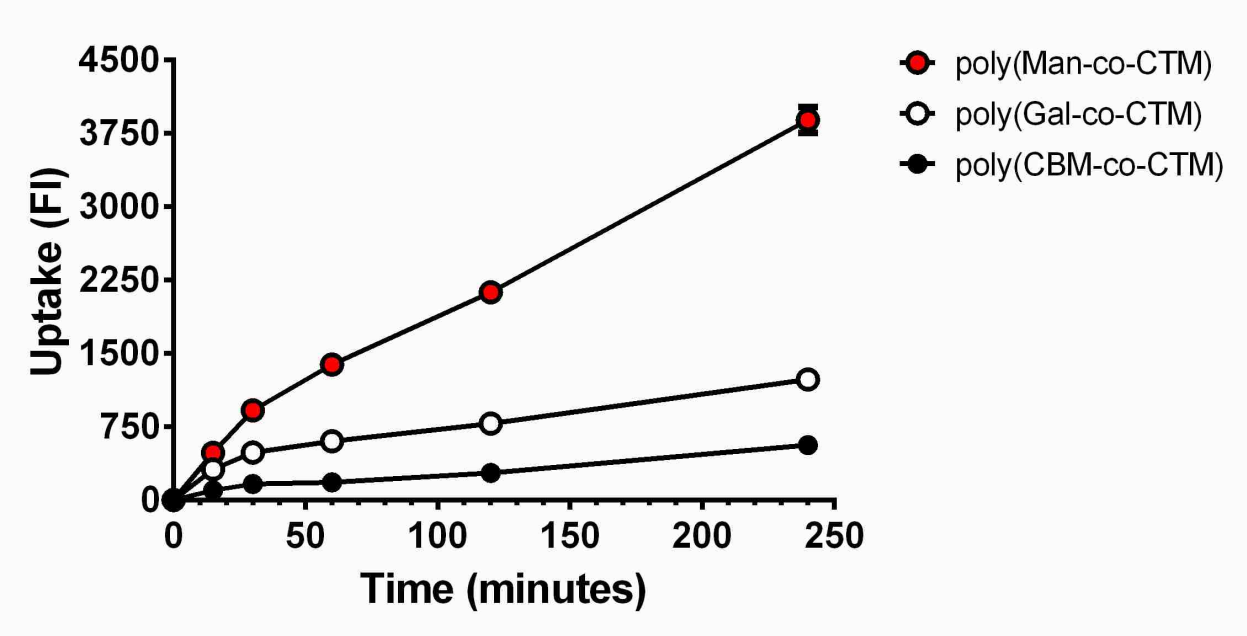

Fig. 3.10 Time-dependent uptake of MPI cells dosed with 20 μg ml^{-1} of fluorescently labelled poly(Man-co-CTM), non-targeted poly(Gal-co-CTM), or non-targeted/non-carbohydrate poly(CBM-co-CTM). The rate of targeted uptake for poly(Man-co-CTM) was significantly greater than the rates of both non-specific polymer prodrugs. Error bars represent means ± s.d. from triplicate samples.

3.D.3 Poly(Man-*co*-CTM) restrict the growth of intracellular *B. thailandensis*

The ability of many pathogenic bacteria to survive intracellularly after the invasion of host eukaryotic cells is crucial as the intracellular niche provides protection from several aspects of host immunity, such as antibodies and the complement and possibly from antibiotic treatment[22]. Poly(Man-*co*-CTM) was tested for its efficacy in killing intracellular bacteria **(Figure 3.11A)**. To determine whether preferentially targeting macrophage cells via CD206 could prevent the spread of intracellular infections, MPI cells were prophylactically dosed with 500 μg ml^{-1} of total ciprofloxacin in poly(Man-co-CTM), poly(Gal-co-CTM), or poly(CBM-co-CTM) or 500 μg ml^{-1} of free ciprofloxacin for 4 hours to allow internalization. After 4 hours, the MPI cells were infected with *B. thailandensis* E264 for 6 hours and 24 hours at an MOI of 05. After 6 hours of infection, only free ciprofloxacin showed efficacy in killing almost all intracellular bacteria, whereas all other

treatment groups showed little efficacy in killing intracellular bacteria **(Figure 3.11B, *left*)**. At 24 hours, however, poly(Man-*co*-CTM), showed approximately 10^3 times less viable intracellular bacteria compared to poly(CBM-co-CTM) and 10^4 times less viable intracellular bacteria compared to poly(Gal-*co*-CTM) **(Figure 3.11B, *right*)**. More importantly, at 24 hours a re-emergence of bacteria was seen for infected MPI cells treated with free ciprofloxacin. Poly(Man-*co*-CTM) and free ciprofloxacin treatment had similar viable CFU well^{-1} at 24 hours, with about a 10 times difference. MPI cells were also infected for 48 hours; however, all bacteria had infiltrated the no treatment, poly(Gal-co-CTM), and poly(CBM-co-CTM) groups resulting in no intracellular bacteria to count.

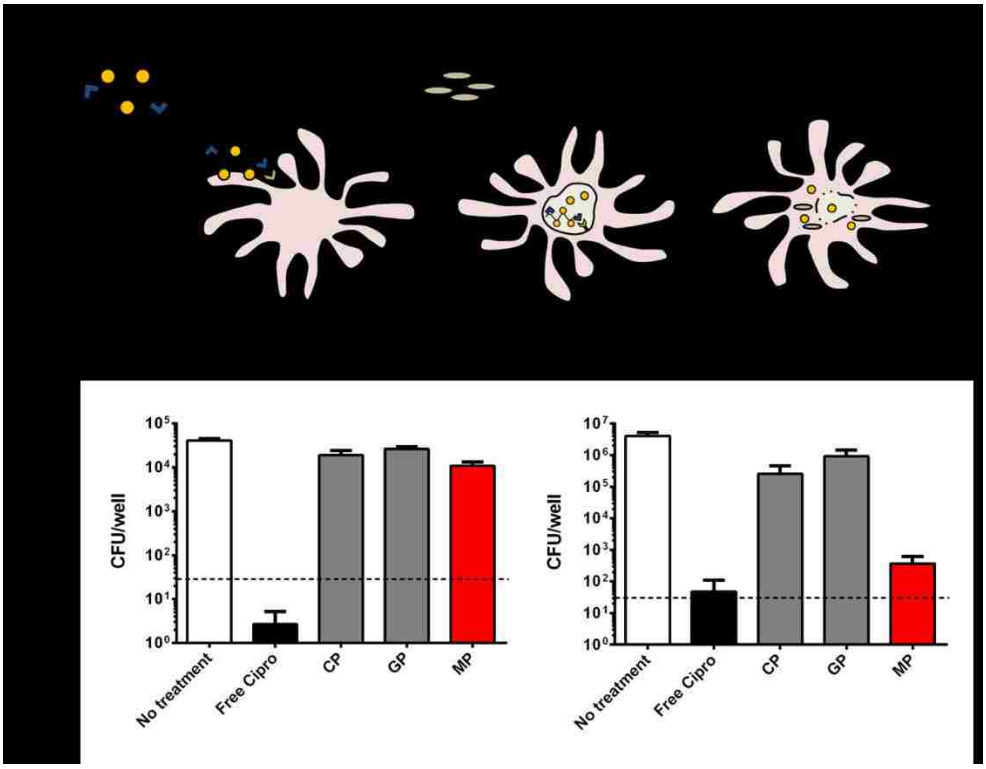

Fig. 3.11
(A) Experimental design for the intracellular killing assay to demonstrate targeted delivery and intracellular antimicrobial efficacy of poly(Man-*co*-CTM) **(B)** Intracellular killing assay in which MPI cells were pre-treated with no drug, 500 μg ml^{-1} free ciprofloxacin, or 500 μg ml^{-1} total ciprofloxacin in poly(Gal-co-CTM), poly(CBM-co-CTM), or poly(Man-co-CTM) to allow internalization. Cells were then infected with *B. thailandensis* E264 for 6 (*left*) and 24 (*right*) hours. Surviving intracellular bacteria were counted in terms of viable CFU well^{-1}. Error bars represent means ± s.d. from triplicate wells. Dashed lines indicate the limit of detection. Data representative of 2 biological replicates.

3.D.4 Mechanism of poly(Man-*co*-CTM) internalization is via CD206

To confirm that CD206 mediates poly(Man-*co*-CTM) internalization in macrophage cells, mannan and galactose were selected as receptor-binding and non-specific competitive inhibitors, respectively. In the competition assay, increasing the ratio of mannan competitor to polymer led to significantly greater inhibition of poly(Man-*co*-CTM) uptake (58%, 68%, and 85%; $P \leq 0.0001$), whereas the presence of galactose did not affect uptake significantly (**Figure 3.12B**). HeLa cells, which lack CD206, showed no uptake inhibition of poly(Man-*co*-CTM) in the presence of either mannan or galactose (**Figure 3.12C**). The uptake of poly(Man-*co*-CTM) in the presence of mannan was further compared to the competitive effect of mannan on negative control polymers, poly(Gal-*co*-CTM) and poly(CBM-*co*-CTM). A significant difference in uptake ($P \leq 0.0001$, $P \leq 0.01$) was observed for poly(Man-*co*-CTM) when compared to the control polymers, such that mannan only inhibited the uptake of the mannosylated ciprofloxacin polymers (**Figure 3.12A**). Non-CD206 targeting polymers, poly(Gal-*co*-CTM) and poly(CBM-*co*-CTM, were also evaluated for inhibited uptake in the presence of mannan and negative control competitor, D-galactose **(Figure 3.12D-E)**. For both polymers, neither mannan nor D-galactose led to a prominent inhibition of uptake.

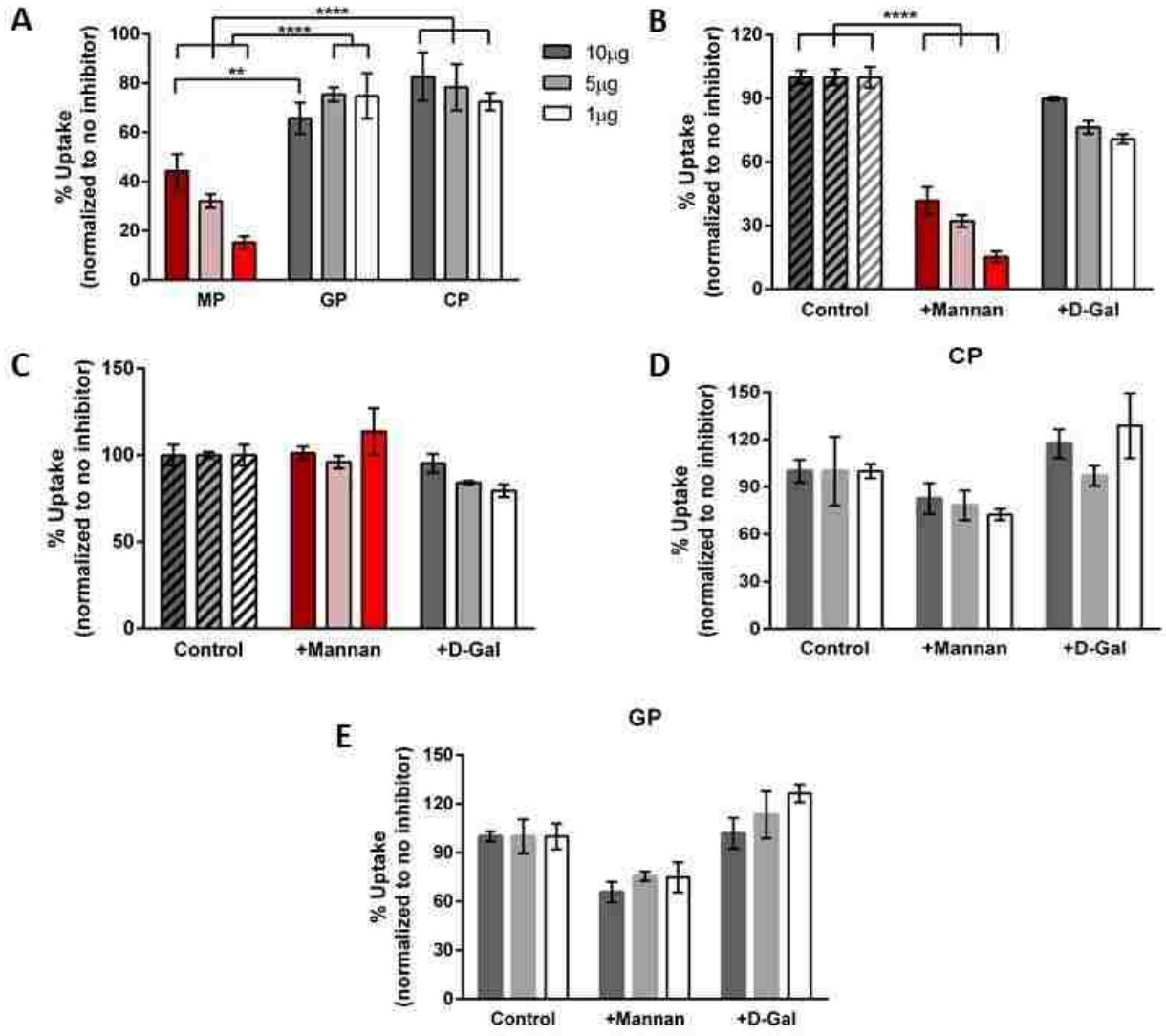

Figure 3.12.
(A) Competition assay comparing poly(Man-*co*-CTM), poly(Gal-*co*-CTM), and poly(CBM-*co*-CTM) with inhibitor mannan. Polymer groups were dosed at 1, 5, or 10µg after MPI cells were incubated with 4mg/ml mannan competitor. **(B)** Competition assay of poly(Man-*co*-CTM) using CD206 receptor-binding and non-specific competitive inhibitors, mannan (4mg/ml) and galactose (18mg/ml), respectively in MPI macrophage cells and **(C)** HeLa cells. The cells were treated with 1, 5, or 10µg of polymer. Competition assay of negative control polymers **(D)** poly(CBM-*co*-CTM) and **(E)** poly(Gal-*co*-CTM) in the presence of inhibitors mannan and D-galactose negative control. Error bars represent means ± s.d. from triplicate samples. (***P* ≤ 0.01, *****P* ≤ 0.0001 analyzed by one-way ANOVA, Dunnett's multiple comparison test).

3.D.5 Enhanced delivery of poly(Man-*co*-CTM) to alveolar macrophage cells in mice

Owing to the promising results for *in vitro* uptake studies with MPI cells, poly(Man-*co*-

CTM) was intratracheally administered to c57bl/6 mice to determine *in vivo* targeting efficacy towards alveolar macrophage cells. The uptake of poly(Man-*co*-CTM) was compared to both poly(Gal-*co*-CTM) and poly(CBM-*co*-CTM), in which 50µl of 2µM of each fluorescently labeled polymer was administered via an aerosole microsprayer to the lungs of mice **(Figure 3.13A)**. 3 hours after administration, alveolar macrophage cells were collected via bronchoalveolar lavage. The percentages of cells positive for fluorescence, and equivalently positive for polymer uptake, were 64% for mice dosed with poly(Man-*co*-CTM), 34% with poly(Gal-*co*-CTM), and 25% with poly(CBM-*co*-CTM) (**Figure 3.13B**). Out of the cell populations positive for fluorescence, the alveolar macrophage cells from mice treated with poly(Man-*co*-CTM) had the greatest content of internalized polymer ($P \leq 0.0001$) as detected via fluorescence intensity (**Figure 3.13C**).

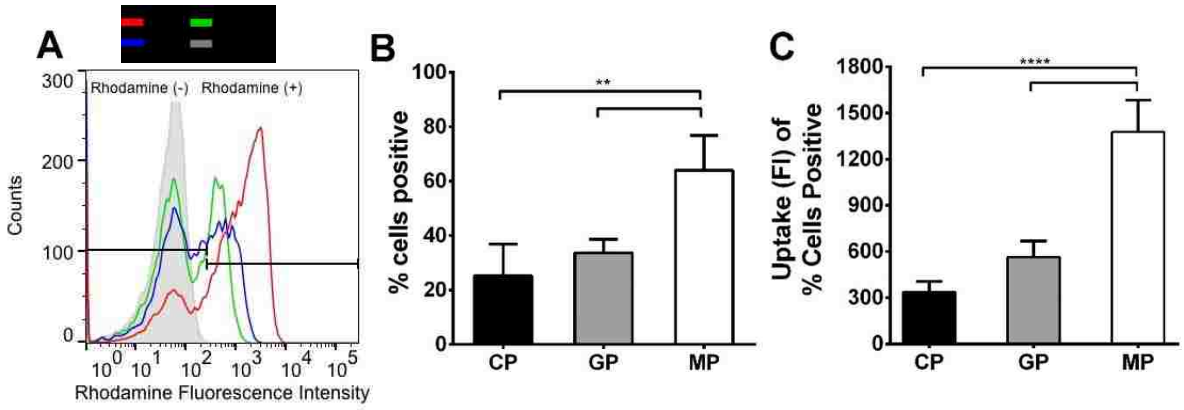

Fig. 3.13
Poly(Man-*co*-CTM), poly(Gal-*co*-CTM), and poly(CBM-*co*-CTM) were intratracheally administered to wild type c57bl/6 mice. A dose of 50µl of 2µM concentration of rhodamine labeled polymers was delivered to the lungs. **(A)** Uptake of polymer treatment groups were compared to PBS treated mice and gated for negative or positive fluorescence. **(B)** Percentage of cells positive for fluorescence was compared for each polymer prodrug treatment group. **(C)** Cells that were positive for polymer uptake, as indicated by fluorescence detection, were further sub-gated and measured for their fluorescence intensity. The uptake of poly(Man-*co*-CTM) was 2.4 times greater than poly(Gal-*co*-CTM) uptake and 4.1 times greater than poly(CBM-*co*-CTM) uptake. Data represent median values ± s.d. (3 mice per group). Significant differences between uptake as measured by fluorescent intensity between treatment groups were analyzed by one-way ANOVA, Tukey's multiple comparison test. (** $P \leq 0.01$, **** $P \leq 0.0001$).

3.E. Discussion & conclusion

Ciprofloxacin was modified into a polymerizable prodrug monomer, such that it is inactive in its polymerized form, but when hydrolyzed becomes an active drug. Phenolic esters were used as the linkage group as they have been shown to be hydrolyzed quickly[23–26]. Mannose monomers were synthesized and subsequently polymerized with the ciprofloxacin monomer to produce copolymers yielding multivalent neoglycopolymer prodrugs. Monomeric interactions with receptors are generally weak due to weak interactions including hydrogen bonds, hydrophobic interactions, and electrostatic interactions[14]. The mannose receptor has multiple interactions that are achieved through having multiple active CRDs in a single polypeptide[27]. The affinity for oligosaccharides is in the micromolar range as a result of the binding of multiple sugar units to extended binding sites on the receptors. Multivalency has shown to lead to significantly higher binding affinities[28], thereby allowing synthetic strategies such as glycopolymers to be utilized for targeted drug delivery. Not only do glycosylated carriers exhibit biological functionality, but these synthetic materials are generally water-soluble, highly polar, and biocompatible[13].

When macrophage cells were treated with poly(Man-*co*-CTM), the rate of uptake was significantly greater than the rate of uptake of non-targeted controls, poly(Gal-*co*-CTM) and poly(CBM-*co*-CTM). This agrees with the recycling ability and high expression level of CD206[29,30], thereby allowing significantly greater amounts of polymeric prodrugs internalized. Research has shown that following internalization, receptors are continually recycled back to the cell surface, or that a group of CD206 stays present within cells and is rapidly and continually replacing those which have been internalized. Internalization of prebound ligand occurs very rapidly at 37ºC ($t_{1/2}$<5 min) and following internalization, binding activity is rapidly recovered ($t_{1/2}$<5 min)[29]. Enhanced uptake may lead to smaller required doses of drugs or therapies sufficient for clinical effects, thereby reducing the toxicity of administered substances.

The importance of internalization rates and rapid recycling of the macrophage mannose receptor was further demonstrated in the ability of poly(Man-*co*-CTM) to prevent intracellular

infection (**Figure 3.11**) whereas non-targeted polymer prodrugs, poly(Gal-*co*-CTM) and poly(CBM-*co*-CTM) were inefficacious towards killing intracellular bacteria. More interestingly, at 24 hours a re-emergence of viable intracellular bacteria was seen in the free ciprofloxacin treatment group, whereas the number of viable intracellular bacteria in the poly(Man-*co*-CTM) treatment group had declined, indicating that targeting and sustained release of antibiotics may play an important role in preventing intracellular bacterial infections.

Competition studies with mannan confirmed that the increased intracellular delivery and subsequent improved efficacy of poly(Man-*co*-cipro) in macrophage cells was mechanistically through the endocytic macrophage mannose receptor. In the competition studies, the percentage of uptake correlated with the ratio of competitor to polymer. As the ratio increased, the percentage of uptake decreased, which further validated receptor-mediated uptake. Two negative controls were evaluated alongside our treatment groups. The first control studied was a negative control cell line, HeLa cells, which lack CD206 receptors. HeLa cells showed no preferential changes in poly(Man-*co*-cipro) uptake in the presence of mannan or D-galactose. The second set of controls tested were negative control polymer groups. Poly(Gal-*co*-cipro) was chosen as a non-targeting carbohydrate analogue to poly(Man-*co*-cipro), while Poly(CBM-*co*-cipro) was a non-carbohydrate negative control. Both polymers showed no inhibition of uptake in the presence of mannan. These results combined confirmed that poly(Man-*co*-cipro), specifically, was being internalized into macrophage cells via CD206. This targeted polymeric prodrug system is a promising drug delivery platform to combat intracellular macrophage infections.

3.F. References

1. General FAQ's about select agents and toxins. *Federal Select Agent Program* (2014).
2. Kortepeter, M. G. & Parker, G. W. Potential biological weapons threats. *CDC Emerg. Infect. Dis.* **5,** (1999).
3. Meric, M. *et al.* Evaluation of clinical, laboratory, and therapeutic features of 145 tularemia cases: the role of quinolones in oropharyngeal tularemia. *APMIS* **116,** 66 (2008).
4. Limaye, A. P. & Hooper, C. J. Treatment of tularemia with fluoroquinolones: two cases and review. *Clin. Infect. Dis.* **29,** 922 (1999).
5. Chocarro, A., Gonzalez, A. & Garcia, I. Treatment of tularemia with ciprofloxacin. *Clin. Infect. Dis.* **31,** 623 (2003).
6. Johansson, A., Berglund, L., Gothefors, L., Sjostedt, A. & Tarnvik, A. Ciprofloxacin for treatment of tularemia in children. *Pediatr. Infect. Dis. J.* **19,** 449–453 (2000).
7. Perez-Castrillon, J. L., Bachiller-Luque, P., Martin-Luquero, M., Mena-Martin, F. J. & Herreros, V. Tularemia epidemic in northwestern Spain: clinical description and therapeutic response. *Clin. Infect. Dis.* **33,** 573–576 (2001).
8. CIPRO® (ciprofloxacin hydrochloride) Tablets. Drug Fact Sheet. *Bayer Pharmaceuticals Corporation* (2004). Available at: http://www.fda.gov/downloads/Drugs/EmergencyPreparedness/BioterrorismandDrugPreparedness/UCM130802.pdf.
9. Kopf, M., Schneider, C. & Nobs, S. P. The development and function of lung-resident macrophages and dendritic cells. *Nat Immunol* **16,** 36–44 (2015).
10. Westphalen, K. *et al.* Sessile alveolar macrophages communicate with alveolar epithelium to modulate immunity. *Nature* **506,** 503–506 (2014).
11. Holt, P. G., Strickland, D. H., Wikström, M. E. & Jahnsen, F. L. Regulation of immunological homeostasis in the respiratory tract. *Nat. Rev. Immunol.* **8,** 142–152 (2008).
12. Aderem, A. & Underhill, D. M. Mechanisms of phagocytosis in macrophages. *Annu. Rev. Immunol.* **17,** 593–623 (1999).
13. Stenzel, M. H. RAFT polymerization: an avenue to functional polymeric micelles for drug delivery. *Chem. Commun. (Camb).* 3486–3503 (2008). doi:10.1039/b805464a
14. Miura, Y. Design and synthesis of well-defined glycopolymers for the control of biological functionalities. *Polym. J.* **44,** 679–689 (2012).
15. Lowe, A. B., Sumerlin, B. S. & McCormick, C. L. The direct polymerization of 2-methacryloxyethyl glucoside via aqueous reversible addition-fragmentation chain transfer (RAFT) polymerization. *Polymer (Guildf).* **44,** 6761–6765 (2003).
16. Albertin, L., Stenzel, M. H., Barner-Kowollik, C., Foster, L. J. R. & Davis, T. P. Well-defined diblock glycopolymers from RAFT polymerization in homogeneous aqueous medium. *Macromolecules* **38,** 9075–9084 (2005).
17. Rautio, J. *et al.* Prodrugs: design and clinical applications. *Nat. Rev. Drug Discov.* **7,** 255–270 (2008).
18. Dizman, B., Elasri, M. O. & Mathias, L. J. Synthesis, characterization, and antibacterial activities of novel methacrylate polymers containing norfloxacin. *Biomacromolecules* **6,** 514–520 (2005).
19. Das, D. *et al.* RAFT polymerization of ciprofloxacin prodrug monomers for the controlled intracellular delivery of antibiotics. *Polym. Chem.* **7,** 826–837 (2015).
20. Fejer, G. *et al.* Nontransformed, GM-CSF-dependent macrophage lines are a unique model to study tissue macrophage functions. *Proc. Natl. Acad. Sci. U. S. A.* **110,** E2191-8

(2013).
21. Spain, S. G. & Cameron, N. R. The binding of polyvalent galactosides to the lectin Ricinus communis agglutinin 120 (RCA120): an ITC and SPR study. *Polym. Chem.* **2,** 1552 (2011).
22. Cossart, P. & Sansonetti, P. J. Bacterial Invasion: The Paradigms of Enteroinvasive Pathogens. *Science (80-.).* **304,** 242–248 (2004).
23. D'Souza, A. J. M. & Topp, E. M. Release from polymeric prodrugs: Linkages and their degradation. *J. Pharm. Sci.* **93,** 1962–1979 (2004).
24. Oh, S. S. *et al.* Synthetic aptamer-polymer hybrid constructs for programmed drug delivery into specific target cells. *J. Am. Chem. Soc.* **136,** 15010–15015 (2014).
25. Biswas, S. *et al.* Biomolecular robotics for chemomechanically driven guest delivery fuelled by intracellular ATP. *Nat. Chem.* **5,** 613–20 (2013).
26. Amir, R. J. *et al.* Multifunctional trackable dendritic scaffolds and delivery agents. *Angew. Chemie - Int. Ed.* **50,** 3425–3429 (2011).
27. Taylor, M. E. & Drickamer, K. Structural requirements for high affinity binding of complex ligands by the macrophage mannose receptor. *J. Biol. Chem.* **268,** 399–404 (1993).
28. Lee, R. T. & Lee, Y. C. Affinity enhancement by multivalent lectin-carbohydrate interaction. *Glycoconj. J.* **17,** 543–551 (2000).
29. Stahl, P., Schlesinger, P. H., Sigardson, E., Rodman, J. S. & Lee, Y. C. Receptor-mediated pinocytosis of mannose glycoconjugates by macrophages: characterization and evidence for receptor recycling. *Cell* **19,** 207–215 (1980).
30. Chen, J. *et al.* Nanostructured glycopolymer augmented liposomes to elucidate carbohydrate-mediated targeting. *Nanomedicine Nanotechnology, Biol. Med.* **12,** 2031–2041 (2016).

4. Chapter 4: *In vivo* efficacy of targeted glycopolymer ciprofloxacin prodrugs to combat intracellular pathogens

4.A. Abstract

Ciprofloxacin, a fluoroquinolone antibiotic, has shown microbiological and clinical success in treating *F. tularensis* infections; however, current standards of treatment involve high frequency administrations of intravenous injections and oral tablets. Common treatment dosing regimens involve 14 days of 400mg IV twice daily followed by 500mg orally twice daily. For post exposure prophylaxis or immediate exposure to the pathogen 14 days of 500mg of oral ciprofloxacin twice daily is usually recommended. The reason for the high frequency dosing lies in the poor pharmacokinetics of free drugs, in which maximum serum concentrations for oral ciprofloxacin tablets are attained 1 to 2 hours after oral dosing and the serum elimination half-life in human patients with normal renal function is approximately 4 hours. Furthermore, in a mass casualty setting, IV treatment may not be a practical option. *F. tularensis* is a classified Tier 1 select agent that, if weaponized, will lead to high morbidity and mortality associated with pulmonary infection. Pulmonary administration is an efficient method for delivering antibiotics directly to the lung and represents a promising alternative to oral administration. Here, we evaluate the efficacy of synthetic aerosolizable targeted ciprofloxacin polymer prodrugs in treating lethal pulmonary intracellular *F. novicida* infections in mice models. We demonstrate that mannosylated ciprofloxacin polymeric prodrugs lead to significantly better protection against lethal infections. The critical factor for these observations lies in significantly improving the pharmacokinetic and pharmacodynamic properties of ciprofloxacin through our targeted polymeric prodrug system.

4.B. Introduction

Francisella tularensis is a highly infectious intracellular pathogen and the causative agent of the life-threatening disease tularemia. As low as 25 colony-forming units can cause illness in 50% of individuals contacted, and half of these cases would result in a 25% case-fatality rate[1]. After 3-5 days of bacterial incubation in a host, the onset of disease is rapid which includes clinical symptoms of fever, chills, malaise, sore throat, and headache[2]. *F. tularensis* primarily infect macrophage cells and are able to escape the phagosome and replicate in the cytosol[3]. Aerosol sprays of select agents are the most likely and effective means of widespread dissemination as infectious material could be easily dispersed, are invisible, and silent[4]. This ultimately highlights the importance for efficacious pulmonary-administered antimicrobial treatments.

Antimicrobial therapy is the current standard of treatment; however, there are currently no specific antibiotic approaches or set regimens. More critical, there are currently no approved inhaled antibiotic treatments to combat pulmonary biowarfare agents. With the introduction to antibiotics and antimicrobial treatment, mortality from tularemia has decreased from about 60% in severely ill patients with pneumonia or typhoidal disease to less than 5%[5,6]. Fluoroquinolones, particularly ciprofloxacin, have shown excellent microbiological and clinical success in treating *F. tularensis* infections in both children and adults[7–11]. Although tetracyclines such as doxycycline have excellent pharmacokinetic properties, some clinicians prefer fluoroquinolones given their lower likelihood of relapse[7,12,13]. Oral administration of ciprofloxacin has been noted as the preferred therapeutic strategy in a mass casualty setting[14,15]. Ciprofloxacin, however, presents several limitations, such as poor aqueous solubility properties and poor pharmacokinetic and pharmacodynamic properties, which lead to exhaustive dosing regimens at high concentrations[16]. No preferential accumulation at target tissues occurs, therefore proper therapeutic levels at target tissue sites, such as the lungs, may not be reached. This failure to eradicate the pathogens leads to persistence of infection and the emergence of bacterial resistance. Therefore, engineering an

inhaled ciprofloxacin product would provide high antibiotic concentrations in the lung and potentially prevent the development of resistance.

Current developments in drug delivery technology have enabled the improvement of ciprofloxacin as an inhalable drug. Several ciprofloxacin drug delivery systems developed by Aradigm Corp. are currently in clinical phase I and II trials. The technology utilizes liposome formulations to encapsulate ciprofloxacin for pulmonary delivery. The advantages provided by Aradigm Corporation's technology include longer retention times of ciprofloxacin in the lung, enabling pulmonary delivery of ciprofloxacin, decreasing serum peak concentrations, and treatment of mice infected with *F. tularensis*[17]. However, the system presents several limitations. Pharmacokinetic studies showed that retention of ciprofloxacin in the lungs following inhalation or intranasal instillation lasted at most 24 hours indicating that frequent doses may be needed for successfully combating respiratory bioagents. The retention time is due to the limited sustained release of drugs from liposomal constructs in which burst release is often seen. Ultimately, an inhaled ciprofloxacin drug delivery system which provides a sustained release profile in the lung with drug concentrations above the MIC for a longer period of time may have superior antimicrobial effects.

Herein, we have engineered a synthetic multivalent mannose ciprofloxacin prodrug neoglycopolymer for efficient pulmonary delivery, targeting, and subsequent internalization in alveolar macrophage cells. We demonstrate that targeting and enhanced internalization of prodrug systems is critical for efficient removal of intracellular pathogens. The physiochemical, pharmacokinetic, and pharmacodynamic properties of ciprofloxacin have been significantly improved via our polymeric prodrug system. Aerosol delivery of the targeted polymeric prodrugs into the lungs of infected mice showed protection against lethal intracellular *F. novicida* infections compared to free ciprofloxacin. These results demonstrate that multivalent targeted ciprofloxacin prodrug copolymers are promising synthetic delivery platforms to combat intracellular pathogens in alveolar macrophages.

4.C. Materials and Methods

Materials were purchased from Sigma-Aldrich unless otherwise specified. All solvents were Fisher HPLC grade.

4.C.1. Ethics statement

All animal procedures and handling were conducted under a protocol approved by the Institutional Animal Care and Use Committee at the University of Washington. C57bl/6 mice were purchased from The Jackson Laboratory.

4.C.2. *In vivo* evaluation of lung inflammation after intratracheal administration

Polymers were prepared by dissolving in PBS pH 7.4 and sterile filtered using 0.22µm syringe filters. Ciprofloxacin hydrochloride was dissolved in Nanopure water and NaCl was added to maintain a 150mM physiological saline solution. The pH was brought up to a maximum of approximately 5.0-5.35 via NaOH. Any pH above that threshold led to precipitation of ciprofloxacin.

Eight-week old female C57bl/6 mice were intratracheally dosed with 50µl of 40mg kg^{-1} of total ciprofloxacin for 3 consecutive days. On days 0, 1, 2, 3, and 4 mice were observed for weight and behavioral change. Mice were euthanized on day 4 (24 hours after the third administration), and lungs were lavaged with 3.4 ml of DPBS containing 1 mM EDTA to obtain macrophages and neutrophils and subsequently harvested. Lavage fluid was kept on ice, centrifuged at 400xg for 15 minutes, and resuspended with 500 µl cold RPMI supplemented with 10% FBS. 250µl of cells were mounted onto glass slides via a Cytospin 3 Cytocentrifuge (Shandon), and slides were allowed to dry. Slides were then stained for HC2 (red) and HC3 (purple). Cell counts were randomized across the slide until a total of 200 cells were counted per slide. The total percentage of neutrophils per mouse lavage was calculated as such: N/(N+M) x 200 where N is the number

of neutrophils counted and M is the number of macrophage cells counted. The remaining 250 µl of lavage fluid were kept for tumor necrosis factor (TNF)-α analysis. The harvested mice lungs were homogenized with 2ml of PBS using a TissueRuptor 115V probe homogenizer (Qiagen). After 30 minutes of allowing the homogenization slurry to settle, the homogenized lungs were centrifuged at 5000xg for 15 minutes. The supernatant was collected and analyzed for TNF-α.

4.C.3. ELISA for quantification of TNF- α in lung lavage fluid and lung tissue

ELISA experiments were performed using standard protocols provided by the vendor for Mouse TNF-α ELISA MAX kits (BioLegend). Briefly, plates were pre-coated with capture antibody and blocked with assay diluent. Lung tissue homogenates were diluted 1.5x with assay diluent. Plates were then incubated with the lung tissue homogenate samples and lung bronchoalveolar lavage fluid. Detection antibody was added to each well, followed by avidin-HRP. The concentrations of TNF-α in both the lung tissues and lavage fluid were calculated by using a calibration curve that was generated with known concentrations of TNF-α standards provided by the manufacturer.

4.C.4. *In vivo F. novicida* U112 challenge studies

Wild type C57bl/6 mice (8-weeks old) were treated with three total doses of aerosolized polymeric prodrugs or free ciprofloxacin on indicated days intratracheally via a Microsprayer Aerosolizer (PennCentury). For pulmonary infection, mice were exposed to aerosolized bacteria via MiniHEART hi-flo nebulizer (Westmed, Arizona, USA). The pressure and environment was controlled by the Biaera Whole-Body Chamber system attached to the nebulizer (Biaera Technologies, Maryland, USA). Bacterial deposition in each experiment was determined from quantitative culture of lung tissue from mice euthanized immediately after infection. Animals were examined daily for health, body weight, and temperature. Abdominal surface temperatures were measured using a Ranger MX4P digital infrared thermometer (Raytek, Santa Cruz, CA, USA). Ill

animals with temperatures <26 °C, body weight loss of greater than 20% with health exceptions, or a combination of ruffled fur, eye crusting, hunched posture, lack of resistance to handling, and isolation from other caged mice were deemed terminal for study purposes and euthanized. Mice surviving 14 days after the third treatment dose were euthanized. Lung, liver, and spleen were harvested and viable bacteria were plated and counted. Bacterial suspensions were serially diluted and plated onto TSB agar plates for quantitative culture. Colonies were counted after incubation at 37 °C for 48 h.

4.C.5. Biodistribution of poly(Man-*co*-CTM) and poly(Gal-*co*-CTM) after intratracheal administration in mice

Eight-week old female C57bl/6 mice were anesthesized with isoflurane and intratracheally dosed with 50µl of 40mg kg^{-1} of total ciprofloxacin incorporated in the rhodamine labeled polymers. Mice were sacrificed at time points of 0.5, 1, 2, 4, 8, 18, 24, 48, and 72 hours via CO_2 and secondary euthanasia was conducted via cardiac exsanguination for terminal blood collection. Immediately after death, lungs, liver, kidney, and spleen were harvested and placed in 2ml reinforced tubes, each filled with 6 2.8mm ceramic beads (Omni International) and 1ml of cold Nanopure water. Tissues were kept on ice until further processing. Plasma was separated and collected from blood by centrifuging the BD PST plasma tubes (BD Biosciences) for 10 minutes at 10000xg at room temperature. Tissue were homogenized using an Omni Bead Ruptor 24 shaken for 25 seconds at 24 ºC. Tissues were subsequently placed back onto ice to allow cooling, and homogenized again on the Omni Bead Ruptor 24. This was repeated for a total of 3 homogenization cycles per tissue sample to ensure full homogenization. Protein was precipitated in all samples by adding 200µl of ice-cold methanol to 100µl of tissue homogenate. Samples were vortexed for at least 1 minute and centrifuged at 18000xg for 15 minutes at 4ºC. The supernatant was analyzed for fluorescent content using a TECAN plate reader at 560 nm excitation and 586 nm emission. The amount of polymers in plasma and each organ were calculated by comparing

to standard curves of fluorescently labeled polymers, in which 100µl of each standard concentration was also added 200µl of methanol. Linearity was established from 0 to 0.56 mg ml^{-1}.

4.C.6. Pharmacokinetics of free ciprofloxacin and ciprofloxacin released from polymer prodrugs after intratracheal administration

Administration of polymers to mice were identical to the methods described in the biodistribution section. After tissue homogenization, homogenate were then diluted 10x with Nanopure H_2O (all except spleen and serum). 300µl aliquots were taken out and 10µl of 500ng ml^{-1} internal standard ciprofloxacin-d8 (CDN Isotopes) stock was added and vortexed. Protein was precipitated with a 3x dilution of ice-cold ACN. Samples were vortexed for at least 1 minute and centrifuged at 18000xg for 15 minutes at 4ºC. The supernatant was collected and stored on ice until analyzed for ciprofloxacin via LC-MS/MS.

To determine the pharmacokinetics of ciprofloxacin in alveolar macrophage cells, 8-week old C57bl/6 female mice were intratracheally administered with polymer groups as mentioned previously. At specified time points, mice were euthanized via CO_2, and bronchoalveolar lavage was conducted to collect lung resident macrophage cells. The lavage solution was kept on ice until centrifugation at 400xg for 15 minutes. The supernatant was aspirated, and the cell pellet was washed with PBS. The cell suspension was centrifuged at 400xg for 15 minutes, and the supernatant was aspirated. The cell pellet was resuspended in 50µl of PBS. An aliquot of 5µl of cell suspension was taken and diluted 10x into a 1% crystal violet with 0.1M citric acid solution for erythrocyte lysis. Macrophage cells were counted and used to determine the total cell volume. The average mouse alveolar macrophage cell volume is 493±161 x 10^{-9} µl[18]. Therefore, the total cell volume collected was calculated. 5µl of 500ng ml^{-1} internal standard ciprofloxacin-d8 stock was added and vortexed. The 50µl of cell suspension (with internal standard) was diluted 2x in ice-cold ACN and incubated for 1 hour to lyse the cells. The cell solution was vortexed and

centrifuged at 18000xg for 20 minutes at 4ºC. The supernatant was collected and stored on ice until analyzed for ciprofloxacin via LC-MS/MS.

Ciprofloxacin was separated on an Agilent 1290 Infinity LC system (Agilent Technologies) under gradient elution using a Hypersil GOLD PFP column (100mm x 2.1 mm internal diameter, 1.9µm particle size) (Thermo Scientific). The column was maintained at room temperature. The mobile phase was a mixture of (A) Nanopure H_2O containing 10mM formic acid and (B) acetonitrile containing 10mM formic acid at a flow rate of 0.3 ml min^{-1}. Ciprofloxacin was eluted with a gradient of 10%-100% B over 4 minutes followed by 1 min 100% B, then 0.1 minute to 10% B to re-equilibrate the column for 1.9 min. The injection volume was 10µl.

The 6460 Triple Quad mass spectrometer (Agilent Technologies) was operated in a positive ion multiple reaction-monitoring (MRM) mode. The ciprofloxacin precursor (Q1) ion monitored was 332 *m/z* and the product (Q3) ion monitored was 288.1 *m/z* with collision energy at 13 eV. Internal standard ciprofloxacin-d8 precursor (Q1) ion monitored was 340 *m/z* and the product (Q3) ion monitored was 296.2 *m/z* with collision energy at 13 eV. The MS/MS setting parameters were as follows: nozzle voltage 500V, capillary voltage 4500V, nebulizer gas 45psi, gas temperature 350 ºC, dwell time 150ms.

4.D. Results

4.D.1. Evaluation of lung inflammation upon intratracheal administration of poly(Man-*co*-CTM)

Prior to conducting exhaustive *in vivo* studies, poly(Man-co-CTM) was evaluated for potential lung inflammation after intratracheal administration along with non-targeted control polymer poly(Gal-co-CTM). More importantly, we were interested in evaluating potential lung

inflammation for free ciprofloxacin delivery to the lungs (**Figure 4.1**). Due to ciprofloxacin's limited solubility in aqueous physiological conditions, ciprofloxacin is currently administered only via intravenous (I.V.) injections or oral tablets. However, in order to more properly compare pharmacokinetics of released drug from poly(Man-co-CTM) with free ciprofloxacin, we believe that the same route of administration was crucial to experimental design. Because ciprofloxacin alone did not dissolve in water, ciprofloxacin hydrochloride was used and readily dissolved in 150mM saline solution. The pH was adjusted to the highest possible pH of 5 without precipitating out the ciprofloxacin. Any pH higher than that led to instability of cipro in aqueous conditions. However, because the pH was below the normal physiological pH of 7.4, we evaluated intratracheal administration of free ciprofloxacin for potential lung inflammation.

Four factors were taken into consideration for evaluating lung inflammation: weight change of the mice, % neutrophil count compared to macrophages, and tumor necrosis factor (TNF)-α content in both lung lavage fluid and lung tissue. A total of three 50 µl doses of 40 mg kg^{-1} of ciprofloxacin were administered for each treatment group including a PBS group, each 24 hours apart, to replicate the dosing scheme of our *in vivo* challenge experiments. Weights of mice were measured on all days prior to administration, and on the day of euthanasia. The percent of weight change was compared between the first day prior to administration and the fourth day in which the mice were euthanized. None of the treatment groups showed statistically different weight change percentages. Lung edema and acute phases of inflammation result in an influx of neutrophils into the bronchoalveolar space, therefore we analyzed for neutrophil to macrophage ratios in bronchoalveolar lavage fluid[19–21]. The ratio of neutrophils to macrophage cells was really low and not statistically different between treatment groups. The last factor for analyzing lung inflammation was comparing TNF-α concentrations between drug treatment groups with the PBS negative control group. TNF-α is a cell signaling protein involved in systemic inflammation and a sign for acute phase reaction. None of the polymer groups tested showed TNF- α concentrations

indicative of tissue inflammation. The overall results show that the polymer prodrugs are safe for pulmonary administration up to 40mg kg^{-1}.

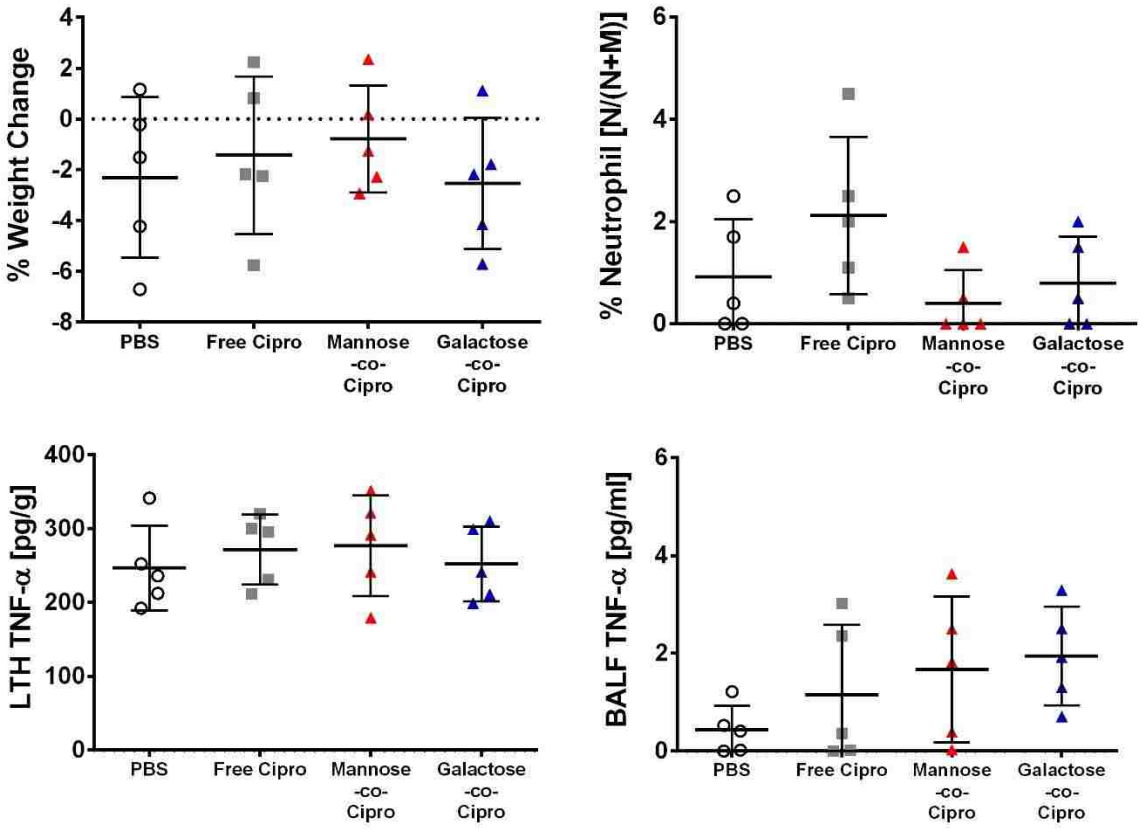

Figure 4.1 Lung inflammation was evaluated after intratracheal administration of 50 µl of 40 mg kg^{-1} ciprofloxacin antibiotic, total ciprofloxacin in poly(Man-co-CTM), total ciprofloxacin in poly(Gal-co-CTM), or PBS treatment in mice. Factors for evaluating lung inflammation involved **(A)** percent weight change of mice between the day of the first administration and the day of euthanasia, **(B)** percent neutrophils compared to macrophages in lung lavage fluid, and TNF-α concentration in **(C)** lung tissue homogenate **(D)** bronchoalveolar lavage fluid.

4.D.2. Targeted polymeric ciprofloxacin prodrug efficacy in lethally infected mice models

To evaluate the antibacterial effect of targeted mannose ciprofloxacin polymeric prodrugs on intracellular infections, poly(Man-*co*-Cipro) was tested in murine models of pulmonary infection. To mimic air-borne routes of infection, C57bl/6 mice were challenged with a lethal dose of *Francisella novicida*, murine counterparts of *F. tularensis*, via a nebulizing. Poly(Man-*co*-Cipro) and controls, poly(Gal-*co*-Cipro) and free ciprofloxacin, were intratracheally administered to the

lungs of mice a total of three times via aerosol delivery either before or after bacterial infection to ensure that the drug was successfully delivered. The survival of the mice was monitored over the course of 14 days after the third drug administration. Lung, spleen, and liver were harvested from mice that survived 14 days after the last drug administration and plated to determine viable bacteria surviving after treatment.

In order to determine whether the targeted and intracellular delivery of poly(Man-*co*-Cipro) enabled prophylactic efficacy, mice (n=8) were dosed with 20mg/kg of total ciprofloxacin in poly(Man-*co*-Cipro) or controls one day before infection. A second dosing of the antibiotic systems was administered the morning before infection, in which the mice were subsequently challenged with a lethal dose of *Francisella novicida* (deposition 194 ± 37 CFU/lung). A third dosing of the polymer prodrugs or free ciprofloxacin was administered 24 hours later, giving a total of 3 administrations. Poly(Man-*co*-Cipro) provided the best protection against *Francisella novicida* (with 4 out of 8 mice surviving) compared to the controls, free ciprofloxacin and glycan control poly(Gal-*co*-Cipro). Within five days after infection, none of the mice treated with free ciprofloxacin survived. Mice treated with non-targeting poly(Gal-*co*-Cipro) showed a 25% survival (2 out of 8 mice) **(Figure 4.2A)**.

A second challenge study was performed to evaluate the post-infection efficacy of the mannose polymeric prodrugs. In this study, mice (n=8) were dosed with 40mg/kg of total ciprofloxacin in poly(Man-*co*-Cipro) or controls on the same day as infection (deposition 556 ± 195 CFU/lung). A second and third administration of the treatment groups were delivered, each 24 hours apart. As observed with the prophylactic study, poly(Man-*co*-Cipro) provided the best protection against *Francisella novicida* **(Figure 4.2B)**. In this post-infection treatment study, 87.5% (7 out of 8) of the mice survived demonstrating that targeted poly(Man-*co*-Cipro) prodrug systems provided nearly complete protection against F. novicida challenge. Mice treated with free ciprofloxacin had negligible protection against the infection, with none of the mice surviving past 10 days after the last antibiotic treatment. Non-targeting poly(Gal-*co*-Cipro) provided mild

protection against *F. novicida* infections, with a survival rate of 25%. For both survival studies, 4 days after infection, the body weight and clinical health signs of mice treated with free ciprofloxacin significantly deteriorated compared to mice treated with the polymeric prodrugs **(Figure 4.2 C,D)**. The extent of weight loss correlated with the clinical health of the mice as observed with the free ciprofloxacin group, whereas the mice treated with polymeric prodrugs had less weight loss. The overall results demonstrate that having a polymeric prodrug version of ciprofloxacin improved protection against *Francisella novicida*.

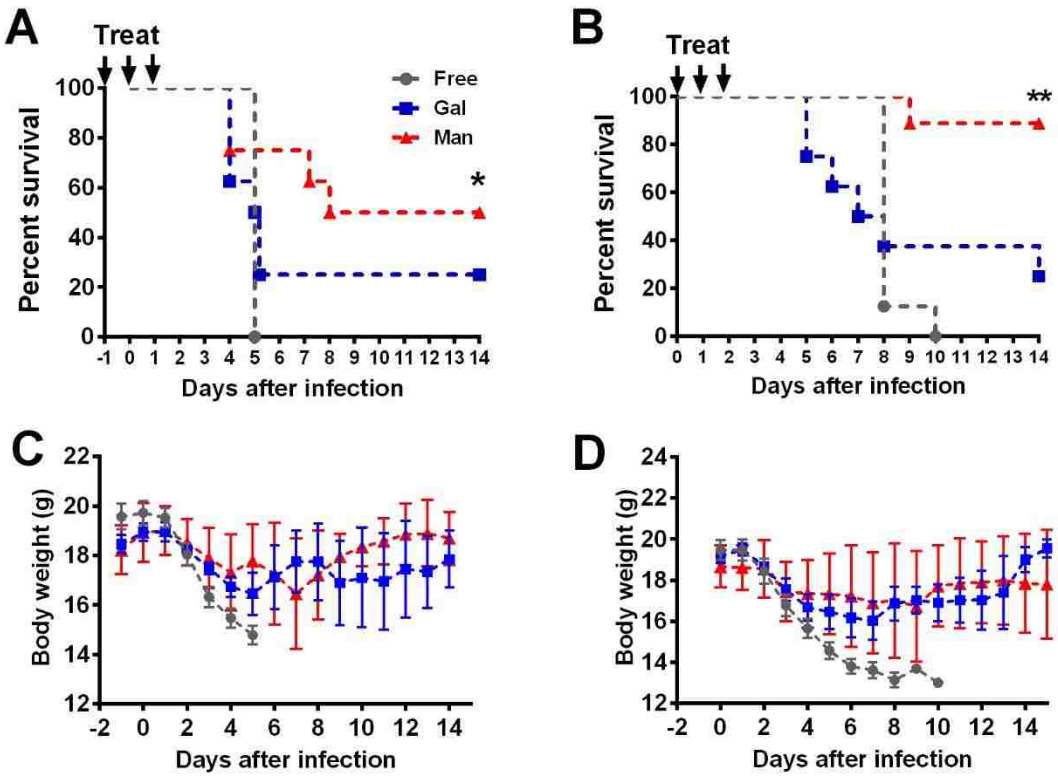

Figure 4.2 Protection against lethal mice F. novicida challenge

(A) The prophylactic efficacy of poly(Man-*co*-CTM) was studied in wild type mice (n=8 per group). Mice were treated with 20mg kg^{-1} of indicated polymeric prodrugs or free ciprofloxacin once daily for a total of three administrations via aerosol delivery to the lungs. The first two administrations were administered before challenging the mice with a lethal dose of F. novicida. The third administration was dosed 24 hours after the second. Protection against infection was monitored by survival of mice 14 days after infection. **(B)** Mice were treated with 40mg kg^{-1} poly(Man-co-CTM) or controls, poly(Gal-co-CTM) or free ciprofloxacin, after being challenged with a lethal dose of F. novicida. A total of three administrations was given, each separated by 24 hours. Protection against infection was monitored by survival of mice 14 days after infection. **(C-D)** During the course of health evaluations of the mice, body weight was recorded.

4.D.3. Biodistribution of glycan antibiotic prodrug polymers

The biodistribution of poly(Man-*co*-CTM) and non-targeting control polymer, poly(Gal-*co*-CTM) were evaluated in healthy mice. A single dose of aqueous suspension of rhodamine labeled polymeric prodrug was administered intratracheally to the lungs of mice via a MicroSprayer

Aerosolizer at a concentration of 40 mg kg^{-1} of ciprofloxacin polymerized to the polymers. Lung, liver, kidney, spleen, and blood were collected at various time points after administration and fluorescent content was measured. Interestingly, both poly(Man-*co*-CTM) and poly(Gal-*co*-CTM) had similar qualitative biodistribution profiles. Both polymers retained in the lungs at detectable values up to 72 hours after polymer administration (**Figure 4.3**). As the polymer content cleared from the lungs, distribution accumulation occurred primarily in the liver and kidneys. The initial distribution half-life ($t_{1/2,\alpha}$) of poly(Man-*co*-CTM) in the lungs was 11.12 minutes and the distribution half-life ($t_{1/2,\alpha}$) of poly(Gal-*co*-CTM) was 18.6 minutes, while the elimination half-life ($t_{1/2,\beta}$) of poly(Man-*co*-CTM) was 14.2 hours and the elimination half-life ($t_{1/2,\beta}$) of poly(Gal-*co*-CTM) was 6.5 hours.

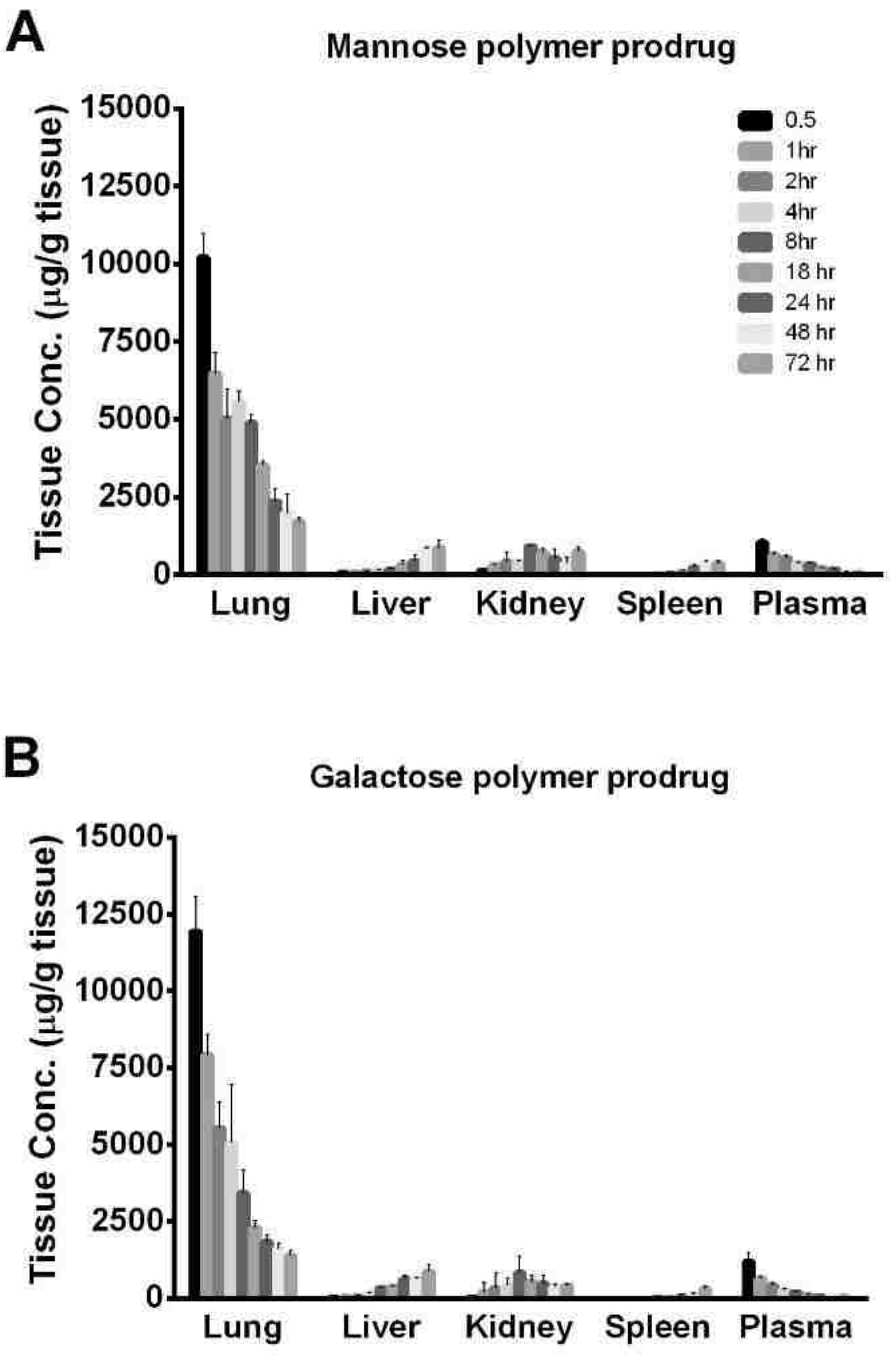

Figure 4.3 Biodistribution of glycan antibiotic prodrug polymers in mice
(A) Poly(Man-*co*-CTM) and **(B)** poly(Gal-*co*-CTM) were administered intratracheally at a dose of 40 mg/kg of ciprofloxacin into the lungs of mice. Animals were euthanized at various time points to determine polymer biodistribution. Values represent µg of polymer per g of tissue. Data represent mean values ± s.d. (*n*=3).

4.D.4. Pharmacokinetics and pharmacodynamics of ciprofloxacin released from poly(Man-*co*-CTM) compared to free antibiotic

The pharmacokinetics of released ciprofloxacin from poly(Man-*co*-CTM) were compared to poly(Gal-*co*-CTM) and intratracheally administered free ciprofloxacin in mice. A single dose of aqueous suspension of polymeric prodrug at 40 mg kg^{-1} of polymerized ciprofloxacin or 40 mg kg^{-1} of free ciprofloxacin was administered intratracheally. Blood, lung, liver, kidney, and spleen were collected at various time points after administration.

Most of the free ciprofloxacin delivered was cleared from the body within 8 hours, which agrees with the short half-life time observed in literature[22–24]. More notably, released ciprofloxacin from the polymeric prodrugs retained in the lungs even after 48 hours (**Figure 4.4**). This observation can be explained by the fact that the glycopolymer retained in the lungs after 48 hours as seen in Figure 4, and consequently explains the differences of ciprofloxacin levels in the lung tissue. Most of the released ciprofloxacin was distributed primarily to the kidneys and liver (with t_{max} occurring at 8 hours for the kidneys and 24 hours for the liver), whereas free ciprofloxacin accumulated in the other organs within 30 minutes. In consistence with the prolonged retention of the polymers in the lung and other tissues, ciprofloxacin released from the polymers had significantly higher total AUCs in all tissue except for the spleen compared to free antibiotic (**Table 4.1**) indicative of the sustained release of the ciprofloxacin from the glycopolymer.

The pharmacodynamics were subsequently evaluated, which showed that even at 72 hours after administration to the lungs, the concentrations of ciprofloxacin released from the polymer in the lungs, liver, and kidneys are above the MIC for ciprofloxacin in treating *F. tularensis* (0.03μg/ml; **Figure 4.5**). The concentrations of ciprofloxacin released from the polymers in the spleen are greater than the MIC up to approximately 48 hours after administration. Because the MIC refers to the minimum inhibitory concentration of drug necessary to prevent visible growth of bacteria generally in liquid suspension (i.e. in plasma), the volume distribution of ciprofloxacin (1.74 to 5.0 L/kg) was used to convert MIC to a more tissue-relatable value (0.05-0.15μg/g)[25]. For

the lung, liver, and kidneys the T>MIC values for both polymeric prodrugs were 100% with the dosage interval being 72 hours, while the T>MIC values for free cipro in the lung and kidneys were 5.5%. This is promising because fluoroquinolones display both concentration-dependent killing characteristics and time-dependent effects[26,27]. Previous studies have suggested that ciprofloxacin should display a C_{max}/MIC ratio of 10 and an $AUC_{0\text{-}24h}$/MIC greater than 125 for successful clinical outcome[28,29]. The C_{max}/MIC value for released ciprofloxacin from the polymers display values significantly greater than 10, and in all tissues studied except the spleens the $AUC_{0\text{-}24h}$/MIC values were also significantly greater than 125.

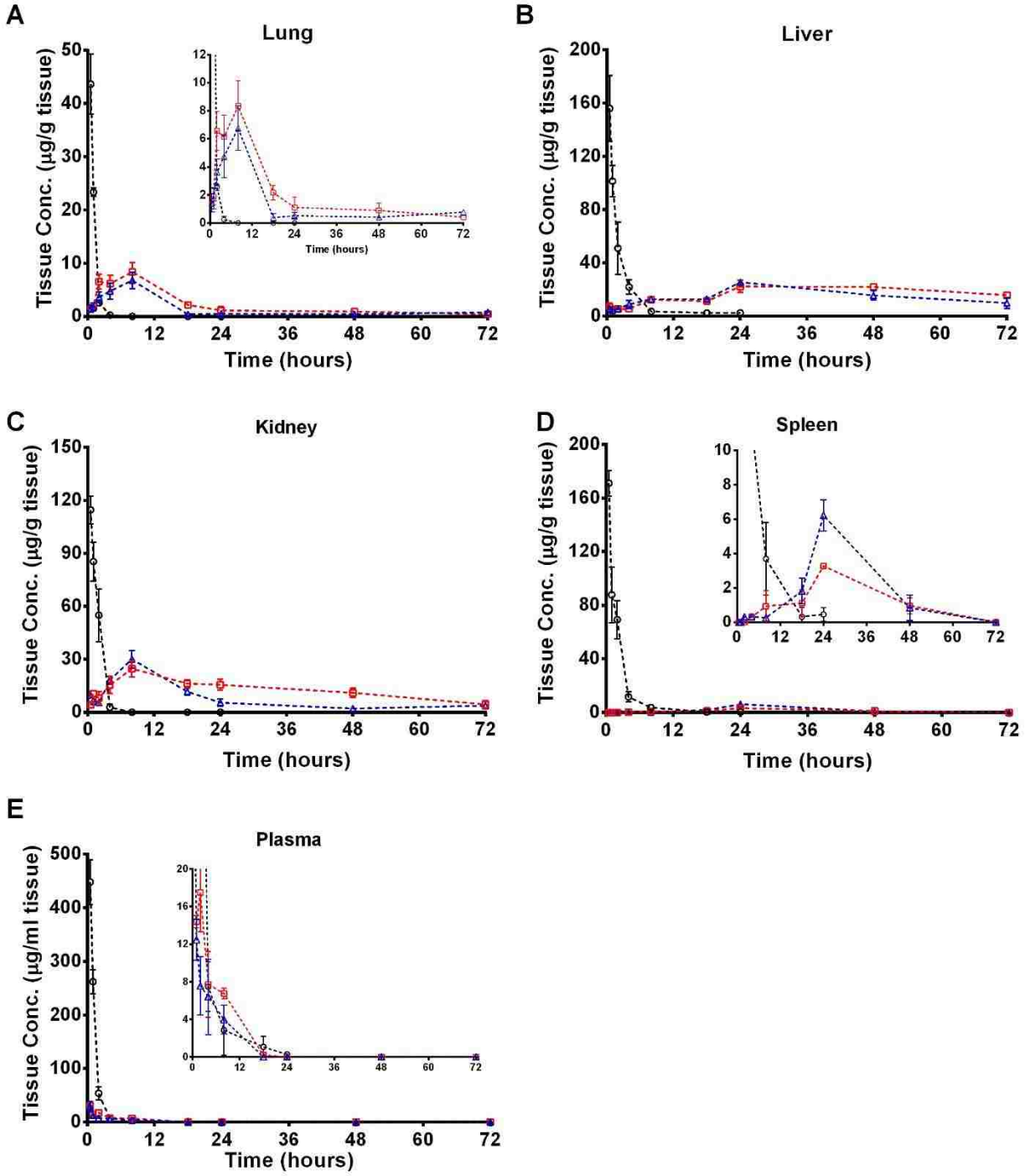

Figure 4.4 Pharmacokinetics of ciprofloxacin

Poly(Man-*co*-CTM) and controls, free ciprofloxacin and poly(Gal-co-CTM), were administered via intratracheal aerosolization at a dose of 40mg kg^{-1} of ciprofloxacin in mice. Animals were euthanized at various time points to determine ciprofloxacin biodistribution and pharmacokinetics in the **(A)** lungs, **(B)** liver, **(C)** kidneys, **(D)** spleen, and **(E)** plasma. Data represent mean values ± s.d. (*n*=3). Significant differences between ciprofloxacin concentrations of the two treatment groups at each time point were analyzed by 2-way ANOVA multiple comparisons test (* *P*<0.05, ** *P*<0.005).

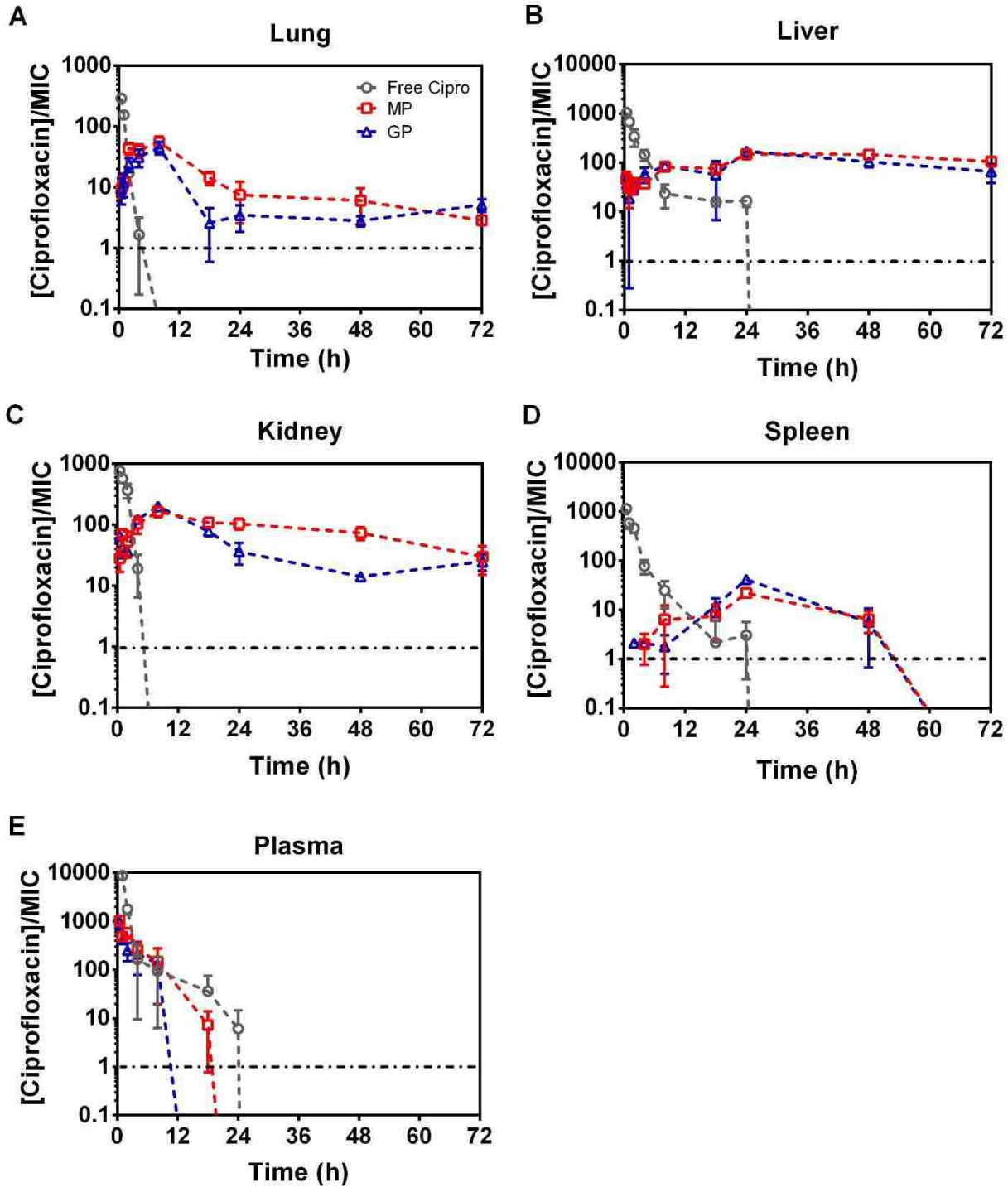

Figure 4.5 Pharmacodynamics of ciprofloxacin
(A-E) The pharmacodynamics of poly(Man-*co*-CTM), poly(Gal-*co*-CTM), and free ciprofloxacin as expressed by the ratio of concentration of ciprofloxacin (μg/g) and the minimum inhibitory concentration (MIC) of 0.03ug/ml. The volume distribution of ciprofloxacin (1.74 to 5.0 l/kg) was used to convert MIC to a more tissue-relatable value (0.05-0.15μg/g). The dotted line represents a ratio of 1. Data represent mean values ± s.d. (*n*=3).

Free Drug released	Organ	AUC (free cipro)	AUC_{total} (μg*h/g)	AUC_{0-24h} (μg*h/g)	C_{max} (μg/g)	t_{max} (h)	C_{max}/MIC	AUC_{0-24h}/MIC (h)
MP	Lung	33.18	149.4	109.1	8.346	8	55.64	727.33
GP			99.11	73.40	6.773	8	45.15	489.33
MP	Liver	308.1	1256	273.1	22.315	24	148.77	1820.67
GP			1106	307.5	25.536	24	170.24	2050
MP	Kidneys	183.7	924.1	417.8	24.701	24	164.67	2785.33
GP			552.5	391.1	30.098	24	200.65	2607.33
MP	Spleen	277.2	88.59	8.416	3.275	8	21.83	56.11
GP			131.1	4.750	6.214	8	41.43	31.67

Table 4.1
Summary of critical pharmacokinetic and pharmacodynamic values of poly(Man-*co*-CTM) and poly(Gal-*co*-CTM).

4.D.5. Cellular pharmacokinetics and pharmacodynamics of ciprofloxacin in alveolar macrophage

To further understand why poly(Man-*co*-cipro) led to greater survival percentages of lethally infected mice compared to those treated with poly(Gal-*co*-cipro), the pharmacokinetics of ciprofloxacin present in alveolar macrophage cells was investigated (**Figure 4.6**). A single dose of aqueous suspension of polymeric prodrug at 40 mg kg^{-1} of polymerized ciprofloxacin was administered intratracheally. Bronchoalveolar lavage was conducted at various time points after administration and centrifuged to collect the alveolar macrophage cell pellet. BAL cells were further washed and centrifuged again at 400xg. Alveolar macrophage cells were stained and counted, and ciprofloxacin was detected via LC-MS/MS.

It is hypothesized that targeting CD206 with poly(Man-*co*-cipro) would enable greater polymer content, and therefore greater antibiotic content in alveolar macrophage cells to combat replication of intracellular pathogens. The pharmacokinetic data show that the concentration of ciprofloxacin residing in alveolar macrophage cells was greater (P<0.0001) in mice treated with

targeted poly(Man-*co*-cipro) compared to the concentration of ciprofloxacin in mice treated with non-targeting poly(Gal-*co*-cipro) for the first 8 hours of dosing (**Figure 4.6A,B**). The concentration of ciprofloxacin remained relatively identical between the two treatment groups after 8 hours, although mice treated with poly(Man-co-cipro) showed slightly higher concentrations of antibiotic between 48 and 72 hours. The AUC_{total} of ciprofloxacin in mice dosed with poly(Man-co-cipro) was 1723, while the AUC_{total} of ciprofloxacin in mice dosed with poly(Gal-co-cipro) was 1582. Despite the differences observed in antibiotic concentration residing in alveolar macrophage cells, pharmacodynamic data show that both polymer prodrug groups have [Ciprofoxacin]/MIC ratios significantly greater than 1 (**Figure 4.6C**).

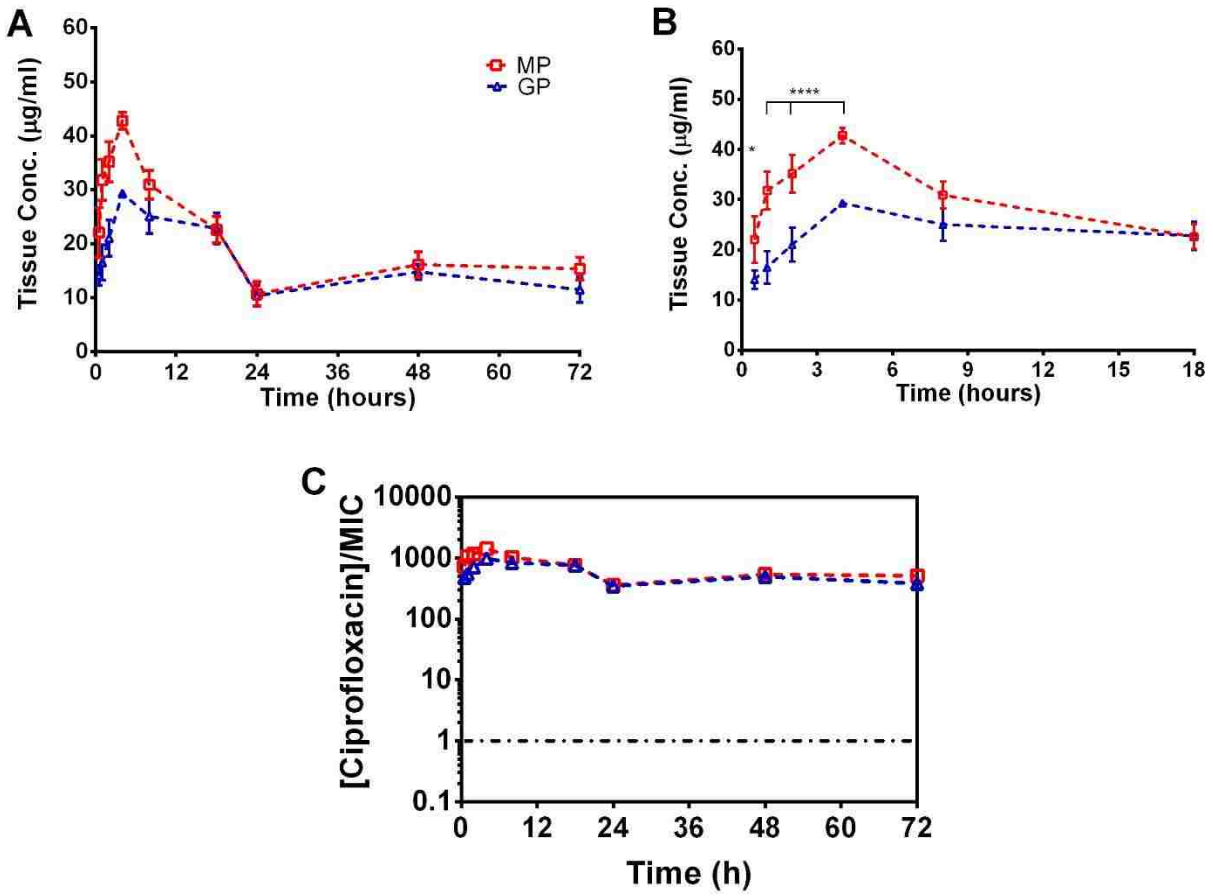

Figure 4.6. Pharmacokinetics and pharmacodynamics of ciprofloxacin in AMs
(A) The pharmacokinetics of ciprofloxacin in alveolar macrophage cells from mice administered with poly(Man-*co*-CTM) or poly(Gal-*co*-CTM). Values are expressed as µg of ciprofloxacin per l of cellular volume. The average volume of murine AM cells used is 493±161 x 10^{-9} µl[18]. **(B)** A zoomed-in figure of the pharmacokinetics up to 18 hours. **(C)** The pharmacodynamic values are expressed as the ratio of concentration of ciprofloxacin (µg/ml) and the minimum inhibitory concentration (MIC) of 0.03ug/ml. The dotted line represents a ratio of 1. Data represent mean values ± s.d. (*n*=3). Significant differences between ciprofloxacin concentrations of the two treatment groups at each time point were analyzed by multiple comparisons t-test (* *P*<0.05, **** *P*<0.0001).

4.E. Discussion & Conclusion

The motivation driving the design of a synthetic ciprofloxacin prodrug glycopolymer delivery system lies on overcoming the limitations presented by free ciprofloxacin delivery. Although ciprofloxacin has shown excellent microbiological and clinical success in treating *F.*

tularensis infections in both children and adults[7–11], ciprofloxacin's limited solubility in aqueous physiological conditions hinder its success as an aerosolizable drug. Ciprofloxacin is currently administered only via intravenous (I.V.) injections or oral tablets. Although, both I.V. and oral administration of ciprofloxacin result in systemic distribution of the drug, no preferential accumulation at target tissues occurs therefore proper therapeutic levels at target tissue sites, such as the lungs, may not be reached. Maximum serum concentrations for oral tablets are attained 1 to 2 hours after oral dosing and the serum elimination half-life in human patients with normal renal function is approximately 4 hours[24]. Because alveolar macrophages (AMs) are the predominant effector cells of the pulmonary innate immune response, it is hypothesized that targeted delivery of neoglycopolymer prodrugs to the macrophage mannose receptor will allow (i) enhanced internalization of polymers and drug to target cells, (ii) increased retention of polymer-drug circulation in the body, and (iii) increased solubility of ciprofloxacin in aqueous conditions thereby enabling aerosol pulmonary delivery.

The ability to protect against lethal pulmonary *F. novicida* infections in mice challenge models ultimately demonstrated the promising intracellular antibacterial functionality of targeted poly(Man-co-CTM). When administered via aerosol to the lungs of mice in a prophylactic setting, poly(Man-co-CTM) improved survival in 50% of the mice, whereas free antibiotic ciprofloxacin was unable to protect any mice. In a post-infection treatment setting, the survival of mice increased to 87.5%, while free antibiotics remained ineffective. This significant improvement in antibacterial effect lies on the improved pharmacokinetic and pharmacodynamic properties of poly(Man-co-CTM). When compared to non-targeting glycan control polymer poly(Gal-*co*-Cipro), poly(Man-co-CTM) had more than double elimination half-life time in the lungs. The C_{max}, AUC, $AUC_{0\text{-}24h}$/MIC, and C_{max}/MIC of active drug were all improved significantly compared to free ciprofloxacin and the galactose control. Overall, the AUC of ciprofloxacin in the lungs was increased 4.5-fold and retention was improved by 64 hours in contrast to free ciprofloxacin. More interestingly, pulmonary administration of our polymeric prodrugs or free ciprofloxacin led to

relatively low serum drug concentrations thus reducing the possibility of systemic side effects. When compared to the pharmacokinetic properties of Aradigm corporation's liposomal platform, the ciprofloxacin released from the polymeric prodrugs demonstrated longer retention in the lungs. This can be attributed to the importance of sustained release of the drugs from the polymer in contrast to the burst release of the liposomes.

It was hypothesized that targeting the alveolar macrophage cells is critical in combatting intracellular pathogens as they provide a niche for bacterial replication while evading the host's immune response. Therefore, we further analyzed the pharmacokinetics and distribution of ciprofloxacin in alveolar macrophage cells to investigate whether high antibiotic concentrations in the target cells leads to the increased survival observed. The concentration of ciprofloxacin in alveolar macrophage cells was greater in mice administered with the targeted poly(Man-*co*-cipro) compared to mice administered with the non-targeted poly(Gal-*co*-cipro) for the first 8 hours, and slightly greater during the 48-72 hour time frame. Surprisingly, the pharmacodynamic data showed similar trends between the two treatment groups. Looking at the data altogether, the increased survival of mice against lethal *F. novicida* can be explained by two possible reasons. The first being that the first 8 hours of antibiotic treatment in alveolar macrophage cells are critical in eradicating pathogen or at least minimizing chances of bacterial replication. This is because *F. tularensis* LVS and *F. novicida* U112 growth are still in the lag phase the first 4-5 hours as the pathogen are acclimating to the new environment and preparing for cell division. The pathogen then display exponential growth phases between 4-24 hours[30,31]. Furthermore, in the first 24 hours of infection the proportions of lung cell types infected with Francisella strain U112, LVS, or Schu S4 are 51.6-78.9% alveolar macrophage cells[32]. Delivering greater amounts ciprofloxacin to the alveolar macrophage the first 8 hours may be a critical reason why we observed better survival for mice treated with poly(Man-co-CTM). The second explanation for the observed differences in survival rates is the overall improvement in pharmacokinetic and pharmacodynamic properties of ciprofloxacin through the prodrug systems. Although alveolar macrophage cells are initially the

predominant target cells of intracellular Francisella pathogens, other lung cell types also get infected, such as dendritic cells, monocytes, neutrophils, and alveolar type II epithelial cells[32,33]. The improved overall pharmacokinetic and pharmacodynamic properties of ciprofloxacin via poly(Man-*co*-cipro) allows for better protection against pulmonary infections. When compared to control polymer poly(Gal-co-cipro), we observed different survival rates with poly(Man-*co*-cipro) leading to greater protection. This may be due to the difference in anatomical locations of target cells, i.e. alveolar macrophage cells, and galactose lectins residing elsewhere throughout the body. A similar observation was seen from Takakura *et al.* in which galactose and mannose lipoplexes were intravenously administered into mice for *in vivo* gene delivery liver applications. They observed different transfections activities between the two lipoplexes[34].

The long retention of the polymers could be explained by two reasons. Firstly, the increased molecular weight of the polymers compared to free drug alone may result in longer retention in tissues. The glycopolymer prodrugs may be more likely to be accumulated in epithelial cells compared to free ciprofloxacin since ciprofloxacin has shown rapid plasma absorption[24]. Secondly, the mannosylated polymers may be interacting with cells of the respiratory tract either by targeting to mannose binding receptors on alveolar macrophage cells or non-specific adhesion between lung epithelial cells. The prolonged retention in the lung, increased drug distribution in the lung, and reduced free drug levels in blood significantly increase antibacterial activity and improve the tolerability of ciprofloxacin. Poor pharmacokinetic properties remain one of the inherent limitations of free drugs; as a result, exhaustive and higher drug doses are required, often times leading to poor compliance and serious side effects. Overall, our results present a promising solution to improving current antibiotics, and provides the possibility of dose sparing and less exhaustive dosing regimens.

Collectively, we have demonstrated that prodrug neoglycopolymers can be engineered to target alveolar macrophage cells thereby increasing drug content in crucial cells to protect against pulmonary intracellular infections. More specifically, preparation of prodrug neoglycopolymers via

aqueous RAFT polymerization of hydrophilic carbohydrates improved conventional antibiotic physiochemical, pharmacokinetic, and pharmacodynamic properties. The modularity, reproducibility, and scalability of this synthetic technique offers advantages over current free drugs, and shows to be a promising platform for new polymeric prodrug systems to treat an array of infections and diseases.

4.F. References

1. *Health Aspects of Chemical and Biological Weapons*. *World Helath Organization* (1970).
2. Evans, M. E., Gregory, D. W., Schaffner, W. & McGee, Z. A. Tularemia: a 30-year experience with 88 cases. *Med.* **64,** 251–269 (1985).
3. Anthony, L. S. D., Burke, R. D. & Nano, F. E. Growth of Francisella spp. in rodent macrophages. *Infect. Immun.* **59,** 3291–3296 (1991).
4. Kortepeter, M. G. & Parker, G. W. Potential biological weapons threats. *CDC Emerg. Infect. Dis.* **5,** (1999).
5. Thomas, L. & Schaffner, W. Tularemia pneumonia. *Infect Dis Clin North Am* **24,** 43 (2010).
6. Tärnvik, A. & Chu, M. C. New approaches to diagnosis and therapy of tularemia. *Ann N Y Acad Sci* **1105,** 378–404 (2007).
7. Meric, M. *et al.* Evaluation of clinical, laboratory, and therapeutic features of 145 tularemia cases: the role of quinolones in oropharyngeal tularemia. *APMIS* **116,** 66 (2008).
8. Limaye, A. P. & Hooper, C. J. Treatment of tularemia with fluoroquinolones: two cases and review. *Clin. Infect. Dis.* **29,** 922 (1999).
9. Chocarro, A., Gonzalez, A. & Garcia, I. Treatment of tularemia with ciprofloxacin. *Clin. Infect. Dis.* **31,** 623 (2003).
10. Johansson, A., Berglund, L., Gothefors, L., Sjostedt, A. & Tarnvik, A. Ciprofloxacin for treatment of tularemia in children. *Pediatr. Infect. Dis. J.* **19,** 449–453 (2000).
11. Perez-Castrillon, J. L., Bachiller-Luque, P., Martin-Luquero, M., Mena-Martin, F. J. & Herreros, V. Tularemia epidemic in northwestern Spain: clinical description and therapeutic response. *Clin. Infect. Dis.* **33,** 573–576 (2001).
12. Tärnvik, A. & Berglund, L. Tularemia. *Eur. Respir. J.* **21,** 361–373 (2003).
13. Eliasson, H., Broman, T., Forsman, M. & Bäck, E. Tularemia: current epidemiology and disease management. *Infect Dis Clin North Am* **20,** 289–311 (2006).
14. Dennis, D. T. *et al.* Tularemia as a biological weapon: medical and public health management. *JAMA* **285,** 2763–2773 (2001).
15. Oyston, P. C., Sjostedt, A. & Titball, R. W. Tularaemia: bioterrorism defence renews interest in Francisella tularensis. *Nat Rev Microbiol* **2,** 967–978 (2004).
16. CIPRO® (ciprofloxacin hydrochloride) Tablets. Drug Fact Sheet. *Bayer Pharmaceuticals Corporation* (2004). Available at: http://www.fda.gov/downloads/Drugs/EmergencyPreparedness/BioterrorismandDrugPreparedness/UCM130802.pdf.
17. Cipolla, D., Blanchard, J. & Gonda, I. Development of liposomal ciprofloxacin to treat lung infections. *Pharmaceutics* **8,** 1–31 (2016).
18. Stone, K. C., Mercer, R. R., Gehr, P., Stockstill, B. & Crapo, J. D. Allometric relationships

of cell numbers and size in the mammalian lung. *Am. J. Respir. Cell Mol. Biol.* **6,** 235–243 (1992).
19. Craig, A., Mai, J., Cai, S. & Jeyaseelan, S. Neutrophil recruitment to the lungs during bacterial pneumonia. *Infect. Immun.* **77,** 568–575 (2009).
20. Grommes, J. & Soehnlein, O. Contribution of neutrophils to acute lung injury. *Mol. Med.* **17,** 293–307 (2011).
21. Walker, J. & Sarmiento, X. Inflammatory mechanisms in the lung. *J. inlammation Res.* 1–11 (2009).
22. Crump, B., WIse, R. & Dent, J. Pharmacokinetics and tissue penetration of ciprofloxacin. *J. Antimicrob. Chemother.* **24,** 784–786 (1983).
23. Bergan, T., Dalhoff, A. & Rohwedder, R. Pharmacokinetics of ciprofloxacin. *Infection* **16,** 3–13 (1988).
24. Begg, E. J. *et al.* The pharmacokinetics of oral fleroxacin and ciprofloxacin in plasma and sputum during acute and chronic dosing. *Br. J. Clin. Pharmacol.* **49,** 32–38 (2000).
25. Vance-Bryan, K., Guay, D. R. P. & Rotschafer, J. C. Clinical Pharmacokinetics of Ciprofloxacin. *Clin. Pharmacokinet.* **19,** 434–461 (1990).
26. Rello, J., Kollef, M., Diaz, E. & Rodriguez, A. *Infectious Diseases in Critical Care*. *Springer* (2007).
27. Firsov, A. A. *et al.* MIC-based interspecies prediction of the antimicrobial effects of ciprofloxacin on bacteria of different susceptibilities in an in vitro dynamic model. *Antimicrob. Agents Chemother.* **42,** 2848–2852 (1998).
28. Preston, S. L. *et al.* Pharmacodynamics of levofloxacin: a new paradigm for early clinical trials. *JAMA* **279,** 125–129 (1998).
29. Forrest, A. *et al.* Pharmacodynamics of Intravenous Ciprofloxacin in Seriously Ill Patients. *Antimicrob. Agents Chemother.* **37,** 1073–1081 (1993).
30. Ma, Z. *et al. EmrA1 Membrane Fusion Protein of Francisella tularensis LVS is required for Resistance to Oxidative Stress, Intramacrophage Survival and Virulence in Mice*. *Mol Microbiol* **91,** (2014).
31. Nallaparaju, K. C. *et al.* Evasion of IFN-γ signaling by Francisella novicida is dependent upon Francisella outer membrane protein C. *PLoS One* **6,** (2011).
32. Hall, J. D. *et al.* Infected-host-cell repertoire and cellular response in the lung following inhalation of Francisella tularensis Schu S4, LVS, or U112. *Infect. Immun.* **76,** 5843–5852 (2008).
33. Hall, J. D., Craven, R. R., Fuller, J. R., Pickles, R. J. & Kawula, T. H. Francisella tularensis replicates within alveolar type II epithelial cells in vitro and in vivo following inhalation. *Infect. Immun.* **75,** 1034–1039 (2007).
34. Takakura, Y., Nishikawa, M., Yamashita, F. & Hashida, M. Influence of physicochemical properties on pharmacokinetics of non-viral vectors for gene delivery. *J. Drug Target.* **10,** 99–104 (2002).

5. Chapter 5: Summary and Future Perspectives

5.A. Overall Summary

Carbohydrates are not only the most abundant biomolecules in nature, but also promising materials for targeted delivery of therapeutics in a cell-specific manner. The recent advances in the design of drug delivery systems have raised the possibility of using carbohydrate moieties that recognize cell surface carbohydrate-binding receptors for targeted drug delivery. In this dissertation, glycopolymer platforms were engineered and evaluated for the context of pulmonary drug delivery. The research was motivated by the physicochemical, pharmacokinetic, and pharmacodynamic limitations and subsequent inefficacies of current antibiotics to properly combat intracellular infections in the lung. Proper, effective, and rapid treatment are crucial for select agent threats. This motivation led to the ultimate goal of designing and engineering a functional ciprofloxacin prodrug system capable of probing and targeting endogenous receptors on alveolar macrophages to promote intracellular delivery and ultimately combat intracellular pathogens either prophylactically or after the onset of infection.

In Chapter 3, we synthesized glycopolymers that could be anchored onto the surface of liposomal constructs and evaluated their bioactivity for receptor-mediated uptake in various macrophage cell lines. The alveolar macrophage express carbohydrate receptors that enable them to recognize microbial-associated markers, localize and isolate infectious events, and trigger adaptive immunity. Therefore, the purpose of the work in Chapter 3 was to understand the nuances of receptor-mediated uptake pathways and demonstrate specific receptor-mediated targeting through multivalent synthetic glycopolymers. Both mannose and galactose glycopolymers were synthesized via RAFT polymerization and we demonstrated that the two carbohydrate polymers targeted their respective receptors, the macrophage mannose receptor (CD206), and the galactose-type lectin receptor (CD301) through competition studies. More importantly, when we compared uptake of the glycan targeted liposomes to conventional

PEGylated liposomes, the targeted liposomes led to greater uptake in macrophage cells. In this work, we also studied the carbohydrate-receptor expression profiles to better understand alveolar macrophage cells as well as commonly used surrogate cell lines. While alveolar macrophages were found to predominantly express the mannose receptor and not the galactose receptor, the CD206 and CD301 expression levels differed widely between macrophage cell lines, in which RAW264.7 and MH-S expressed high levels of the galactose-type lectin. These observations have significant implications regarding the translation of results from *in vitro* cell models to *in vivo* experiments, as carbohydrate-mediated targeting and uptake varies by receptor expression levels. Ultimately, we demonstrated that CD206 carbohydrate-receptor targeting is a promising method to improve delivery and therapeutic applications involving alveolar macrophage cells.

In Chapter 4, we investigated mannosylated glycopolymeric ciprofloxacin prodrugs as a pulmonary drug delivery system to combat alveolar intracellular infections. Utilizing aqueous RAFT polymerization techniques, we synthesized and characterized random copolymers consisting of mannose ethyl methacrylate monomers and ciprofloxacin prodrug ethyl methacrylate monomers. The ciprofloxacin prodrug monomer contains a phenolic ester linker that enables hydrolysis of the antibiotic drug to its active form. When polymerized with hydrophilic glycans, the physicochemical properties of ciprofloxacin in aqueous conditions are significantly improved, thus allowing pulmonary aerosol administration to the lungs. We found, both *in vitro* and *in vivo*, that the targeted mannose polymer prodrugs lead to enhanced uptake and greater internalization rate of polymer content into macrophage cells through CD206 receptor-mediated uptake. The importance of enhanced uptake and internalization rates were further shown in the intracellular killing assay, such that the targeted polymeric prodrugs killed 3-4 log fold more intracellular bacteria than non-targeted polymeric prodrug systems. These results demonstrate a promising modular platform that can be fine-tuned and altered to synthesize a combination of antibiotics and targeting monomers to treat intracellular infections.

In Chapter 5, we evaluated the efficacy of the mannosylated glycopolymeric ciprofloxacin prodrugs in treating lethal pulmonary infected mice and addressed the limitations of free ciprofloxacin. When administered via aerosol to the lungs of mice in a prophylactic setting, poly(Man-co-CTM) improved survival in 50% of the mice, whereas free antibiotic ciprofloxacin was unable to protect any mice. In a post-infection treatment setting, the survival of mice increased to 87.5%, while free antibiotics remained ineffective. These results are indicative of the limitations of conventional antibiotic treatment. This significant improvement in antibacterial effect of our polymeric prodrug systems lies on the improved pharmacokinetic and pharmacodynamic properties of ciprofloxacin. We showed that targeted mannose polymer prodrugs had more than double elimination half-life time in the lungs compared to non-specific polymer prodrugs. Overall, the AUC of ciprofloxacin in the lungs was increased 4.5-fold and retention was improved by 64 hours in contrast to free ciprofloxacin. More interestingly, pulmonary administration of our polymeric prodrugs or free ciprofloxacin led to relatively low serum drug concentrations thus reducing the possibility of systemic side effects. Poor pharmacokinetic properties remain one of the inherent limitations of free drugs; as a result, exhaustive and higher drug doses are required, often times leading to poor compliance and serious side effects. Overall, our results present a promising solution to improving current antibiotics, and provides the possibility of dose sparing and less exhaustive dosing regimens.

5.B. Future Directions

The work presented in this dissertation presents a promising and exciting antibiotic platform for combatting intracellular respiratory pathogens. However, there is much left to be explored and investigated. The latter portion of this chapter will delve into possible future directions towards exploring poly(Man-co-Cipro) and steps towards clinical translation.

5.B.1. Evaluating combinatorial roles of poly(Man-co-Cipro) with the host immune system

Macrophages were originally identified as having two distinct activation states, M1 and M2. M1 is described as classically activated pro-inflammatory cells with a function to mediate defense of the host, whereas M2 cells are known as alternatively activated cells and are anti-inflammatory with a function to regulate wound healing[1]. In recent years, it has become widely established that macrophage cells are actually highly dynamic and heterogeneous cells[2,3]. The plasticity of these cells is largely due to the various functional roles that these cells partake in. The immediate and common response of macrophages upon bacterial infections involves the upregulation of genes involved in M1 polarization, such as TNF, IL-6, IL-12, and NO synthase 2. The preference for an M1 state is a common response associated with foreign particle interaction and independent of the specific bacterial species involved[4]. The M1 classically activated state is usually associated with acute infectious diseases in which macrophages have a protective role to control infection. However, prolonged M1 states lead to many diseases and ultimately, tissue damage and multiple organ failure. Therefore, macrophages transition to M2 cells by producing anti-inflammatory mediators and respond to M2 promoting cytokines, such as IL-10 and IL-4. Chronic inflammation and wound healing is thought to be associated with the M2 profile.

More recently, the phenotypic and functional properties of macrophages have been shown to be directly influenced by the specific pathogens invading the cells. Specifically, for *Francisella* infections, several studies have shown that macrophages can be polarized toward an M2 phenotype. Shirley *et al*., have hypothesized that *F. tularensis* avoid macrophage-mediated killing by reprogramming the macrophage differentiation from M1 to M2[5]. As expected, in the early stages of infection (24 hours post-infection), *F. tularensis* induced strong proinflammatory responses *in vitro* and *in vivo* which are most likely due to the protective and pro-inflammatory roles of macrophage cells, independent of pathogen species. However, by 48 hours postinfection, majority of macrophage cells acquired an alternatively activated phenotype, as determined by an increase in FIZZ1 expression. In a different study, Mares *et al*. also showed that alternatively

activated macrophages are generated at later stages of *Francisella* infection; however, they hypothesize that the activations occurs as a result of damaged lung tissue associated with sepsis as a way to promote wound healing and repair[6]. They further hypothesize that the infection and cytotoxic nature of the pathogens lead to a downregulation of efferocytosis receptors, which leads to an accumulation of dead cell debris. The accumulation of dead cell debris is what leads to the alternative activation of macrophages.

Investigating the synergy between the host's natural immune defense system with our targeted polymeric prodrug systems would be important in understanding a more optimal dosing regimen. First, to assess whether *in vivo* infection with *F. tularensis* results in alternatively activated macrophages, specifically whether CD206 is upregulated, C57BL/6 mice will be infected with *F. tularensis* via nebulization. Mice will be euthanized at 6, 24, 48, and 72 hours post-infection. Mice treated with PBS will be used for the control group. Further processing of the lungs will either be conducted via bronchoalveolar lavage for alveolar macrophage (AM) collection or collected via whole lung harvest from methods in literature[7]. Cells will be stained for viability dye Aqua (Invitrogen) or eFluor 506 (eBioscience) and incubated with Fc block. Alveolar macrophage cells can be identified with the expression of Siglec F, CD11c, CD64, F4/80, and the absence of CD11b, with high side scatter, and high autofluorescence. Expression of CD206 will also be assessed. Cell populations will be identified using sequential gating strategies. Compensation and data analyses will be performed via FlowJo.

To study synergy between the immune system and poly(Man-*co*-cipro), mice challenge studies with either IL-4 receptors or IFN-γ receptors knocked out should be evaluated. It was shown by Shirley *et al*. that failure in mice models to induce alternatively activated macrophages (M2) protected against lethal infections with *F. novicida LVS* by allowing M1 macrophages to control bacterial replication. It is therefore hypothesized that in mice models in which macrophage fail to induce the classically activated macrophages, bacterial burden will take over. In the presence of poly(Man-*co*-cipro), mice models that fail to induce classically activated macrophages

should provide protection against bacterial infection due to an upregulation of CD206 in M2 macrophages. A *F. novicida* challenge study can be conducted with the following mice model groups: *Fn* WT, *Fn* IL-4Rα$^{-/-}$, *Fn* IFN-γR$^{-/-}$[8]. All treatment groups will either be treated with or without poly(Man-*co*-cipro). If the *Fn* IL-4Rα$^{-/-}$ group shows better protection than *Fn* WT, and if *Fn* IFN-γR$^{-/-}$ with poly(Man-*co*-cipro) show better protection than *Fn* IFN-γR$^{-/-}$ alone, then the targeted polymeric prodrugs may work synergistically with the host's immune system.

5.B.2. Evaluating alternative drugs

Ciprofloxacin was chosen as the antibiotic for the prodrug system due to relevance in treating *F. tularensis* as well as the capability to chemically engineer and synthesize the ciprofloxacin monomer. Much can be explored in the realm of utilizing other more relevant antibiotics for various applications, as well as fine tuning the functional linker on the prodrug monomer. The significance of the work presented in this thesis is the modular and plastic, yet extremely well-controlled polymerization techniques. Streptomycin or tetracycline-class drugs are common antibiotic choices for tularemia. As mentioned in this dissertation, *Burkholderia pseudomallei* is another highly lethal bacteria that poses a great threat to public health. The current drugs of choice to treat melioidosis include ceftazidime, meropenem, or doxycycline as they lead to minimal antibiotic resistance[9]. The polymer prodrug platform can be expanded for alternative drug usage and drug combinations. Type A and B strains of *F. tularensis* are sensitive to rifampicin, so it is possible to evaluate the combination of rifampicin with ciprofloxacin[10].

5.B.3. Moving towards nebulization administration

The *in vivo* work presented in this dissertation uses a MicroSprayer™ aerosolizer to deliver the drugs into the lungs of mice. The MicroSprayer aerosolizer is widely used for intratracheal administration of drugs into the lungs[11] and acts as an alternative to true aerosol systems. Evaluations of the MicroSprayer have shown that it delivers a more uniform distribution of the

instilled material in the lung compared to a standard gavage needle[12]. However, for clinical translation purposes, the MicroSprayer is not a practice method of administering drugs to the lungs. Even though intratracheal instillation is used as an alternative method for studying inhalation exposure, it has been shown that localization of delivered materials differ between actual inhalation and intratracheal instillation. Inhaled materials deposit thinly and uniformly throughout the entire lungs, whereas intratracheal instillation showed uneven distribution[13,14]. Despite these limitations, our results have shown very promising data, and it would be very exciting to investigate the efficacy of our polymeric prodrug systems with a true inhalation device. Currently, Aradigm Corporation is using the PARI LC Sprint nebulizer for ongoing clinical trials for the Lipoquin and Pulmaquin liposome-ciprofloxacin drug systems. Perhaps future experiments can use the PARI LC Sprint nebulizer to evaluate the antibiotic efficacy of our systems for comparison.

5.B.4. Evaluating scalability and storage life of polymeric prodrugs

Materials-based therapeutics or "smart" drug delivery systems, have greatly advanced over the past years; however, few of them have been able to be clinically translated **(Table 5.1)**. Several factors to take into consideration for the design of drug carriers include (i) biocompatibility and biodegradation (ii) good storage life and stability (iii) high drug loading capacity and low toxicity (iv) industrial scalability. With our polymeric prodrug systems, we have shown exciting and promising *in vivo* data in murine models, including efficacy, toxicity, and pharmacokinetic and pharmacodynamic data. To further bridge the gap between bench to bedside, it would be important to evaluate the optimal drug loading, scalability, and storage life of the polymer prodrug systems.

Table 1. Select FDA-Approved Agents Utilizing Nanomedicine

PRODUCT	COMPOSITION	INDICATION	APPROVED
	Lipid-Based Nanoparticles		
Abelcet	Lipid complex formulation of amphotericin B	Invasive fungal infections	1995
AmBisome	Liposomal preparation of amphotericin B	Fungal and protozoal infections	1997
DaunoXome	Liposomal preparation of daunorubicin	HIV-related Kaposi's sarcoma	1996
DepoCyt	Liposomal formulation of cytarabine	Lymphomatous meningitis	1999
DepoDur	Liposomal formulation of morphine sulfate	Relief of postsurgical pain	2004
Doxil/Caelyx	PEGylated liposomal formulation of doxorubicin	Various cancers	1995
Inflexal V	Liposomal influenza vaccine	Influenza	1997
Visudyne	Liposomal formulation of verteporfin	Wet age-related macular degeneration	2000
	Polymer-Based Nanoparticles		
Adagen	PEGylated adenosine deaminase enzyme	Severe combined immunodeficiency disease	1990
Cimzia	PEGylated Fab' fragment of a humanized anti-TNF-alpha antibody	Crohn's disease, rheumatoid arthritis	2008
Copaxone	Polymer composed of L-glutamic acid, L-alanine, L-lysine, and L-tyrosine	Multiple sclerosis	1996
Eligard	Leuprolide acetate and PLGH polymer formulation	Advanced prostate cancer	2002
Macugen	PEG-anti-VEGF aptamer	Neovascular age-related macular degeneration	2004
Mircera	Chemically synthesized ESA, methoxy PEG-epoetin beta	Symptomatic anemia associated with chronic kidney disease	2007
Neulasta	Conjugate of PEG and filgrastim	Chemotherapy-induced neutropenia	2002
Oncaspar	PEGylated formulation of L-asparaginase	Acute lymphoblastic leukemia	1994
Pegasys	PEGylated interferon alfa-2a	Hepatitis C	2002
Peglntron	PEGylated interferon alfa-2b	Hepatitis C	2001
Renagel	Polyamine (polymer loaded with amine groups)	Chronic kidney disease	2000
Somavert	PEGylated human growth hormone receptor antagonist	Acromegaly	2003
	Protein-Based Nanoparticles		
Abraxane	Albumin-bound paclitaxel (nab-paclitaxel)	Breast cancer	2005

ESA: erythropoiesis-stimulating agent; PEG: polyethylene glycol; PLGH: poly (DL-lactide-co-glycolide); TNF-alpha: recombinant human tumor necrosis factor-alpha.
Source: Reference 7.

Table 5.1. A list of FDA-approved nanotechnology or material-based drug delivery systems. Figure taken from Ledet *et al*. [16].

From characterization data, our glycopolymer prodrugs have an average molecular weight of 20-25 kDa, with a drug weight percent of approximately 11-14%. Our initial molar feed ratio choice of glycan:CTM was 8:1 owing to the solubility mismatch between the hydrophobic ciprofloxacin monomer and the glycomonomers. This ratio prevented the hydrophobic CTM from self-assembling into nanoparticles under physiological conditions and allowing multivalent targeting. The total drug polymerized averaged to about 9 ciprofloxacin molecules per polymer. However, the polymeric systems could be further optimized to maximize the drug loading, while

still allowing targeting and aqueous solubility. In order to do so, different molar feed ratios will be experimentally investigated. Each polymerization will compare the $T_{3\ hours}$ and T_0 samples to evaluate monomer conversion. NMR and GPC will provide the molar ratios and molecular weights respectively. *In vitro* planktonic studies will evaluate the MIC of each polymer system, and uptake or binding studies will evaluate targeting. The optimal system will provide the best combined results. The significance of higher drug loading is to minimize the amount of polymer content delivered to the host or patient, therefore lowering the actual concentration of polymer administered.

One of the advantages to the polymer prodrug system presented in this dissertation is the potential scalability. We are currently capable of manually synthesizing the monomers on the gram-scale. However, there are also third-party companies who provide synthetic monosaccharides and oligosaccharides (i.e. Carbosynth) as well as custom synthetic polymers (i.e. PolySciTEch). Furthermore, researchers at the Commonwealth Scientific and Industrial Research Organization (CSIRO) have established an automated RAFT polymerization instrument enabling RAFT synthesis on an industrial scale. CSIRO has further established an automated characterization method for determining monomer conversion and molecular weight distribution of polymers, which allows for high throughput screening[15].

The physical stability and storage shelf life are important parameters to evaluate. Currently, after purification, the polymers are dried via a lyophilizer for a minimum of 4 days. The polymer is then stored in a conical tube, parafilm-sealed, and placed in a -20˚C freezer. To date, we have stored the polymer for at most 4-6 months, and no apparent degradation has been observed via NMR or LC-MS/MS. Stability and storage life can be further evaluated for 12-24 months. The presence of vinyl peaks via ^{1}H NMR or LC-MS/MS m/z fragmentations can be used to determine monomer degradation or release of drugs from the polymer. Polymer degradation can be evaluated by GPC via the changes in the chromatogram (i.e. increased width or polymer distribution).

5.B.5. Evaluation of CD206 expression profiles in human alveolar macrophage cells

The work presented in this dissertation focuses on murine cells; however, for clinical translation purposes, it would be crucial to study the CD206 receptor expression profile in human alveolar macrophage cells and the targeting ability of poly(Man-*co*-cipro). It has been shown in previous studies that 50% of human alveolar macrophages are $CD206^{+}$ in healthy individuals, and patients with pulmonary fibrosis had alveolar macrophage cells that were 80% positive for CD206[17]. However, there are minimal literature results studying how CD206 is affected after the onset of tularemia or melioidosis. *F. tularensis* species can induce the M2 phenotype characteristics in host macrophages to manipulate their replication environment. It would be interesting to study human macrophage cells via GM-CSF differentiated primary human monocytes in an in vitro setting, or directly study clinical patient BAL samples from both healthy and infected patients.

5.C. References

1. Murray, P. J. & Wynn, T. a. Protective and pathogenic functions of macrophage subsets. *Nat. Rev. Immunol.* **11,** 723–737 (2011).
2. Gordon, S. & Taylor, P. R. Monocyte and macrophage heterogeneity. *Nat. Rev. Immunol.* **5,** 953–964 (2005).
3. Gordon, S. Alternative activation of macrophages. *Nat. Rev. Immunol.* **3,** 23–35 (2003).
4. Benoit, M., Desnues, B. & Mege, J.-L. Macrophage polarization in bacterial infections. *J. Immunol.* **181,** 3733–3739 (2008).
5. Shirey, K. A., Cole, L. E., Keegan, A. D. & Vogel, S. N. Francisella tularensis live vaccine strain induces macrophage alternative activation as a survival mechanism. *J. Immunol.* **181,** 4159–67 (2008).
6. Mares, C. a *et al.* Defect in efferocytosis leads to alternative activation of macrophages in Francisella infections. *Immunol. Cell Biol.* **89,** 167–172 (2011).
7. Misharin, A. V., Morales-Nebreda, L., Mutlu, G. M., Budinger, G. R. S. & Perlman, H. Flow cytometric analysis of macrophages and dendritic cell subsets in the mouse lung. *Am. J. Respir. Cell Mol. Biol.* **49,** 503–510 (2013).
8. Lee, E. Y., Schultz, K. L. W. & Griffin, D. E. Mice Deficient in Interferon-Gamma or Interferon-Gamma Receptor 1 Have Distinct Inflammatory Responses to Acute Viral Encephalomyelitis. *PLoS One* **8,** 1–13 (2013).
9. Wiersinga, W. J., van der Poll, T., White, N. J., Day, N. P. & Peacock, S. J. Melioidosis: insights into the pathogenicity of Burkholderia pseudomallei. *Nat. Rev. Microbiol.* **4,** 272–

82 (2006).
10. Ikäheimo, I., Syrjälä, H., Karhukorpi, J., Schildt, R. & Koskela, M. In vitro antibiotic susceptibility of Francisella tularensis isolated from humans and animals. *J. Antimicrob. Chemother.* **46,** 287–290 (2000).
11. Bivas-Benita, M., Zwier, R., Junginger, H. E. & Borchard, G. Non-invasive pulmonary aerosol delivery in mice by the endotracheal route. *Eur. J. Pharm. Biopharm.* **61,** 214–218 (2005).
12. Hasegawa-Baba, Y., Kubota, H., Takata, A. & Miyagawa, M. Intratracheal instillation methods and the distribution of administered material in the lung of the rat. *J. Toxicol. Pathol.* **27,** 197–204 (2014).
13. Brain, J. D., Knudson, D. E., Sorokin, S. P. & Davis, M. A. Pulmonary distribution of particles given by intratracheal instillation or by aerosol inhalation. *Environ. Res.* **11,** 13–33 (1976).
14. Leong, B. K. J., Coombs, J. K., Sabaitis, C. P., Rop, D. A. & Aaron, C. S. Quantitative morphometric analysis of pulmonary deposition of aerosol particles inhaled via intratracheal nebulization, intratracheal instillation or nose-only inhalation in rats. *J. Appl. Toxicol.* **18,** 149–160 (1998).
15. Becer, C. R., Groth, A. M., Hoogenboom, R., Paulus, R. M. & Schubert, U. S. Protocol for automated kinetic investigation/optimization of the RAFT polymerization of various monomers. *QSAR Comb. Sci.* **27,** 977–983 (2008).
16. Ledet, G. & Mandal, T. K. Nanomedicine: Emerging Therapeutics for the 21st Century. *U.S. Pharm.* **37,** 7–11 (2012).
17. Pechkovsky, D. V. *et al.* Alternatively activated alveolar macrophages in pulmonary fibrosis-mediator production and intracellular signal transduction. *Clin. Immunol.* **137,** 89–101 (2010).